EXTENDED PERFORMANCE SOLAR ELECTRIC PROPULSION THRUST SYSTEM STUDY

Final Report

Volume III

Tradeoff Studies of Alternate Thrust System Configurations

September 1977

By

Ion Physics Department Staff

Hughes Research Laboratories

and

Technology Division Staff

Space and Communications Group

of

Hughes Aircraft Company

Prepared For

NATIONAL AERONAUTICS AND SPACE ADMINISTRATION

NASA Lewis Research Center

Contract NAS 3-20395

1. Report No. CR 135281	2. Government Accession No	3. Recipient's Catalog No
4. Title and Subtitle EXTENDED PERFORMANCE SOLAR ELECTRIC PROPULSION THRUST SYSTEM STUDY VOLUME III — TRADEOFF STUDIES OF ALTERNATE THRUST SYSTEM CONFIGURATIONS		5. Report Date December 1977
		6 Performing Organization Code
7 Author(s) E.I. Hawthorne, et al.		8. Performing Organization Report No.
9. Performing Organization Name and Address Hughes Aircraft Company Hughes Research Laboratories Hughes Space & Com.Group 3011 Malibu Canyon Road P.O. Box 92919 Malibu, California 90265 Los Angeles, CA 90009		10. Work Unit No.
		11 Contract or Grant No NAS 3-20395
		13 Type of Report and Period Covered Final Report 14 Feb 1977–29 Aug 1977
12. Sponsoring Agency Name and Address National Aeronautics and Space Administration Lewis Research Center 21000 Brookpark Road Cleveland, Ohio 44135		
		14 Sponsoring Agency Code

15. Supplementary Notes

Project Manager: James Cake, NASA Lewis Research Center, Cleveland, Ohio

16. Abstract

Ion-thruster technology has progressed during the past decade to the point that it is considered ready for application. During this study, several thrust system design concepts were evaluated and compared using the specifications of the most advanced 30-cm engineering model thruster as the technology base. Emphasis was placed on relatively high-power missions (60 to 100 kW) such as a Halley's comet rendezvous. The extensions in thruster performance required for the Halley's comet mission were defined and alternative thrust system concepts were designed in sufficient detail for comparing mass, efficiency, reliability, structure, and thermal characteristics. Confirmation testing and analysis of thruster and power-processing components were performed, and the feasibility of satisfying extended performance requirements was verified. A baseline design was selected from the alternatives considered, and the design analysis and documentation were refined. The baseline thrust system design features modular construction, "conventional" power processing, and a "concentrator" solar array concept and is designed to interface with the Space Shuttle. A program development plan was formulated that outlines the work structure considered necessary for developing, qualifying, and fabricating the flight hardware for the baseline thrust system within the time frame of a project to rendezvous with Halley's comet during December 1985. An assessment was made of the costs and risks associated with a baseline thrust system as provided to the mission project under this plan. Critical procurements and interfaces were identified and defined. The results of this study are presented in the five volumes of this report.

17 Key Words (Selected by Author(s)) Solar Electric Propulsion Thrust System	18 Distribution Statement Unclassified-Unlimited

19. Security Classif. (of this report) UNCLASSIFIED	20 Security Classif (of this page) UNCLASSIFIED	21. No. of Pages 158	22 Price*

*For sale by the Clearinghouse for Federal Scientific and Technical Information, Springfield, Virginia 22151

FOREWORD

The work described herein was performed by the coordinated efforts of personnel within two divisions of the Hughes Aircraft Company. Responsibility for the study resided in the Ion Physics Department of the Research Laboratories Division. This department is managed by Mr. J.H. Molitor. A major portion of the thrust system design activity was performed by a team of individuals assembled from the Technology Division of the Space and Communications Group and coordinated and directed by Dr. E.I. Hawthorne. The work was funded under contract NAS3-20395 and monitored by Mr. James E. Cake of the NASA Lewis Research Center. The key technical contributors were

R.L. Poeschel	– Study manager for the final phases of the study and project engineer for the approach confirmation task
E.I. Hawthorne	– Manager of all thrust system design and program development activities
Y.C. Weisman	– Project engineer for structural design
M. Frisman	– Project engineer for structural design
G.C. Benson	– Project engineer for power management and control design
R.J. McGrath	– Project engineer for thermal control design
R.M. Martinelli	– Project engineer for capacitor diode voltage multiplier development and evaluation
T.L. Linsenbardt	– Thermal analysis
J.R. Beattie	– Thruster evaluation

SUMMARY

The primary objective of this study was to provide a data base for a program plan for the development of the ion-propulsion thrust system for the Halley's comet mission spacecraft. This data base was to include: the definition of a design concept, selected from among alternate candidate configurations; the identification of required supporting technology, including the definition of critical areas and potential technical risks; the definition of a program development plan, including a development schedule and an assessment of potential schedule risks; and a preliminary estimate of yearly and total program costs.

A concurrent objective of the study was to conduct a hardware "approach confirmation" technology effort to evaluate the ion thruster's performance and lifetime at the power level required for the Halley's comet mission, to design and evaluate the thruster isolator required for operation at the higher power level, and to evaluate the design of a capacitor-diode voltage multiplier.

A thrust system baseline configuration was identified for the 30-cm extended-performance mercury ion thruster that can perform the Halley's comet rendezvous mission. The configuration is comprised of 10 thrusters configured with a power management and control system and a structure and thermal control system in a modular thrust system design. The power management and control system uses conventional power processing. Power is provided to the thrust system with an 85 kW concentrating solar array. The thrust system mass is 1010 kg (including 15% contingency), the average system efficiency is 70%, and the estimated reliability upper bound is 72%.

Adaptability of the 900-series 30-cm thruster design to the 6 to 7 kW range required for the Halley's comet mission was demonstrated with only minor design modification required, and an acceptable high-voltage isolator design was validated by laboratory tests. The design and performance of an alternate power management and control system design approach utilizing the capacitor-diode voltage multiplier was successfully demonstrated by laboratory model tests in excess of 1 kW.

The technology efforts mentioned above assisted in the identification of the level of technical risks associated with the thrust system design. These risks have been found amenable to resolution through normal engineering development and, therefore, judged to be acceptable for mission application.

The program plan, which includes the procurement plan generated for the baseline configuration, is a viable plan that provides for delivery, in May 1981 of the flight thrust system to be integrated with the mission module and solar array. The cost of the thrust system development program is projected to be 54 million dollars (in fiscal year 1977 dollars) excluding contractor fee, of which approximately 13.5 million dollars will be required in fiscal year 1978.

In contrast to the low technical risk, the schedule risk for initiating this program development is of particular concern. Timely approval of the authorization of 13.5 million dollars for fiscal year 1978 must be granted so that the pre-project, or advanced development, activities can be initiated.

TABLE OF CONTENTS

LIST OF ILLUSTRATIONS

x

SECTION 1

INTRODUCTION

This report summarizes the results of a six-month study to define the design, program plan, and costs of the ion-propulsion thrust system for the Halley's comet mission spacecraft. The modular characteristics of the design developed during this study also make it applicable as the prime space propulsion system for other potential missions.

This study, which is based on an initial system characterization (completed 7 February 1977) performed by the National Aeronautics and Space Administration's Lewis Research Center (NASA LeRC), was performed in three parts:

- Design tradeoff studies (14 February to 15 April 1977)
  to define and compare alternate design approaches.

- Conceptual design definition, program plan, and costs
  of a selected design approach (15 April to 15 June 1977).

- Approach confirmation of supporting technology in
  selected areas.

The results of this study are presented in four volumes. Volume I summarizes the results of the entire program. Volume II discusses the conceptual design, program development plan, and cost estimates for the selected baseline thrust system design. This volume, Volume III, describes the design tradeoff studies performed to compare alternate design approaches. Volume IV describes the evaluation of thruster technology for extended performance applications.

A.   BACKGROUND

In the fall of 1976, the Office of Aeronautics and Space Technology (OAST) was given the responsibility of assessing the capability of the electric propulsion technology under development at NASA LeRC and of the solar array technology under development at Marshall Space Flight Center (MSFC) and the Jet Propulsion Laboratory (JPL) to perform the Halley's comet rendezvous mission proposed by JPL. OAST established an "August

1

Project" team from members of the three organizations to develop a preliminary program plan to support a fiscal year (FY) 1979 new start.

The August Project consisted of parallel efforts by JPL, NASA LeRC, and MSFC to define the design approach, program plan, costs, and risks of the Halley's comet mission. Three areas were considered: the spacecraft (including the science payload), the ion propulsion subsystem (referred to as the thrust system in this report), and the solar array. The NASA LeRC program was conducted in two phases. First, initialization studies (completed 15 February 1977) were conducted to define requirements and to identify preliminary design characteristics. Second, during the 15 February to 15 July period, the design of the thrust system was defined, the program plan and projected costs were generated, and a risk assessment was made. The results of the second phase of the program are reported in this volume. The design selection process included tradeoff studies among alternate design approaches, followed by a refinement of the conceptual design that had been selected. Iteration with design data available from the parallel activities at JPL and MSFC, and concurrent approach confirmation tests and analyses included in this study, strengtnen the conclusions of the thrust system study.

NASA directed us to begin the study by identifying two candidate solar array configurations (flat or concentrator), three candidate power management and control (PMaC) approaches (conventional, direct drive, or voltage multiplier), and two structural design approaches (modular or integrated). A comparative assessment of the various configurations possible from combinations of these design choices was desired in terms of performance, mass, efficiency, reliability, and technical and schedule risks.

The thrust systems being considered are based on the electric propulsion technology that NASA LeRC has been developing for over a decade. The technical baseline for this application is the most recent operational engineering model thruster (EMT), the 900-series 30-cm mercury ion EMT. This thruster is a scaled-up version of the 15-cm thruster developed and flight tested during the 1960-1969 period for the SERT II program. The EMT operates at a 3-kW power level with a specific impulse

of 3,000 sec. By making minor modifications in the existing thruster design, extended performance at approximately 6-kW power level, 4,800 sec specific impulse, and 15,000-hr pre-wearout life (as required for a Halley's comet mission) was believed to be achievable at a low technical risk. This supposition was evaluated as part of this study.

In addition to the extended-performance thruster, the key elements of the thrust system for this extended-performance application are the PMaC subsystem, gimbal system, propellant storage and distribution system, thermal control system, and supporting structure. The background of extensive development in power-processing technology for mercury ion thrusters and technology developments in the other areas were the basis for the high level of confidence that the required extended performance levels could be achieved.

B. SCOPE

The scope of this study included: the development of conceptual designs for various candidate systems; the selection, definition, and evaluation of a baseline design concept and its critical interfaces; an evaluation of the sensitivity of the baseline design to critical data base and design parameters; the generation of a development program plan for the baseline concept; estimation of costs and fiscal year funding requirements; fabrication of a demonstration scale model; and the conduct of supporting technology studies (including fabrication and testing of critical hardware components) to estimate the physical and electrical performance and to provide a baseline for subsequent work.

The design characteristics, program plan, and costs of the baseline system were defined in parallel with the supporting technology effort. Design definition was carried out in two consecutive phases:

- Phase 1: Definition and comparison of alternate configurations, leading to baseline selection.

- Phase 2: Design definition and evaluation of the baseline configuration, culminating in the generation of a program plan and cost estimates.

3

The concurrent technology effort comprised thruster performance and lifetime evaluation, thruster isolator design and evaluation, and the design and evaluation of a CDVII breadboard.

The design study was necessarily limited to the conceptual definition of the key design features and characteristics. However, sufficient understanding was achieved in all important areas to provide realistic estimates of masses; power requirements, which led to efficiency calculations; complexity and parts count, which led to reliability estimates; development, procurement, fabrication, and test requirements, which led to schedule definition; potential areas of uncertainty and concern, which led to an assessment of the technical and schedule risks; the scope and nature of system interactions, which led to the definition of principal interfaces; and requirements and phasing for hardware and manpower, which led to a cost estimate.

The tradeoff studies of alternate configurations presented in this volume led to the selection of one thrust system configuration as the baseline. The studies considered two solar array design concepts, several approaches to the design of the power management and control subsystem (PMaC), and two structural design approaches (modular versus integrated). From the various possible combinations of these design approaches, seven candidate thrust system configurations were defined. A conceptual design was developed for each of these seven configurations in sufficient detail to estimate their performance in terms of mass, reliability, and efficiency and to assess their potential technical, system-interface, and program (schedule) risks. The configurations were then compared with respect to these factors to select the recommended baseline for subsequent design definition, program plan development, and cost estimation.

Section 2 of this volume defines the seven configurations selected for comparative assessment from the matrix of potential configurations, using the data base furnished by NASA LeRC. Section 3 presents the key

4

features of the various PMaC design concepts developed during this preliminary analysis to the degree required to define the design characteristics of the seven selected thrust system configurations. Section 4 presents the structural and thermal conceptual designs generated for the seven configurations, using the PMaC design data, the solar array characteristics furnished by NASA LeRC, and the design characteristics developed for the other components of the thrust system. Section 5 presents the comparative assessment of the seven configurations, and the rationale for the selection of the recommended baseline.

SECTION 2

CANDIDATE THRUST SYSTEM CONCEPTS

A. CONFIGURATION OPTIONS

The block diagram in Figure 1 defines the key components of the thrust system and its principal interfaces with the other systems of the Halley's comet spacecraft. Figure 1 also identifies the options available for defining the alternate thrust system configurations that we considered.

The key components of the thrust system are

- PMaC subsystem (interface and thrust module units)

- Thrusters and gimbals

- Thrust system structure

- Thermal control subsystem

- Mercury propellant storage and distribution

- Solar array drive

The other major systems of the Halley's comet spacecraft (shown in Figure 1) are the solar array and the mission module (assumed in this study to include the science payload). The principal interfaces are shown in Figure 1 and are the interface between the solar array and the mission module and the interface between the thrust system and the Interim Upper Stage (IUS). The adapter between the thrust system and the IUS was considered as part of this study.

The initial system characterization performed at NASA LeRC before the start of this study evaluated thrust systems incorporating conventional, direct drive, and voltage multiplier power management and control subsystems in combination with a flat solar array. Preliminary trajectory analysis results available at the conclusion of the characterization indicated that the performance of the conventional and voltage multiplier thrust system approaches was marginal if not sufficient. Concurrently, trajectory analyses evaluating a concentrator solar array option showed

7
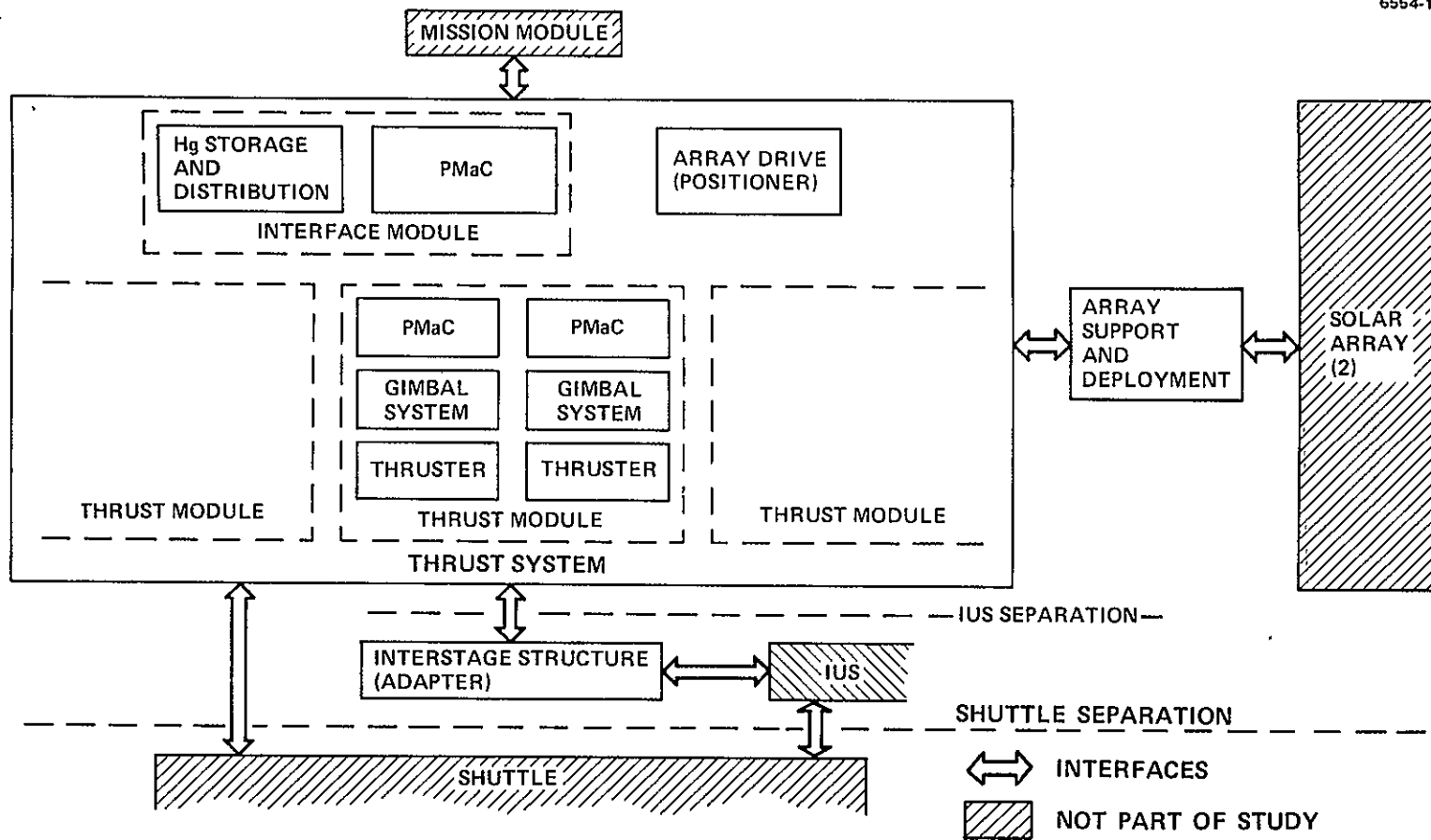
Figure 1. Thrust system block diagram showing principal interfaces.

a substantial increase in the delivered mass capability to the comet. The feasibility of the conventional and voltage multiplier options was thereby enhanced with the concentrator solar array.

Table 1 shows the coding adopted for the PMaC subsystem, solar array, and modularity options. The integrated design was compared to the modular design concept to assess any mass benefits of the integrated design. The specific thrust system configuration options selected for the tradeoff study are shown in Table 2. They are believed to provide a reasonable cross section of the available choices:

- A comparison of the four PMaC concepts is presented for the modular designs which employ the flat solar array concept.

- The four combinations of flat versus concentrator array and modular versus integrated design are examined for the conventional PMaC concept.

The principal comparisons of performance capability and technical risk could therefore be obtained from the study of these seven configurations for the purpose of selecting the recommended baseline.

Table 2 also indicates the number of thrusters required for each configuration, as determined from a preliminary analysis of the solar array power profile. The numbers were selected jointly with NASA LeRC at the start of the study and may be considered to be part of the data base (presented in the next subsection).[*]

The thruster and gimbal designs are common to all options. The same dual-tank mercury propellant subsystem was assumed for each candidate configuration. Alternate approaches to the design of this subsystem (e.g., one versus two tanks) are secondary tradeoffs that do not significantly influence the assessment of the alternate thrust system configurations. These tradeoffs were subsequently performed for the selected baseline configuration (see Section 2.D of Volume II). The same solar array drive was assumed for all candidate configurations.

---

[*] Variations in the number of thrusters was subsequently analyzed for the selected baseline configuration, as reported in Volume II.

Table 1. Study Option Codes

Option	Code
Solar array	
Flat	A
Concentrator	B
PMaC	
Direct Drive	1
Conventional discharge supply	(none)
Direct drive discharge supply	X
Conventional	2
CDVM	3
Modularity	
Modular design	(none)
Integrated design	I
Number of thrusters (modules): determined by mission requirements	(none)

T5816

Table 2. Selected Study Configurations

Option Code	PMaC	Solar Array	Modularity	No. of Thrusters
1A	Direct drive Conventional discharge supply	Flat	Modular	12
1AX	Direct drive Direct drive discharge supply	Flat	Modular	12
2A	Conventional	Flat	Modular	10
2B	Conventional	Concentrator	Modular	10
2A/I	Conventional	Flat	Integrated	10
2B/I	Conventional	Concentrator	Integrated	10
3A	Capacitor-diode voltage multiplier	Flat	Modular	10

T5816

B. DATA BASE

The data base for defining the seven configurations comprised:

● Mission module interface characteristics and requirements

● Solar array design assumptions and interface characteristics (flat and concentrator concepts)

● IUS and shuttle design characteristics and interface assumptions

● PMaC conceptual design definition (all four concepts)

● Design definition of other thrust-system elements: thrusters, gimbals, propellant storage and distribution subsystem, and solar array drive

● Certain supplementary ground rules and assumptions.

The mission module characteristics assumed were the same as those summarized in Volume II, Section 2.A for the selected baseline, and will not be repeated here.

The electrical, structural, and thermal characteristics of the two solar array configurations, furnished by NASA LeRC, are presented below. A total mass allocation of 700 kg (including the deployment system) was assumed for both the flat and the concentrator arrays. It was also assumed that both arrays would have the following structural natural frequencies:

● Each wing (uncoupled): 0.04 Hz

● Each wing and boom (uncoupled): 0.035 Hz

● Each array wing at the root of the drive structure: 0.025 Hz*

---

*Subsequently changed for the baseline configuration to 0.015 Hz; this is discussed in Volume II, Section 2.A.

The flat array was a 100 kW array whose power profile is shown in Figure 2. Corresponding voltage and current profiles, not included here, were also provided. The deployed and stowed configurations are shown in Figure 3. The deployed length of each wing is 55 m. The arrays are deployed by pulling the restraining pins and unfolding and rotating the wings, as illustrated in Figure 4. Thermal characteristics are given in Figure 5.

The stowed configuration shown in Figure 3(b) was one of several acceptable designs that was considered; it was ultimately selected for all the modular configurations using the flat array (i.e., 1A, 1AX, 2A, and 3A). An alternate configuration, one in which the four blanket containment boxes were placed side by side (as initially suggested by NASA LeRC), was also considered (as discussed in Section 4)[*] but was rejected because the net structural mass would have been higher even though the thrust system would have been shorter. A still different stowed configuration was chosen for the integrated configuration 2A/I; in it, the blanket containment boxes were placed vertically, as discussed in Section 4.

In addition to the degree of freedom available for the specific placement and arrangement of the blanket containment boxes, Figure 3 indicates the two dimensions X and Y left open as design variables, depending on the thrust system configuration. Dimension X, given in Table 25, was ultimately defined by the requirement to prevent solar array contamination by mercury ions, as discussed later in this subsection. Dimension Y was determined by the length requirements of each thrust system design, primarily determined by thermal radiator size (as discussed in Section 4).

[*]In effect, therefore, eight alternate configurations were analyzed.
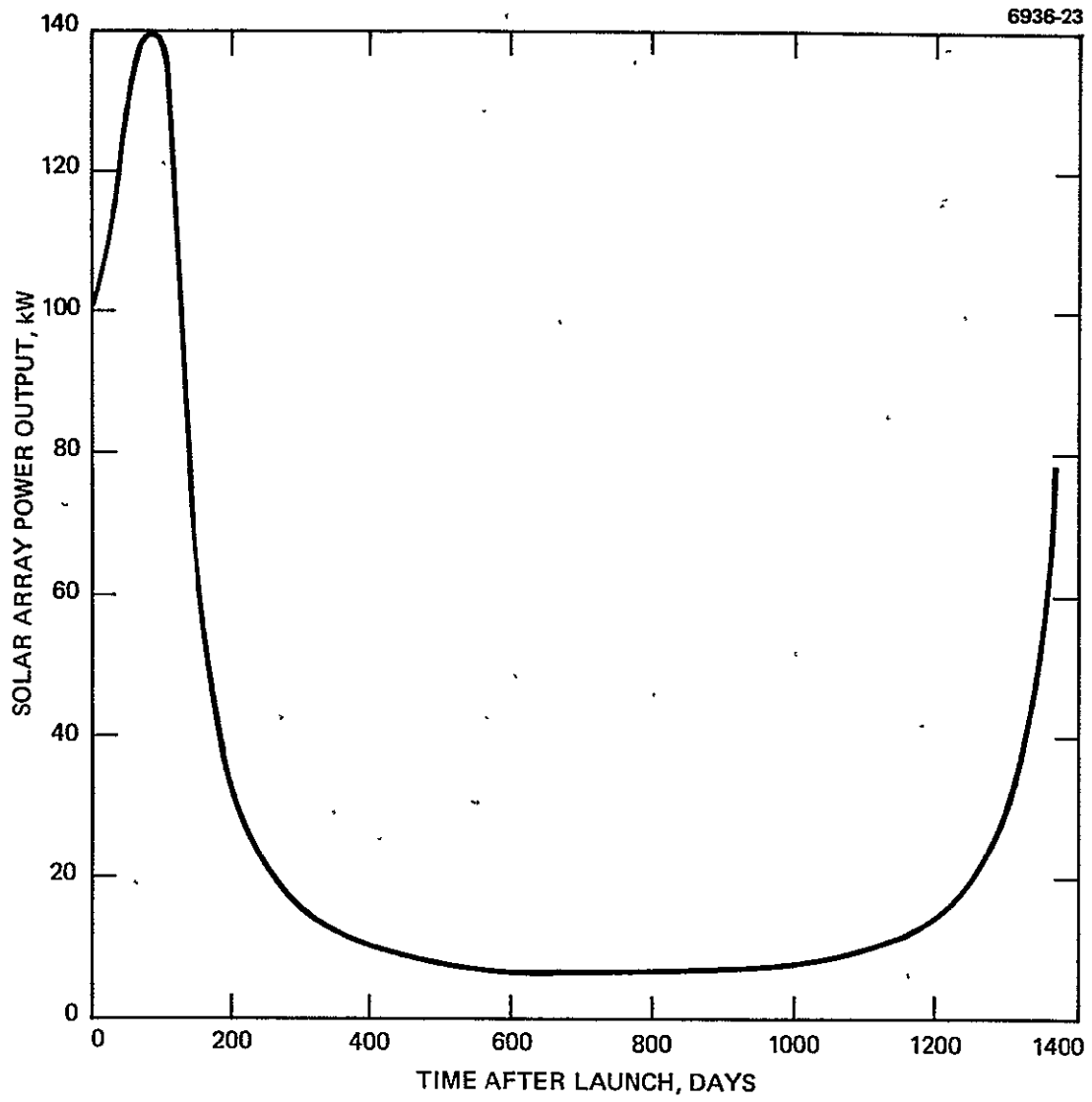
Figure 2. Flat solar array power profile.

6926-22

0 44

SECTION A - A

~ 55

A

~ 8 2

X

2.1

CANISTER

4.1

2 05

0 66 DIA

THRUST SYSTEM

FOLD LINES
(HINGES)
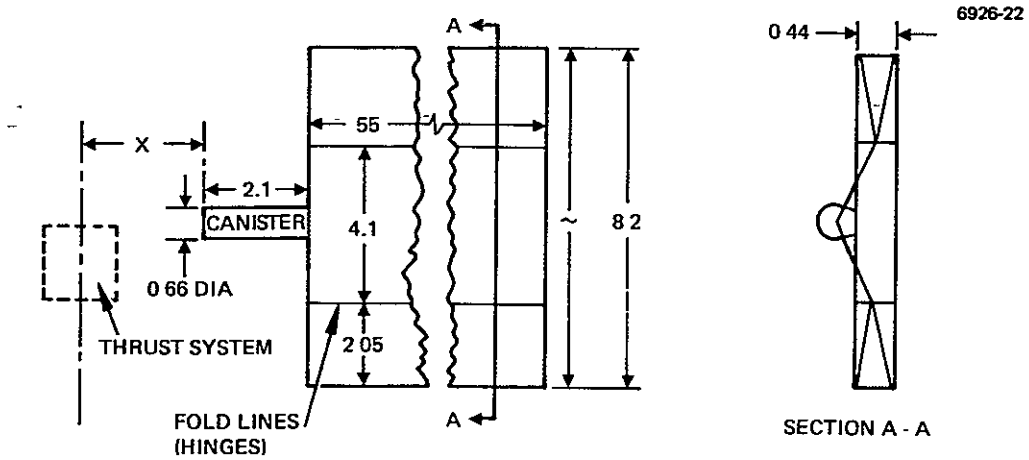
NOTE. NOT TO SCALE; ALL DIMENSIONS IN METERS,
DIMENSION X DEPENDS ON CONFIGURATION

(a) DEPLOYED

6936-21

1 3

BLANKET
CONTAINMENT
BOXES (4)

POSITIONER
MOTORS

0 81

0 43

2 0

Y

0 66

4 11
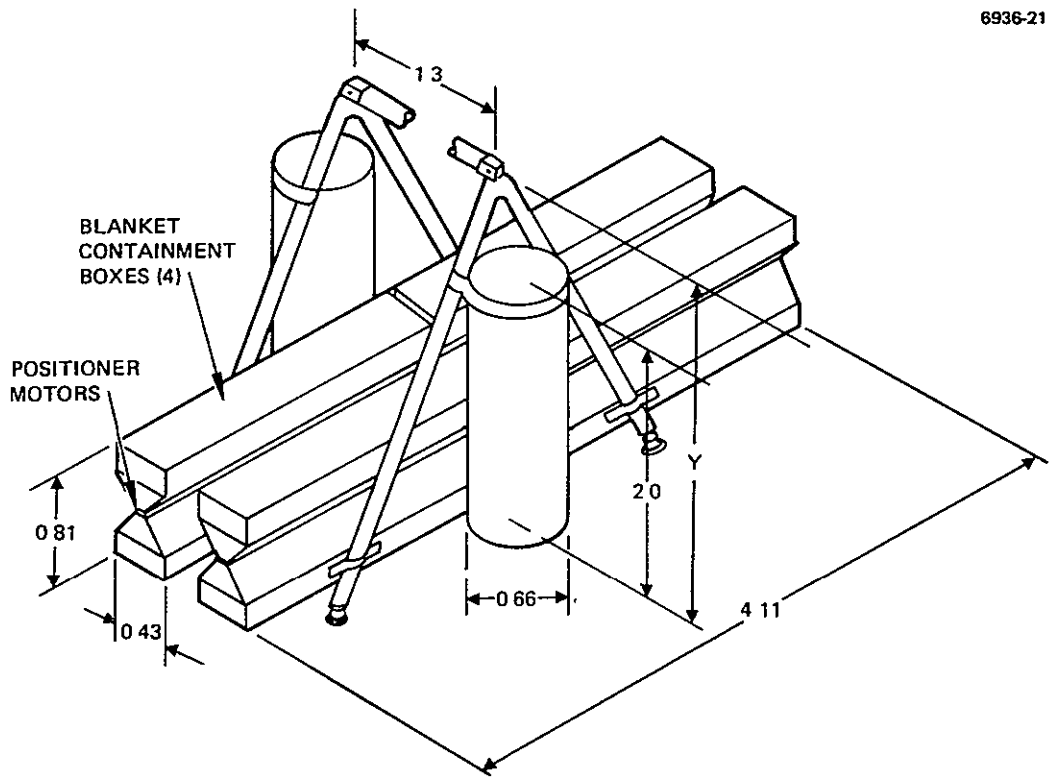
NOTE ALL DIMENSIONS IN METERS, DIMENSION Y DEPENDS ON CONFIGURATION

(b) STOWED

Figure 3. Flat solar array configuration.

14

6936-20

ASTROMAST EXTENSION
DIRECTION

DEPLOYED POSITION
LOCK

LAUNCH
LOCK

SOLAR ARRAY
DEPLOYED STAGE

HINGE

1/4 SOLAR ARRAY
STOWED

DEPLOYMENT
BOOM

ASTROMAST
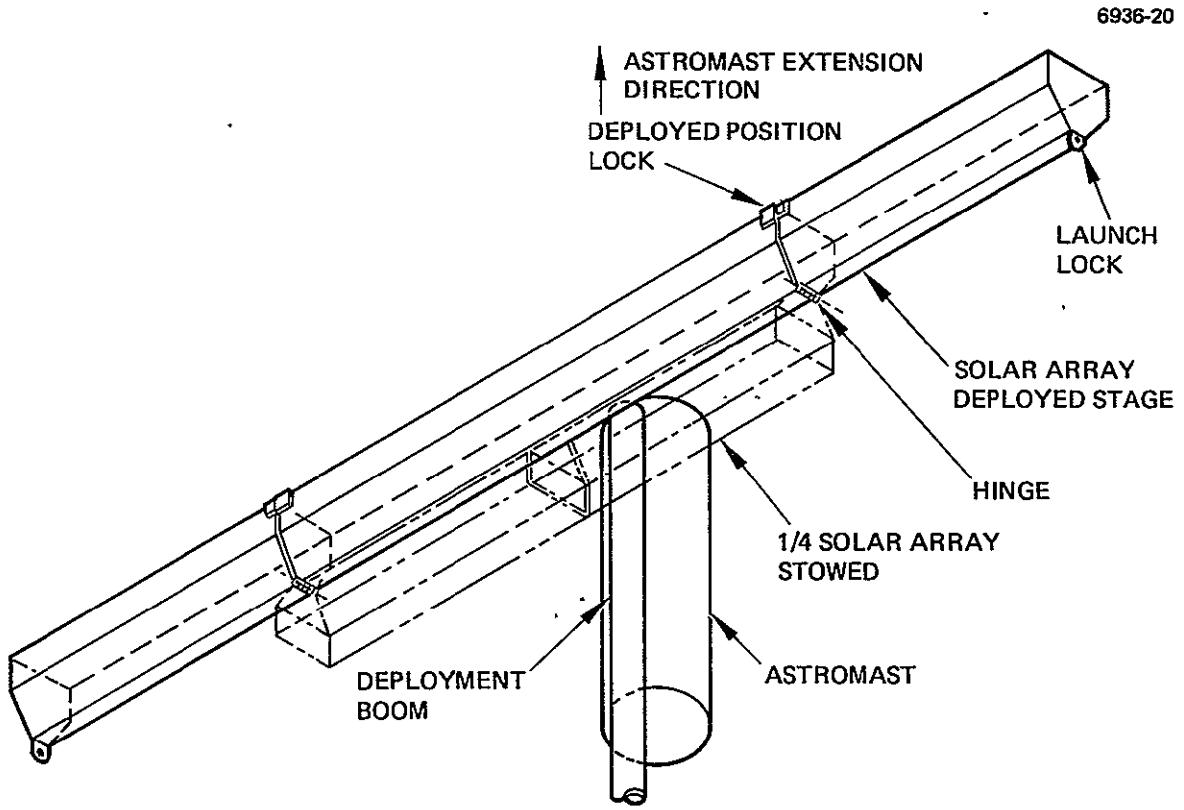
Figure 4.   Flat solar array deployment.
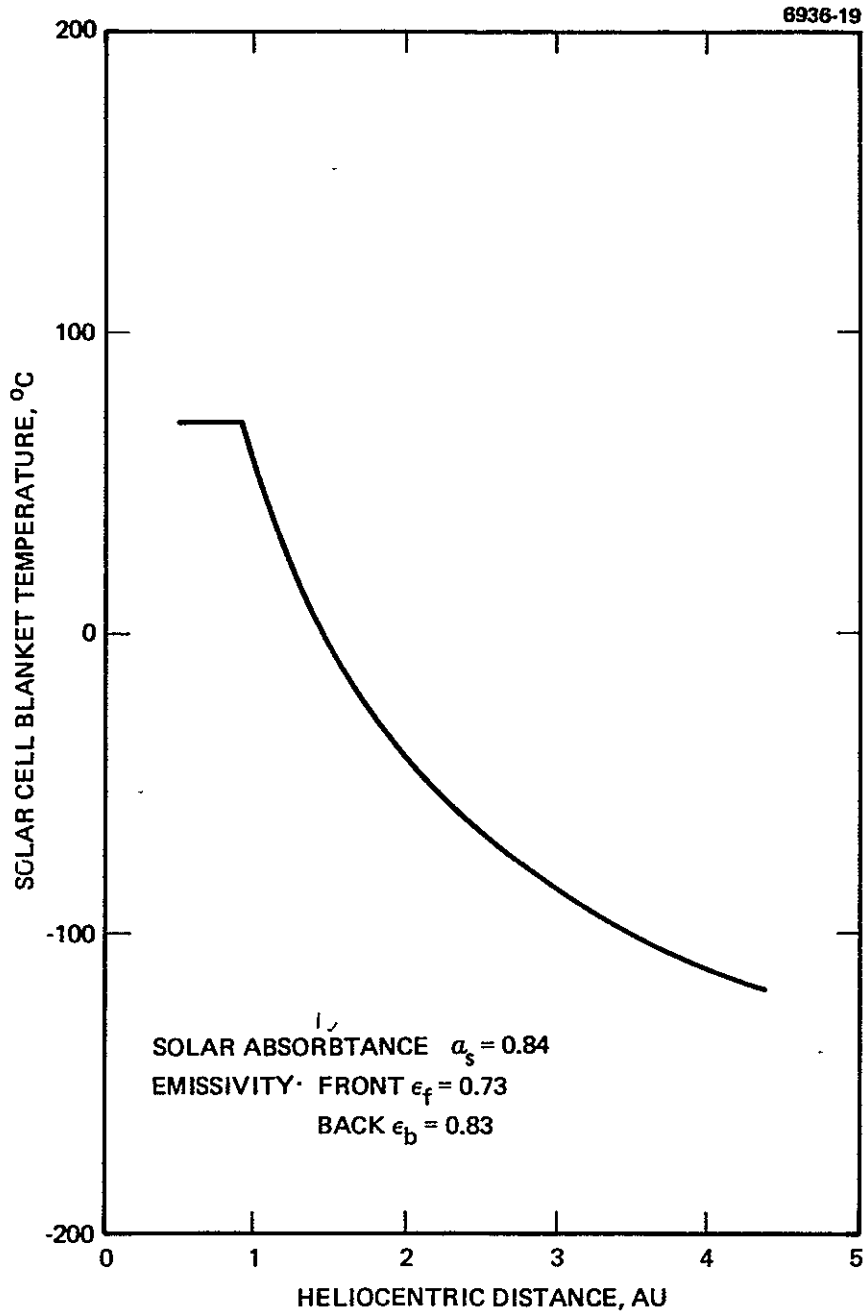
Figure 5. Thermal characteristics of the flat solar array.

The concentrator array was an 85-kW array with a 3:1 concentration ratio; its power profile is shown in Figure 6. Corresponding voltage and current profiles not shown here were also furnished. The deployed and stowed configurations are shown in Figure 7. The 3:1 concentration at distances greater than 1.4 AU is provided by the side reflectors deployed at a 60° angle, as shown in Figure 7(a). Inside 1.4 AU, the reflectors are coplanar with the cell blanket. The deployed length of each wing is 60 m. Thermal characteristics are given in Figure 8.

The separation distance X for the flat array in the deployed configuration shown in Figure 7(a) was ultimately determined by the requirement that Hg ion contamination be prevented. A value of X = 2.25 m was used in preparing layouts.

This concentrator solar array design, which was used for comparing the seven configurations, was not the same as the design of the array subsequently furnished by NASA LeRC for the analysis of the selected baseline (the latter design is discussed in Volume II, Section 2.A). Concentrator array configurations 2B and 2B/I and the comparative assessment of all seven configurations are, therefore, based on the earlier design. Although the solar array design selected was changed, the results of our comparative analysis are still considered valid because the modifications only make the concentrator array more desirable for the baseline. These modifications improved thrust system performance, in particular by reducing the size of the stowed array.

The characteristics that the IUS was assumed to have are those given in Ref. 1 and 2 and subsequently updated by Ref. 3. The key specifications were the envelope dimensions, mechanical interface requirements, structural loads, and payload capability. IUS length ranges from about 5.4 m (17.8 ft) in Ref. 1* for the standard two-stage configuration to 8.4 m (27.5 ft) for the three-stage planetary configuration. A maximum length of 8.4 m was therefore postulated. The structural

---

*Subsequently updated in Ref. 3 to 5.0 m.

17
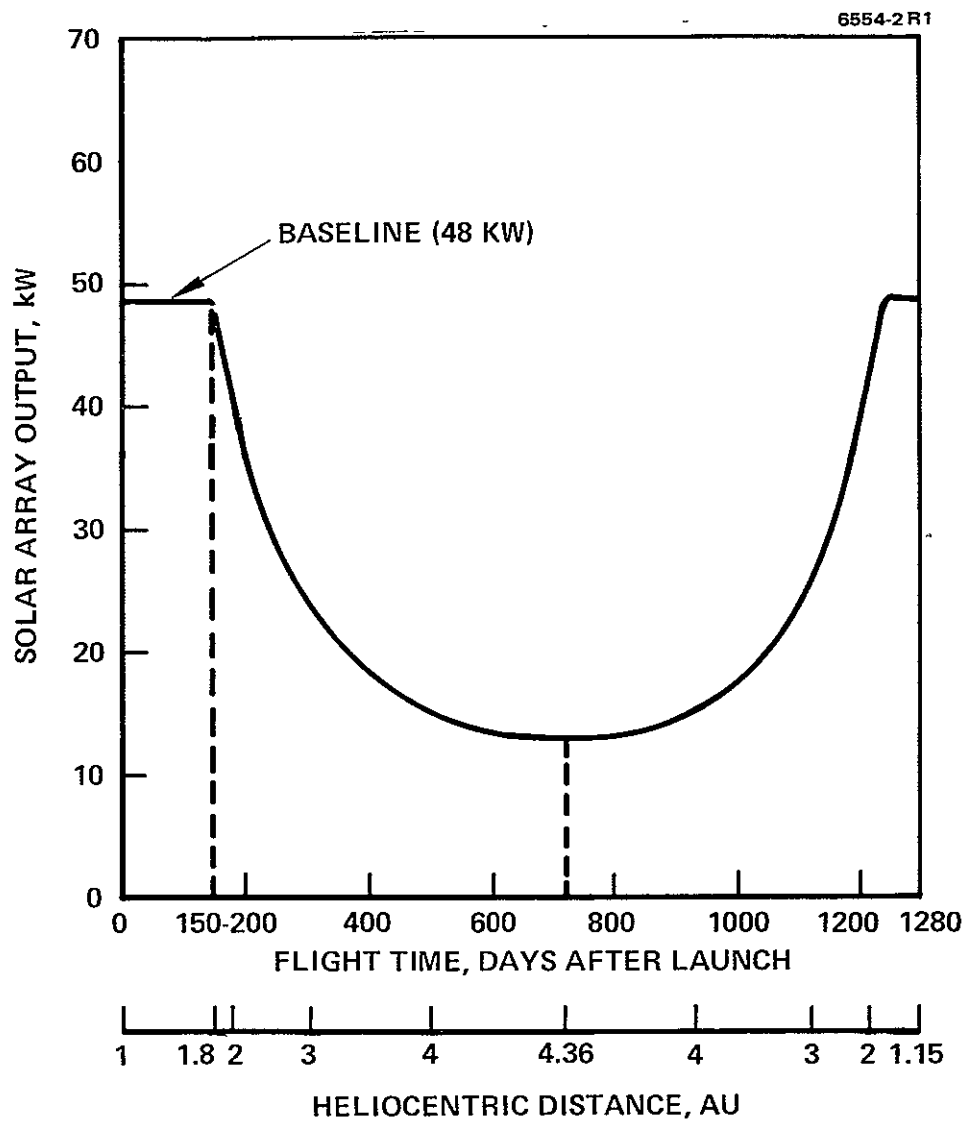
Figure 6. Concentrator solar array power profile.

6936-18

REFLECTOR

~60

~24

CANISTER

08 DIA

X

θ

THRUST SYSTEM

REFLECTOR

~ 12M

37

60°

4M

08

4M

4

4

NOTE   NOT TO SCALE, ALL DIMENSIONS IN METERS,
DIMENSION X TO BE DETERMINED

(a) DEPLOYED

6936-17

REFLECTOR
CONTAINER

SOLAR ARRAY
CONTAINER

1 25

1 0

1 0

4 0

08 DIA

4 42

2 85

NOTE   ALL DIMENSIONS IN METERS

(b) STOWED
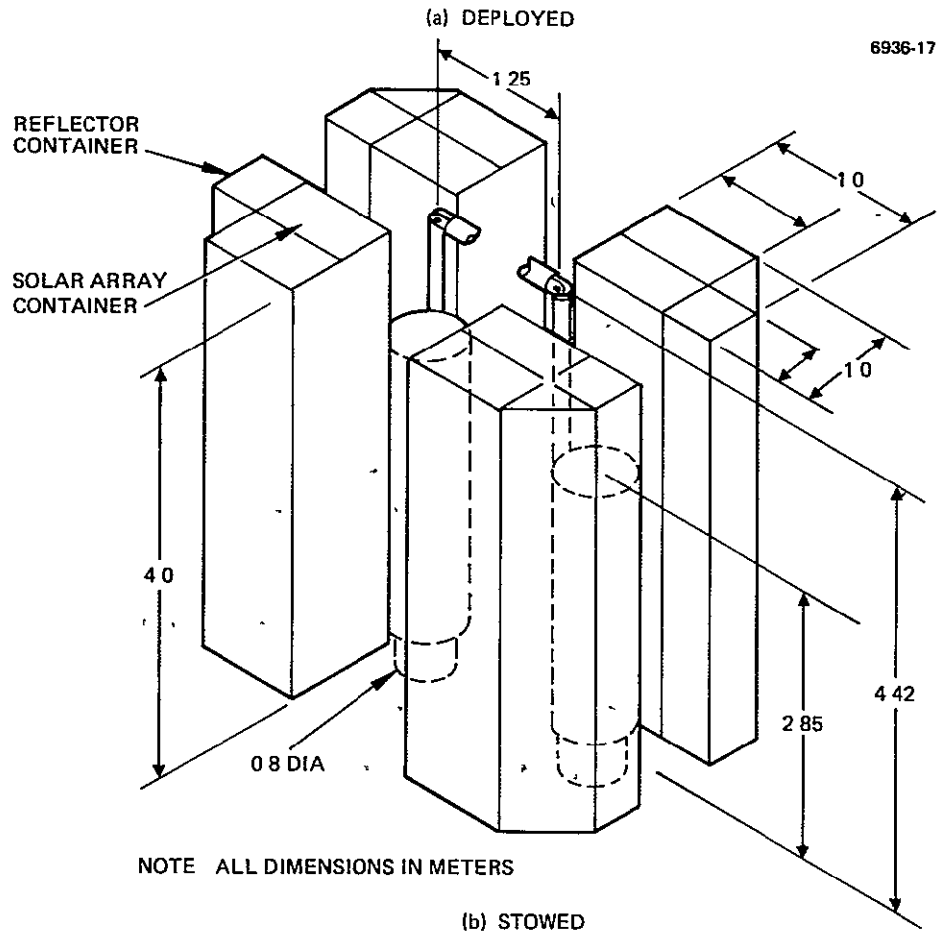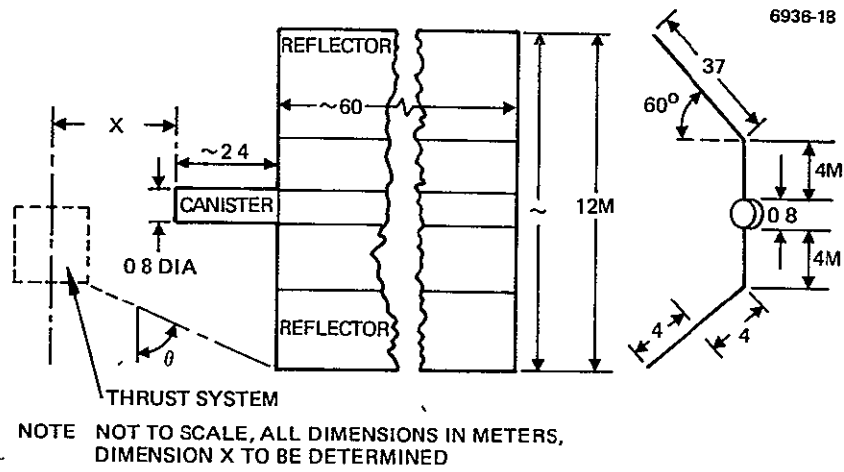
Figure 7.   Concentrator solar array configuration.

19

6936-16
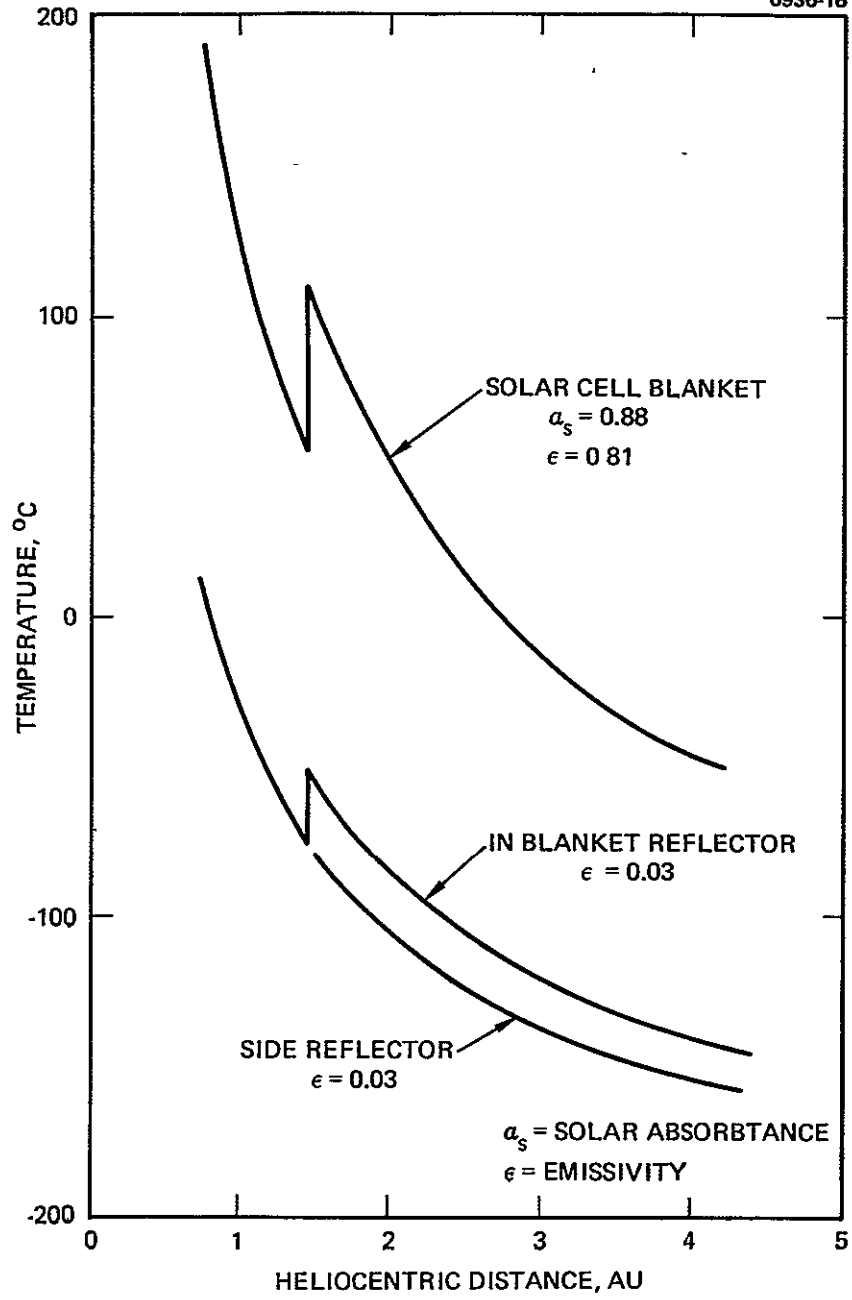
Figure 8.   Concentrator solar array thermal
characteristics.

interface was defined in terms of the standard bolt circle given in Ref. 1 and 2, although it would be acceptable to provide transverse extension fittings if the diameter of the configuration were to exceed the bolt circle diameter as a result of the size of the stowed array. IUS loads governed the structural design requirements. Results of the loads analysis (presented in Volume II, Section 2.D, and not repeated here) were therefore used in designing each of the seven configurations. IUS payload capability could not be readily determined. Furthermore, the allowable mass for the complete spacecraft does not depend only on the IUS payload capability; it also depends on the mission trajectory ultimately selected through system-level analysis. The allowable mass for the thrust system depends, in turn, on the mass allocated to the solar array and to the mission module. Consequently, IUS payload capability was not considered to be an imposed constraint. Instead, the design goals established were to minimize thrust system mass for each configuration.

The shuttle characteristics assumed are those given in Ref. 4. As discussed in Volume II, Section 2.D, compliance with shuttle load requirements was assumed to be met by providing a "forward cradle" support structure that will remain in the shuttle after the payload is deployed.

The PMaC design data developed during this study are presented in Section 3. The conventional PMaC design data was based on inputs from NASA LeRC (from the initialization study). Direct-drive PMaC design data (for use of both conventional and direct-drive discharge supplies) and the CDVM design data was generated during the thrust system configuration design study.

The design characteristics of the remaining thrust system elements are the same for all seven configurations (except for the number of thrusters). These were described in Volume II.

The data base for the design of the seven configurations also included the following ground rules and assumptions (established with NASA LeRC concurrence):

- There is no requirement to jettison any thrust system elements.

- There will be no direct sunlight incident on thermal radiation surfaces (i.e., spacecraft orientation throughout the mission will keep the planes of the thermal radiators always parallel to the line to the sun).

- The spacecraft attitude control sensing and command functions will be performed by the mission module; commands will be executed by gimballing the thrusters within their gimbal angle range capability, stipulated as $\pm 5°$ along the solar array centerline and $\pm 30°$ about the solar array centerline.

- The solar array drive is part of the thrust system and executes the commands generated by the mission module to orient the deployed array (initial solar array deployment is a function that is mechanized by actuators that are part of the solar array subsystem*).

- The distinction between "modular" and "integrated" designs is based on different approaches to the arrangement of subsystems and to structural and thermal design. The electrical unit designs are the same for both approaches. The modular design approach assures thermal and structural module similarity for assembly and test, and allows changing the number of thrusters (in multiples of two) used in the configuration with only relatively minor design modifications.

---

*The relative complexity of deployment is, however, considered in the comparative evaluation of the seven configurations in Section 5.

22

● Potential impingement of mercury ions on the solar array from the thruster ion beam plumes could result in substantial power degradation if not prevented. Impingement will be prevented by several available design measures (e.g., by providing adequate separation distance between the thrust system and solar array) and therefore need not be considered as constraining the physical design of the thrust systems nor as a significant factor in the comparative assessment of the resulting configurations. ·

The last ground rule was adopted following an analysis of the distribution of the Hg ions in the ion beam plume, which indicated that impingement effects were negligible outside of a 45° cone about the thrust axis (50° cone allowing for 5° gimbal angle along the array centerline). This geometry can be achieved relatively easily by providing an adequately long solar array arm for all configurations to ensure the required separation between the array and the thrusters without imposing any design constraints on the length of the thrust system or on the location of thrusters. The Hg ion impingement geometry is illustrated in Figure 9, which was constructed for the conventional PMaC, concentrator solar array configuration (2B).

23

REFLECTOR ATTITUDE	*θ	REF. POINT
CLOSED 60°	29 8°	B
OPENED (COPLANAR WITH ARRAY)	26.0°	C

*θ = IMPINGEMENT ANGLE
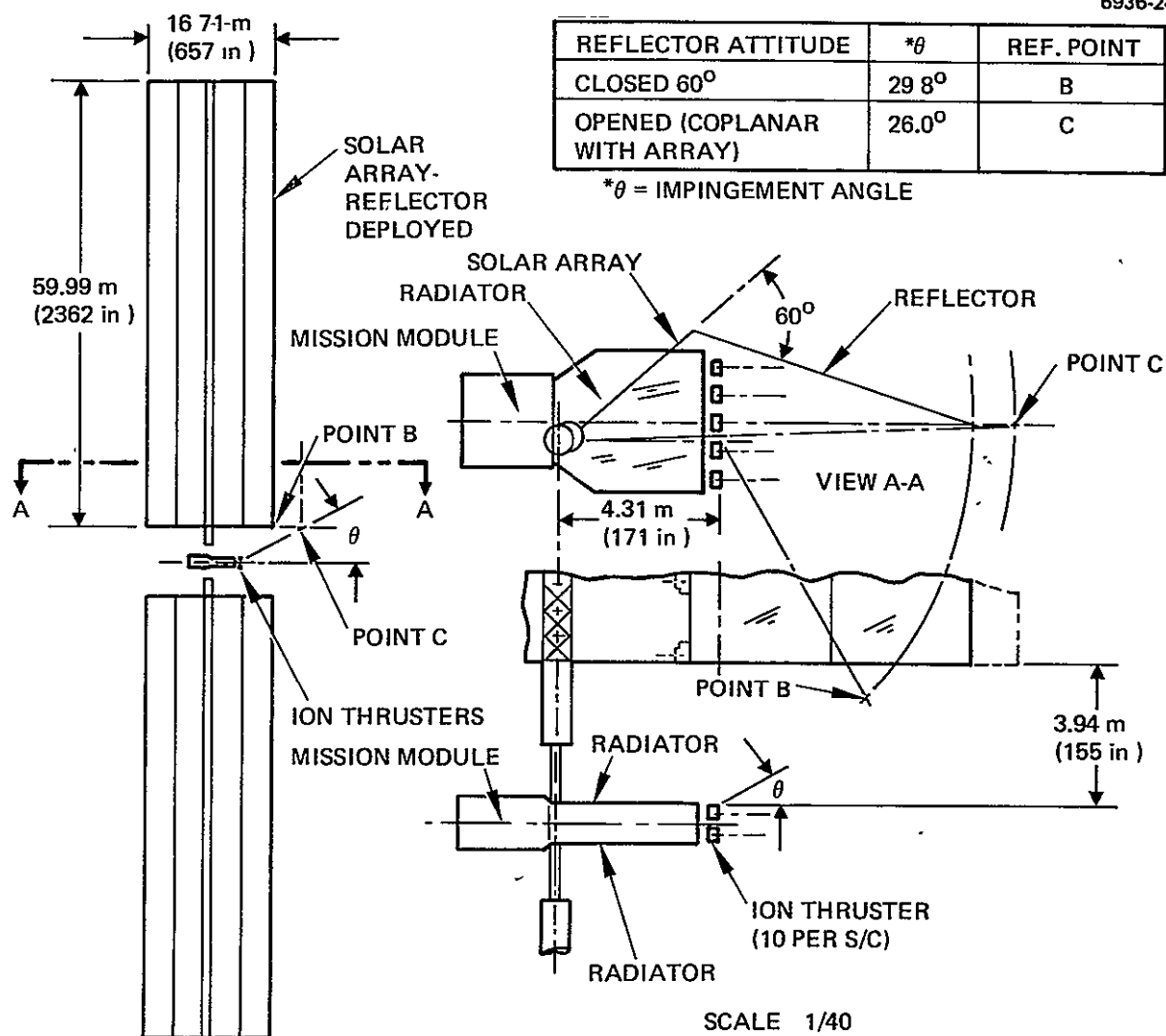
Figure 9. Hg impingement angle geometry for configuration 2B (for solar array — thrust system separation).

SECTION 3

ALTERNATE PMaC SUBSYSTEM DESIGNS

This section presents the design characteristics of the four PMaC
subsystems, thereby completing the data base for the conceptual design
definition of the seven configurations. The conventional PMaC design
approach was ultimately chosen for the baseline configuration. It is
fully described in Volume II, Section 2.C. The three other PMaC design
concepts (the direct drive approach with either a conventional or direct
drive discharge supply, and the CDVM beam supply concept with conventional
discharge supply) developed during the study phase differ from the con-
ventional PMaC approach in the design of the beam supply and the source/
load reconfiguration unit of the interface module. This reconfiguration
unit performs the functions of electrical control of the solar array out-
put and of controlled power distribution, as required in each approach.
The design features of the three alternate PMaC concepts are presented
here primarily in terms of these two units, using as the baseline refer-
ence the conventional PMaC design. Based on the design analysis, this
section summarizes the characteristics of all four PMaC design concepts
in terms of size, mass, power dissipation (efficiency), and reliability.

A.   DESIGN DEFINITION

The PMaC subsystem serves to process, condition, and manage the power
furnished by the solar array: (1) to provide the voltages and currents
required for the operation of the thrusters, (2) to furnish power for the
thrust system housekeeping and control functions, and (3) to provide the
required mission module power. Preliminary analysis (later done in
greater depth for the selected baseline) led to the partitioning of these
functions among PMaC components according to their application in either
the thrust modules or the interface module. This partitioning was iden-
tical for all four PMaC concepts. The thrust module units comprise
beam, discharge, and low-voltage power supplies for the operation of
individual thrusters. Control functions common to all thrust modules are

incorporated in the interface module components. The interface module units perform power control, distribution, and conversion functions, and include a thrust system controller.

1. Functional Requirements

The PMaC subsystem designs were developed to comply with the following data inputs and functional design requirements:

- Compliance with the electrical requirements of the thrusters and with the thrust system housekeeping and mission module power requirements.

- Compliance with the two solar array designs and with the specified design characteristics (reconfiguration concepts) for each array as applicable to the various PMaC concepts.

- Compliance with several design guidelines and ground rules furnished by NASA LeRC or generated during the study.

The thruster, housekeeping, and mission-module electrical requirements stipulated by NASA LeRC are listed in Tables 3 and 4. The system battery, provided in the mission module, furnishes power before the solar array is deployed, including power for thrust-system housekeeping, firing the release squibs, and deploying the solar array.

The original functional requirements furnished by NASA LeRC after the initialization study as a study guideline are represented by the block diagram in Figure 10. In particular, the designs of the conventional beam and discharge supplies were essentially those specified by NASA LeRC, and were to be capable of operating over a 200 to 400 V range of solar array output.

Other design requirements adopted, which were essentially common to all four PMaC concepts, included: provision of adequate filtering and electromagnetic interference (EMI) protection, implementation of controller functions, and compliance with certain additional general ground rules. The last two are discussed below.

26

Table 3. Thruster Power Requirements

| Supply Number | Supply | Maximum Ratings[b] | | | Static Load Regulations Type and Percent | Static Load Ripple, Percent, P-P |
		Voltage, V	Current, A	Power, W		
1	Main vaporizer	9	1.5	13.5	I ± 5	10[c]
2	Cathode vaporizer	6	1.5	9	I ± 10	10[c]
3	Cathode heater	15	4 4	66	I ± 5	10[c]
4	Main isolator and cathode isolator	9	4 0	36	V ± 10	10[c]
5	Neutralizer heater	15	4.4	66	I ± 5	10[c]
6	Neutralizer vaporizer	6	1 5	9	I ± 10	10[c]
7	Neutralizer keeper[a]	25 [20]	2.5 [2.1]	62.5	I ± 5	2
8	Cathode keeper[a]	15 [5]	1.0 [0 5]	15	I ± 10	10
9	Discharge	60	16 3	815	I ± 1	2
10	Accelerator	500	0 02	10	V ± 10	10
11	Screen	3000	2 0	6000	V ± 10	10
12	Magnetic baffle	2	5 0	10	I ± 5	5

[a]Boost supply· 400 V at 10 mA, 25 V at 100 mA.

[b]Maximum rating is defined as that voltage and current level that each supply can deliver continuously to the thruster Where two V/I characteristics are indicated, a condition during startup is shown and the norminal condition is bracketed

[c]Applies only to ac heaters

5918

Table 4. PMaC Housekeeping and Mission Module Power Requirements

Power Source	Voltage Requirements, V	Power Requirements, W
Mission module	+30 ± 2	400 (during thrusting phase)
		650 (during rendezvous)
PMaC system housekeeping[a]	+30 ± 2	75
	±15	140 (max)
	±5	10 (max)

[a]During thrusting phase.

5903

27
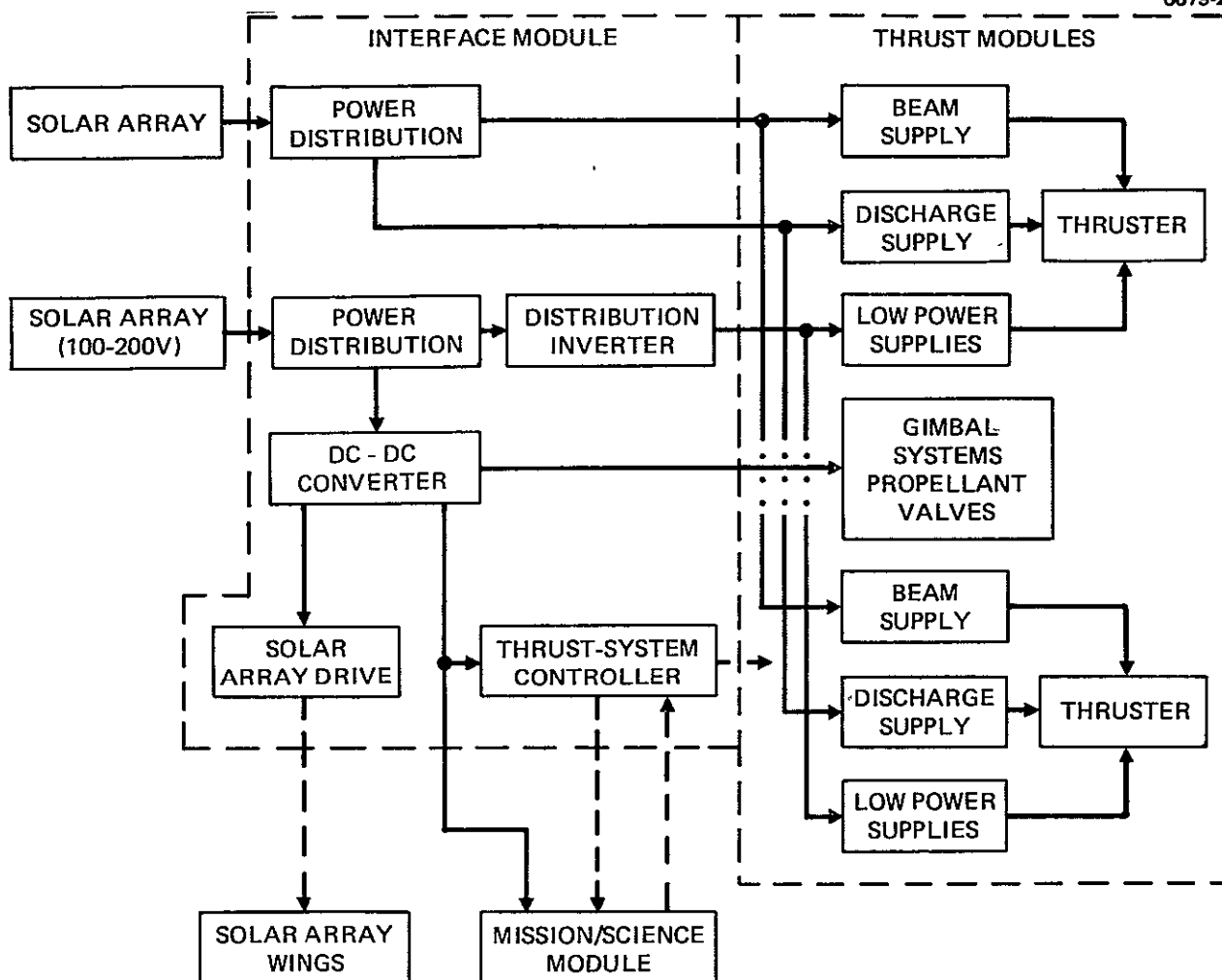
Figure 10.   Conventional PMaC block diagram
furnished by NASA LeRC.

28

The logic to perform the thruster control functions and other thrust system management functions was placed centrally in a controller (one of the PMaC interface module units). The controller was to be capable of ensuring autonomous thruster operation for an extended period of time. Its functions include: sensing the operating parameters of power supplies, analysis of PMaC system and thruster operation, generation and execution of control signals, data exchange with the ground via the mission module.

The following additional general design requirements and ground rules were adopted:

- Common (single) bus for power distribution

- Thruster ground isolated from spacecraft ground

- Capability of withstanding transient or sustained shorts by all thruster power supplies

- Provision of thruster grid clearing circuit

- Input/output power bus fault protection for all inverters

- Operation of thrusters not influenced by malfunction of single thruster/PMaC subsystem

- Provision of redundancy for critical units

- PMaC mounting surface temperature range from -30°C to +60°C.*

---

*Later changed to 50°C for the selected baseline.

2. Description of Alternate Designs

The PMaC designs are described in this section to provide a common framework for discussing the four concepts and for defining the specific design features which distinguish them. The description also establishes a convenient format for defining the PMaC design and performance characteristics that are required to design and assess the seven thrust system configurations.

The PMaC subsystem is basically an interface between the solar array and the power consuming components of the spacecraft: thrusters, mission module, and housekeeping units. These requirements are identical for all four PMaC concepts. Thruster requirements and operational modes are similar. The PMaC subsystem must provide the required voltages and currents because the solar array output power level and the operating point on its current-voltage (I-V) curve vary over the mission trajectory and with the number of operating thrusters. The differences among the various PMaC design concepts relate to the different methods and design techniques employed to utilize the solar array output, particularly with respect to the provision of thruster beam and discharge powers. The different design approaches are also reflected in different PMaC subsystem design features (size, thermal characteristics) and performance characteristics (mass, efficiency, reliability).

Figure 11, a simplified schematic of thruster operation, shows the basic current paths and gives the principal thruster power requirements: high voltage beam (screen and accelerator) supply and discharge supply. The four PMaC concepts differ in the way in which these requirements are implemented in terms of: (1) design features of these two power supplies, and (2) the method in which they are connected to the solar array. The other thruster requirements (i.e., the various low-voltage power supplies) are identically satisfied by the PMaC subsystem in all four design concepts. Also, the PMaC units which furnish power to the mission module and which power and manage the housekeeping functions are identical in all four designs.

A generalized block diagram for all four PMaC concepts is presented in Figure 12, which shows the units and functions common to all four

30
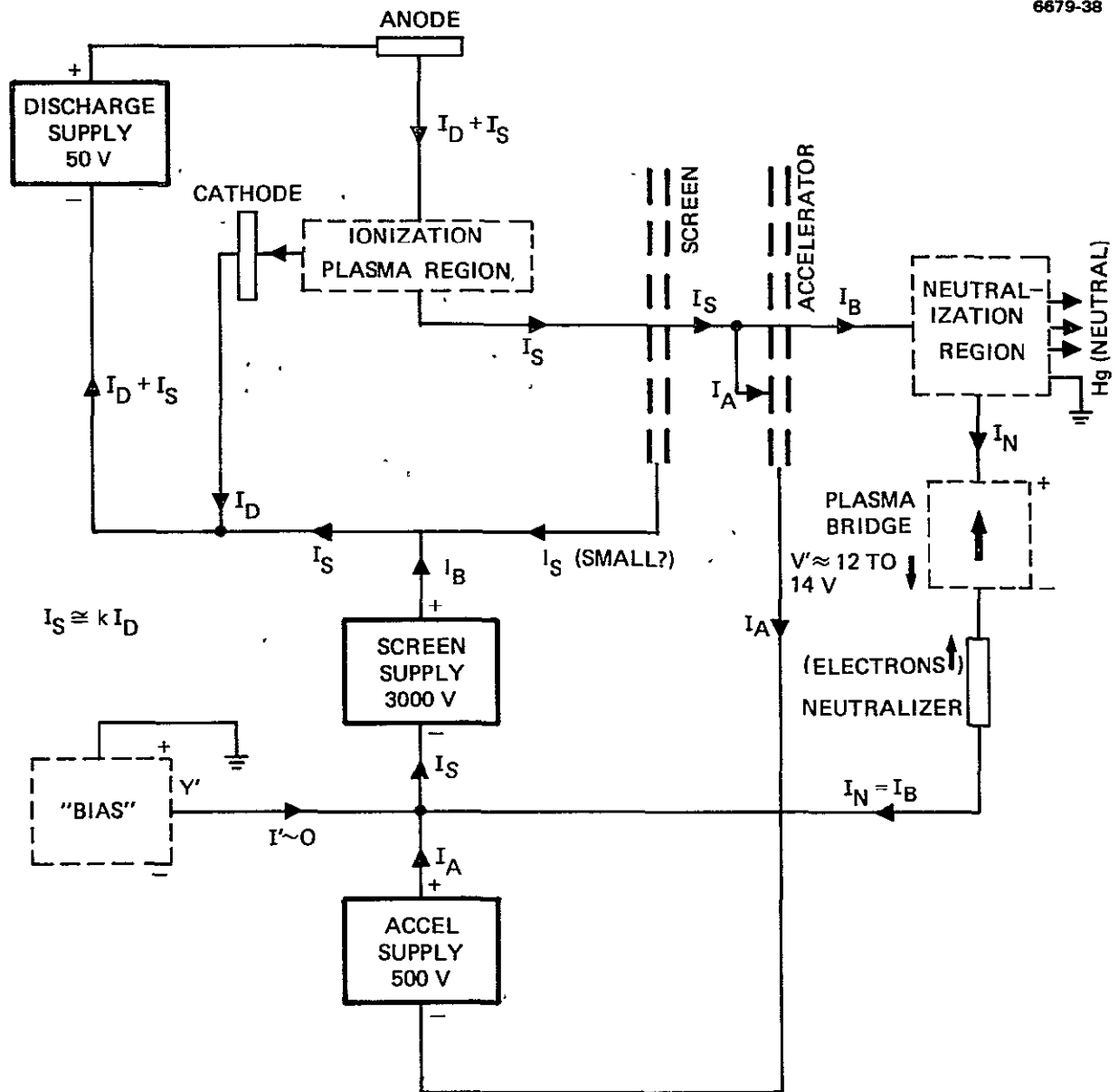
Figure 11. Basic current paths.
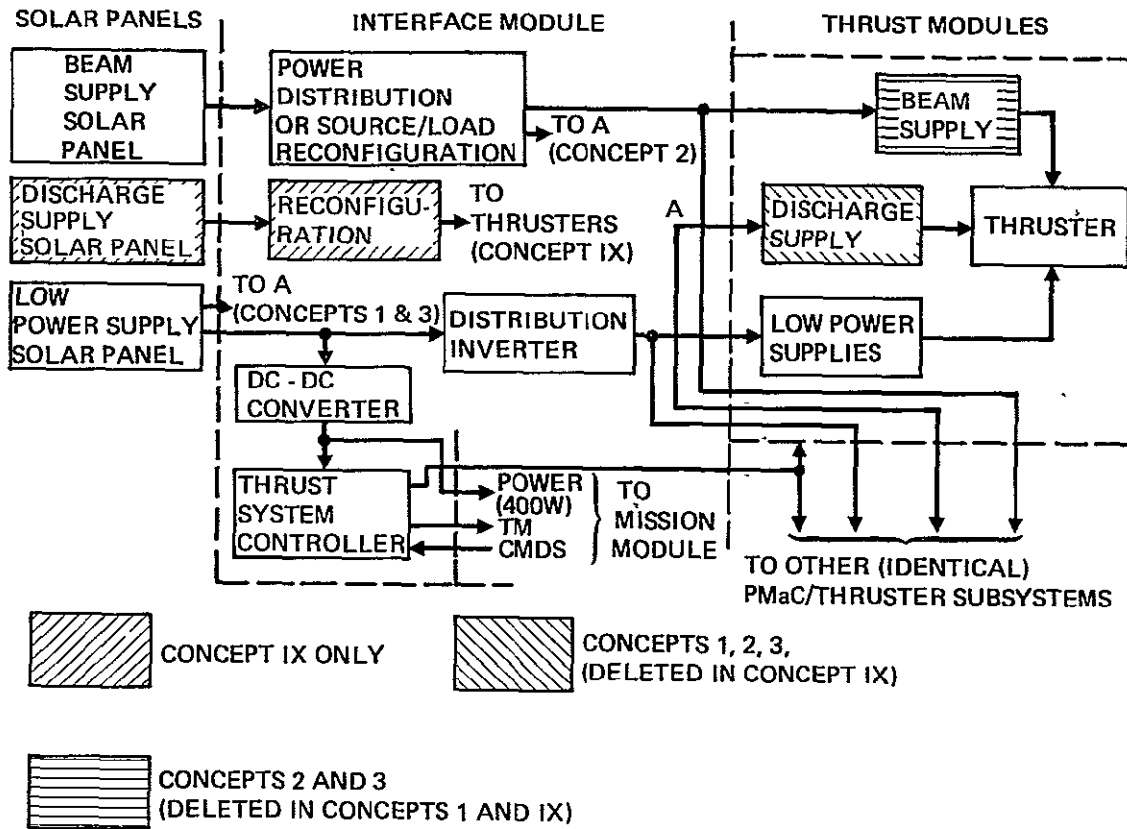
SOLAR PANELS	INTERFACE MODULE	THRUST MODULES

Figure 12. Block diagram of the generalized PMaC subsystem.

concepts. The figure also indicates the differences between the four concepts. Units and functions common to all four concepts were described for the baseline configuration in Volume II, Section 2.C. Units and functions that are different for the four concepts are presented in some detail in the succeeding subsections. Specifically, the differences among the four designs pertain to:

- The design of the beam supply and the method of furnishing thruster discharge power

- The functional requirements and the design of the source/ load reconfiguration unit connecting the main solar array to the beam supply.

The conventional PMaC approach, concept 2, uses beam and discharge supplies of conventional design. Both supplies are fed from the main solar panel and furnish power to the thrusters at a constant voltage level, provided that the input to the supplies is within a 2:1 (200 to 400 V) range. This is accomplished because they have a built-in regulation capability. The solar array is configured so that its output delivers power at the corresponding low-voltage level. The reconfiguration unit (or units) on the interface module basically performs the filtering/isolation function;* power distribution is automatic. The power distribution filters are packaged in five separate units to distribute the total mass more evenly. Design modularity is enhanced by mounting the units on the interface module side of the cold plate (one per module).

Discharge current to each thruster is required to track the beam current. Since the two supplies are adjustable, the controller simply compares the two currents and sends appropriate commands to maintain them in the proper ratio.

---

*Solar array control unit is included in the baseline system to provide for variations in the output voltage of the selected solar array that are anticipated to exceed the allowable 2:1 range during the mission.

PMaC concept 3 uses a CDVM beam supply. The solar array output is furnished at a low voltage (200 to 400 V), and voltage multiplication is achieved without transformers to obtain a high-voltage output. This affords significant potential payoffs in reducing mass, increasing reliability, and increasing efficiency although a development program is required. Present specifications call for the CDVM beam supply to be unregulated, although some regulation is provided at the input so that the beam voltage supplied to the thrusters varies only over a 1.75:1 range during the mission. Much better regulation could be achieved with some mass penalty. The resulting thruster operational parameters accordingly would be sowewhat different from those for the conventional system, but this would not significantly alter thruster performance.[*]

The reconfiguration unit for the CDVM PMaC concept in Figure 12 is, however, considerably more complex than for the conventional system. In addition to the power distribution and isolation functions,[**] a switching matrix is required to reconfigure the solar array output because each CDVM has an individual neutralizer return for each thruster. The solar array must be partitioned so as to create separate sections for each CDVM. The reconfiguration unit is fed by a series of separate inputs, one for each thruster. The switching matrix connects these inputs to the individual CDVMs to provide the required isolation. As the number of operational thrusters changes, this switching matrix can reconfigure the available power from the various sections of the solar array to utilize the full solar array capability optimally. Many reconfigurations

---

[*]The conventional system could also have been designed with no regulation provision in the beam and discharge supplies, with some mass saving; existing designs, however, already incorporated this regulation feature.

[**]The CDVM beam supply designs incorporate input filtering.

are required during the mission not only for this thruster on-off control, but also to respond to changing power levels and I-V characteristics, which change with time during the mission and with thruster throttling requirements. The switching matrix and reconfiguration frequency required will depend on the number of sections. More reconfigurations would require reducing the variation in thruster operating modes. The NASA LeRC initialization study yielded the solar array partitioning concept that was used in designing the switching matrix.

The CDVM PMaC subsystem uses a conventional discharge supply. Since such a supply does not require a switching matrix, system simplicity is achieved by powering the discharge supplies from a common auxiliary solar panel rather than from the main solar panel (see Figure 12). Control of the discharge current in proportion to the beam current is accomplished by the controller in the same manner as for the conventional system.

PMaC concept 1 (direct drive with conventional discharge supply) uses the conventional discharge power supply, but has the main solar array interconnected so as to provide the high-voltage beam power directly to the thrusters. Separate beam supplies are not required. The solar panel is divided into sections individually connected to the reconfiguration unit. The reconfiguration unit performs the switching functions needed to connect these sections in the series/parallel combinations to fulfill thruster requirements. This reconfiguration unit is more complex than the one used with the CDVM. It does offer potentially significant benefits in reduced PMaC system complexity, lower mass, and improved reliability, although it requires developing the yet unproven technology high-voltage solar arrays and solving any associated problems. Discharge supplies are fed from the common auxiliary solar panel (as with the CDVM concept) and discharge current tracking of the beam current is also done by the controller.

PMaC concept 1X (direct drive with direct-drive discharge supply) is similar to concept 1, except that conventional discharge supplies are not used. Instead, part of the main solar array provides the discharge power directly. This is done (see Figure 12) by adding an extra reconfiguration

unit to couple the discharge supply solar panel section to the discharge circuits of the individual thrusters. This function is performed at the required high potential relative to spacecraft ground. With the exceptions that the input and output voltages are lower (30 to 60 V range) and that the power level is considerably less, the reconfiguration/switching/ isolation functions of this unit are similar to those for the direct-drive beam supply reconfiguration unit. Beam-discharge current tracking cannot be done by the controller: currents and voltages at the thruster input are determined directly by the solar array output. Since circuit parameters cannot be adjusted, simultaneous reconfiguration of both beam and discharge circuits is required. This automatically maintains the fixed proportionality between the beam and discharge currents. This concept offers potential improvements relative to concept 1 (direct drive with conventional discharge supply) in terms of simplicity, mass, and reliability, but for the penalty of a higher technical risk.

The four concepts are compared in Table 5 in terms of the type and number of units required. The number of units listed reflects the assumptions regarding the number of thrusters required for each concept (defined in Table 2): 12 for the direct drive concepts and 10 for the conventional and CDVM concepts. In addition, one spare is provided for better reliability for the following units: distribution inverter, dc-dc converter, and controller.

B. CONVENTIONAL PMaC DESIGN CONCEPT

The conventional PMaC design concept selected for the baseline thrust system configuration is essentially that presented in Volume II, Section 2.C, with the following principal differences:

- The selected baseline PMaC system includes a solar array reconfiguration unit that was not included in this initial tradeoff study.

- The mass of the beam supply was increased from 14.3 kg to 20 kg for the selected baseline (as specified by NASA LeRC).

36

Table 5. Type and Number of Units Required
for the Four PMaC Designs

Unit	Number of Units for Design Concept[a]			
	1	1X	2	3
Source load reconfiguration (direct drive)	2	2		
Source load reconfiguration (CDVM)				2
Source load reconfiguration (direct-drive discharge)		2		
Power distribution			5	
Distribution inverter[b]	3	3	3	3
DC-DC converter[b]	2	2	2	2
Controller[b]	2	2	2	2
Conventional beam supply			10	
CDVM beam supply				10
Discharge supply	12		10	10
Low power supplies	12	12	10	10

[a] 1 = Direct drive beam supply
1X = Direct drive beam and discharge supplies
2 = Conventional
3 = Voltage multiplier

[b] One spare unit added for reliability.

T5916

37

- The length and width of the beam and discharge supplies (with total volume unchanged) and the length of the low-voltage power supply unit were modified for the selected baseline. This was done so all units would be in the NASA Z-frame modular package and fit within the available mounting surface area.

The design features of the conventional PMaC concept are taken directly from Volume II in the following discussion.

C. DIRECT-DRIVE PMaC DESIGN CONCEPTS

The two direct-drive PMaC concepts differ from the conventional approach primarily with respect to the functions of the reconfiguration units. Neither the direct drive discharge supply nor the conventional discharge supply approaches include a beam supply unit. One function of the reconfiguration unit in both concepts is to transfom the solar array output to provide the beam power to all the thrusters. In addition, concept 1X requires solar array power reconfiguration/switching to provide the discharge power to the thrusters.

Since the reconfiguration units for PMaC concept 3 and for PMaC concepts 1 and 1X are similar, these units are described jointly and those differences which do exist are highlighted.

Table 6 summarizes the basic requirements for the three reconfiguration units. Electrical differences result from differences in input voltages, accessory circuits (filters, inductors, and grid clearing circuits) switching logic, number of sections switched, and switch drivers. The number of reconfigurations (essentially the same for each unit) govern the overall unit designs. Since half of the thrusters are powered by each solar array wing, the reconfiguration function can be divided between two identical units to optimize mass distribution, with each unit handling the switching requirements for one wing. The corresponding physical configurations vary only slightly among the three PMaC concepts.

The direct drive reconfiguration unit must handle voltages ranging from 2000 to 4000 Vdc at 2.5 A. The direct drive discharge reconfiguration unit switches a voltage of 30 to 60 Vdc at 16.3 A, and is referenced to the beam voltage. The discharge reconfiguration unit must

Table 6. Design Requirements and Characteristics of the
Reconfiguration Units for PMaC Concepts 1, 1X, and 3

Requirement or Characteristic	Direct Drive	Direct-Drive Discharge	CDVM Beam
Functional mechanization			
High-voltage relays	Yes	Yes	Yes
Relay redundancy	Yes	Yes	Yes
Hybrid relay driver	Yes	Yes	Yes
Relay driver redundancy	Yes	Yes	Yes
Line filter	Yes	No	No
Line inductor	No	Yes	No
Fault protection with a grid clearing circuit	Yes	No	No
Baseline parameters			
Input voltage, V	2000-4000	30-60[a]	200-400
Number of outputs	12	12	10
Power dissipation, W	34	34	17
Size, in.^{3}	3600	3600	3000
Weight, kg	44.8	32.8	20.6
Reliability	0.998	0.998	0.999

[a]Referenced to 2000 to 4000 V array panel.

T5916

reconfigure the solar panel at the same time the beam panel is recon-
figured and switching circuitry will be identical to that of concept 1.
The CDVM reconfiguration unit must carry currents as high as 30 A at a
voltage of 400 V. The number of solar panel segments and the frequency
of reconfiguration are lower than for the other units.

The maximum excursion of the solar array output voltage was assumed
in the initial tradeoff study to be 2:1. For the selected baseline, the
design was subsequently changed to include an additional solar array
control/reconfiguration function that would allow increasing this ratio.

High-voltage relays and hybrid switching logic were selected for
all three designs. Figure 13 is a block diagram of a typical reconfigura-
tion unit. Serial commands are received from the controller and decoded
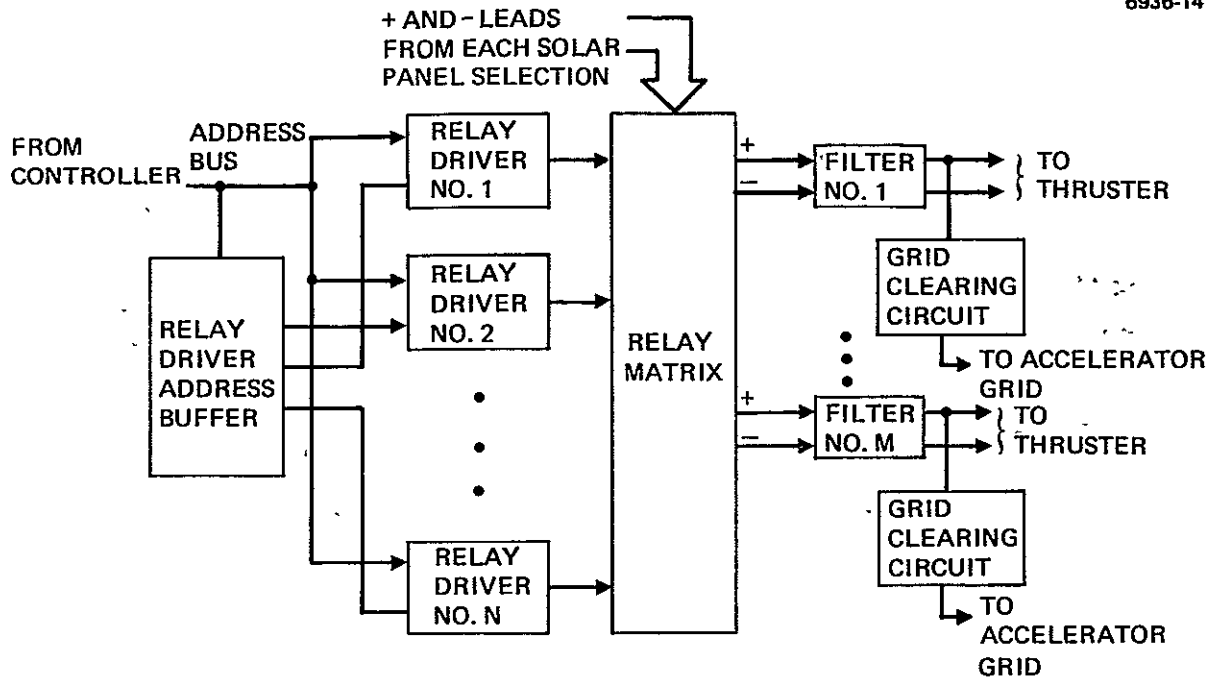
Figure 13.   Block diagram of a typical source/load reconfiguration unit.

in the relay driver address buffer. The appropriate hybrid relay driver and high-voltage relay are then commanded to switch. A relay matrix performs the series/parallel connections of the solar panel segments to operating thrusters. Input power isolation is maintained by dedicating solar panel segments to a particular thruster. The positive and negative power terminals of each operating thruster are electrically isolated from adjacent operating thrusters. This prevents possible interaction during a thruster malfunction. To reduce EMI effects during normal arcing or during a malfunction, line filters were added to two of the units, but not to the CDVM unit.* A grid-clearing circuit was also included in all three approaches.

Figure 14 is a schematic of the concept 1 unit for one wing and six thrusters; two such units are required per spacecraft. To improve reliability, three redundant single-pole single-throw relays are used for each relay shown. The required switch position for each reconfiguration is shown in Table 7. Relay position A in Table 7 corresponds to the position of the relays shown in Figure 14. The small figure below Table 7 shows the thruster positions with respect to the center of gravity. The thrusters are arranged to operate in pairs on the opposite sides of the center of gravity (e.g., 1 and 2, 3 and 4).

A simplified representation of the five switching configurations encountered during the mission is shown in Figure 15 for the direct drive reconfiguration unit. With the exception of Configuration A (in which all thrusters are operating), each configuration has at least one standby thruster to cope with faults that cannot be cleared.

Figures 14 and 15 and Table 7 are assumed to also apply to the direct-drive discharge.reconfiguration unit.**

---

*The CDVM beam supply incorporates these filters.

**The data furnished by NASA LeRC for direct drive is also assumed to apply to the direct-drive discharge panel.
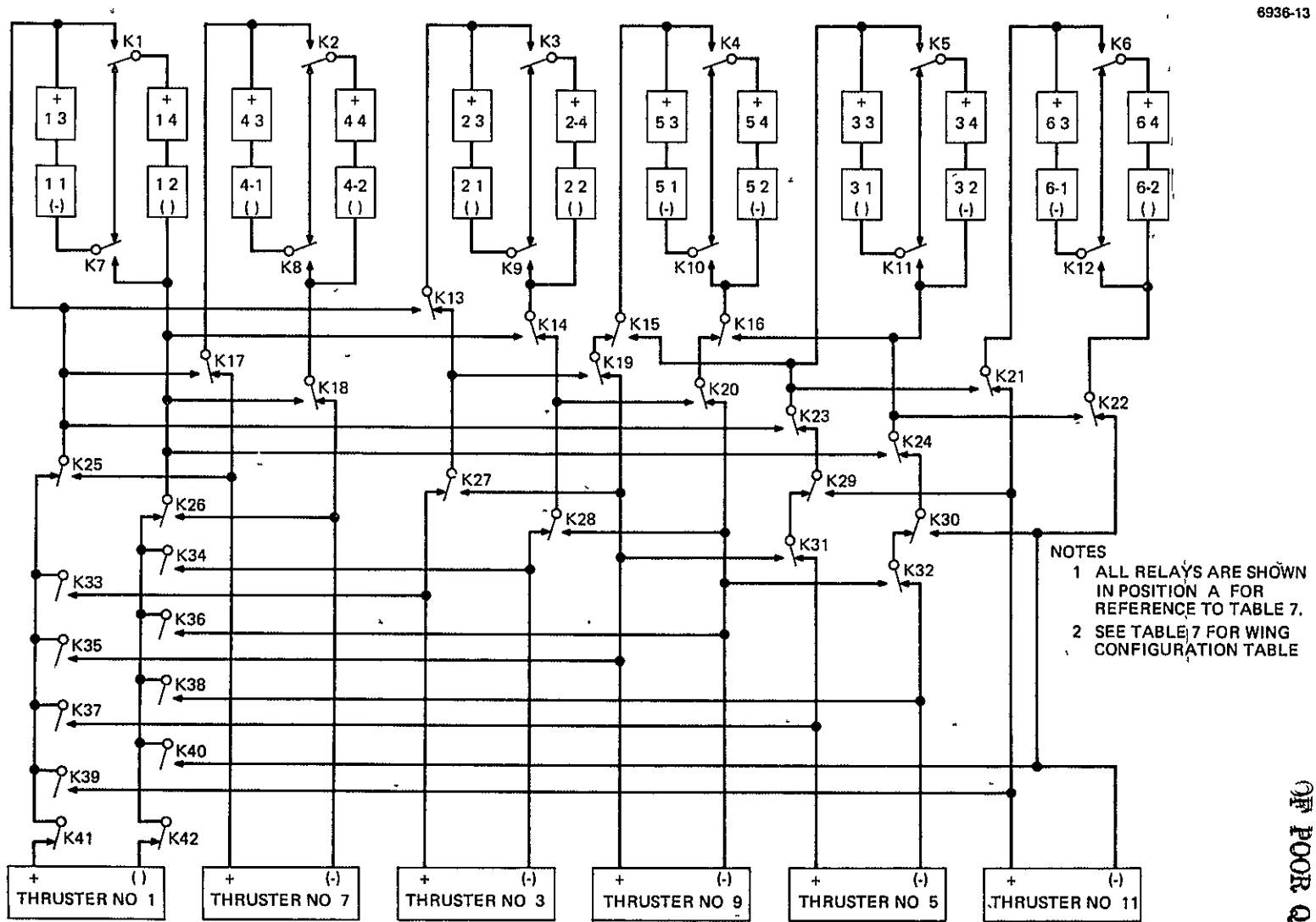
Figure 14.   Schematic of the one wing of direct drive reconfiguration unit.

42

Table-7. Switching Diagram, Direct Drive Reconfiguration Unit

SHADED AREA INDICATES THRUSTER ON

Thruster/Relay switching diagram with top scale markings: 1 6 AU, 2 2 AU, 2 6 AU, 3 4 AU, 3 2 AU, 2 9 AU, 2 7 AU, 2 4 AU, 1 8 AU.

Wing Configuration columns: B1, C, D1, D2, D3, E1, E2, E3, E4, E5, E6, O3, D2, C, B2, A

(Upper portion — Thruster No. 1 through 12 — shaded cells indicate thruster ON, per configuration.)

Relay No	B1 A	B1 B	C A	C B	D1 A	D1 B	D2 A	D2 B	D3 A	D3 B	E1 A	E1 B	E2 A	E2 B	E3 A	E3 B	E4 A	E4 B	E5 A	E5 B	E6 A	E6 B	O3 A	O3 B	D2 A	D2 B	C A	C B	B2 A	B2 B	A A	A B
1	X		X			X		X		X		X		X		X	y			y		X		X		X		X	X	X		X
2	X		X			X		X		X		X		X	y		X			X		X		X		X	X	X	X	X		X
3	X		X			X		X		X		X		X	X		X			X		X		X	X	X	X	X		X
4	X		X					X		X		y		X		X		X	X			X		X		X	X	X		X
5	X		X			X		X		X		X	y		X		X			X		X		X	X	X	X	X		X
6	X		X			X		X		X		X		X		X		X	X			X		X	X	X	X	X		X
7	X		X			X		X		X		X	y			X		X		y		X		X	X	X		X
8	X		X			X		X		X		X		X	y		X			X		X		X	X	X	X	X
9	X		X			X		X		X		X		X	y		X			X		X		X	X	X	X	X
10	X		X			X		X		X		X	y		X		X			X		X	X	X	X	X		X
11	X		X			X		X		X		X		X		X		X			X		X	X	X	X	X		X
12	X		X			X		X		y		X		X	y		X			X		X	X	X	X	X
13	X		X	X			X	X			X		X		X	y			X		X	X		X		X
14	X		X	X			X	X		X		X		y		X		X	X		X	X		X		X
15	X		X		X			X		X			X		X		X			X	X	X		X		X
16	X		X		X			X		X		X	X			X		X		X		X	X	X		X
17	X			X	X		X			X		X		X	X		X			X		X	X	X		X
18	X		X	X		X			X		X		X	y			X		X		y		X		X		X
19	X		X	X		X		X		X		X		X		X	X			X		X		X		X
20	X		X	X		X		X		X		X		X		X	X		X		X		X		X	
21	X		X	X			X		X	y		X		X		X	X		X		X	X		X		X
22	X		X	X			X		X	X		X		X		X	X		X		X	X		X		X
23	X		X		X		X		X			X	X		X	X		X	X		X		X		X		X
24	X		X		X		X		X			X	X		X		X		X	X		X		X		X
25	X		X			X		X		X	X		X		X	X		X		X		X		X	X	X
26	X		X			X		X	X		X			X	X		X		X		X		X		X	X	X
27	X			X	X		X		X		X		X		X		X		X		X		X		X	X	X
28	X		X		X		X		X		X		X		X		X		X		X		X		X	X	X
29	X		X		X		X			X	X		X		X		X	y		X		X	X		X		X	X	X
30	X		X		X		X			X	X		X		X		X		X		X	X		X		X	X	X
31	X		X		X			X	X		X		X	X		X		X		X		X		X		X
32	X		X		X			X	X		X		X		X		X		X		X		X		X		X
33	X		X		X			X	X		X		X		X		X	X		X		X	X		X		X
34	X		X		X		X		X		X		X		X		X	X		X		X	X		X		X
35	X		X	X		X		X		X		X		X	X		X		X		X		X		X		X
36	X		X		X		X		X		X			X	X		X		X		X		X		X		X
37	X		X		X		X		X		X		X		X	X		X		X		X	X		X		X
38	X		X		X		X		X		X		X		X	X		X		X		X		X		X
39	X		X		X		X		X		X		X		X		X	X		X		X		X		X
40	X		X		X		X		X		X		X		X		X	X		X		X		X		X
41	X		X		X		X		X	X		X		X		X	X		X	X		X		X		X
42	X		X		X			X	X		X		X		X		X		X	X		X		X		X

Relay Position (A / B for each Wing Configuration)

WING NO 1

| 1 | 5 | 9 | 8 | 4 | — THRUSTERS |
| 3 | 7 | 10 | 6 | 2 | |

WING NO 2

43

6936-8
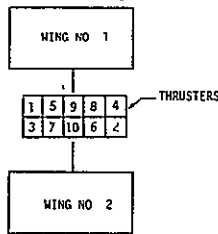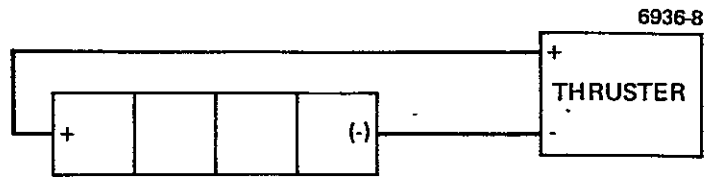
(a) CONFIGURATION A (12 SUCH CONFIGURATIONS
COMPRISE THE FULL SYSTEM)

6936-9
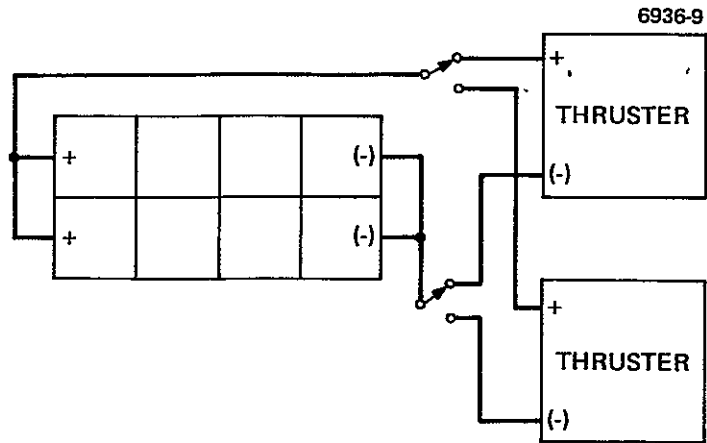
(b) CONFIGURATION B (6 SUCH CONFIGURATIONS
COMPRISE THE FULL SYSTEM)
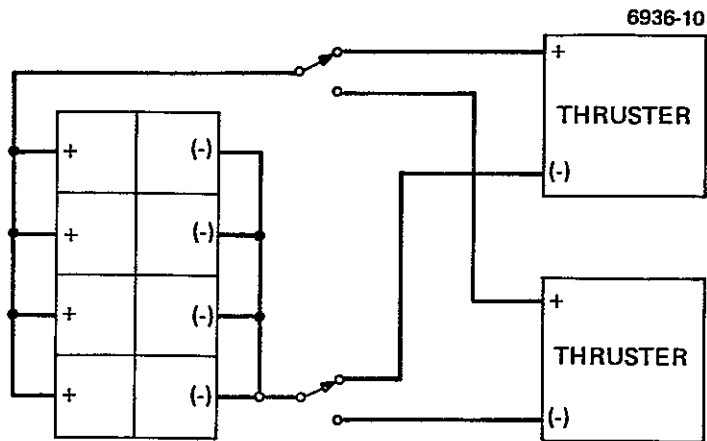
6936-10

(c) CONFIGURATION C (6 SUCH CONFIGURATIONS
COMPRISE THE FULL SYSTEM)

Figure 15. Switching configurations for direct-drive
reconfiguration unit.

44
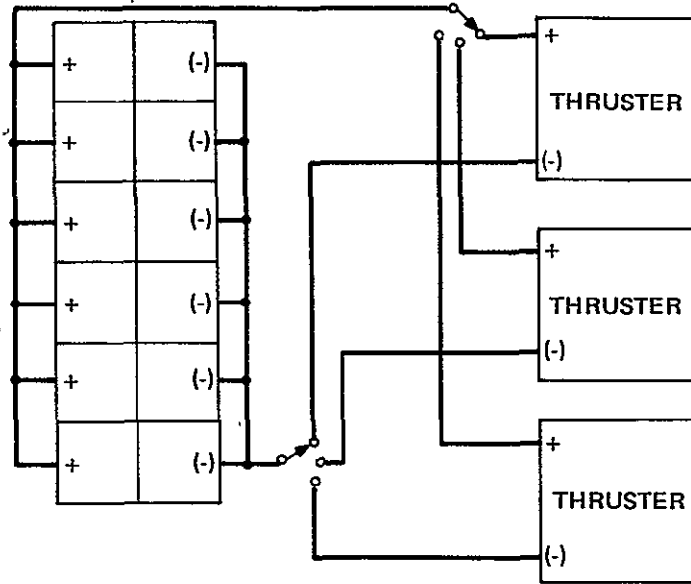
6936-11

(d) CONFIGURATION D (4 SUCH CONFIGURATIONS COMPRISE THE FULL SYSTEM)

6936-12

(e) CONFIGURATION E (PER WING, 2 SUCH CONFIGURATIONS COMPRISE THE FULL SYSTEM)

Figure 15. Continued.

45

Corresponding diagrams for the CDVM reconfiguration units are shown in Figure 16 and 17 and Table 8. This unit differs from the direct-drive unit in that only four reconfigurations are required for the 10 thrusters (versus five reconfigurations required for 12 thrusters). The switching diagram in Table 8 indicates that all 10 thrusters would be operational at the beginning and end of the mission; a minimum of two thrusters would be operating midway through the mission. The corresponding four switching configurations are shown in Figure 17, which indicates how the solar array segments are connected through the power-processing units to the thrusters. Configuration A (and partially in configuration B) does not allow other thruster/PMaC units to be selected in case of a malfunction. The switching hardware could be simplified by requiring fewer spares during the low-power phase of the mission.

This preliminary design effort sized the reconfiguration units. The physical dimensions and design characteristics, common to all three units, are shown in Figure 18. The unit consists of an aluminum honeycomb panel, components mounted on this panel, and two aluminum covers. The honeycomb panel minimizes vibration and provides an adequate thermal path to the mounting surface.

All high-voltage circuitry, filters, and grid-clearing circuits are mounted on one side of the panel. The low-voltage circuitry, including relay driver logic, is located on the other side of the panel. The relays (SPST Kilovac KC-4, latching) are rated at 10 kV. There are 18 high-voltage connectors: 1 per thruster and 1 per wing segment. The connectors are Reynolds Industries series 1804 (four pin). A seven-pin version of this connector has previously been used on the power electronics unit for our 8-cm ion thruster. All wiring is redundant, and precautions must be taken to minimize high-voltage arcing. The 12 solar panels used in the direct-drive solar array are switched redundantly with 126 relays (252 relays for both wings). The 10 solar panels used in the CDVM reconfiguration unit are switched redundantly with 96 relays (192 relays for both wings).

Table 9 summarizes the major components used in the three units, their quantities, and the mass breakdown. Table 10 summarizes the
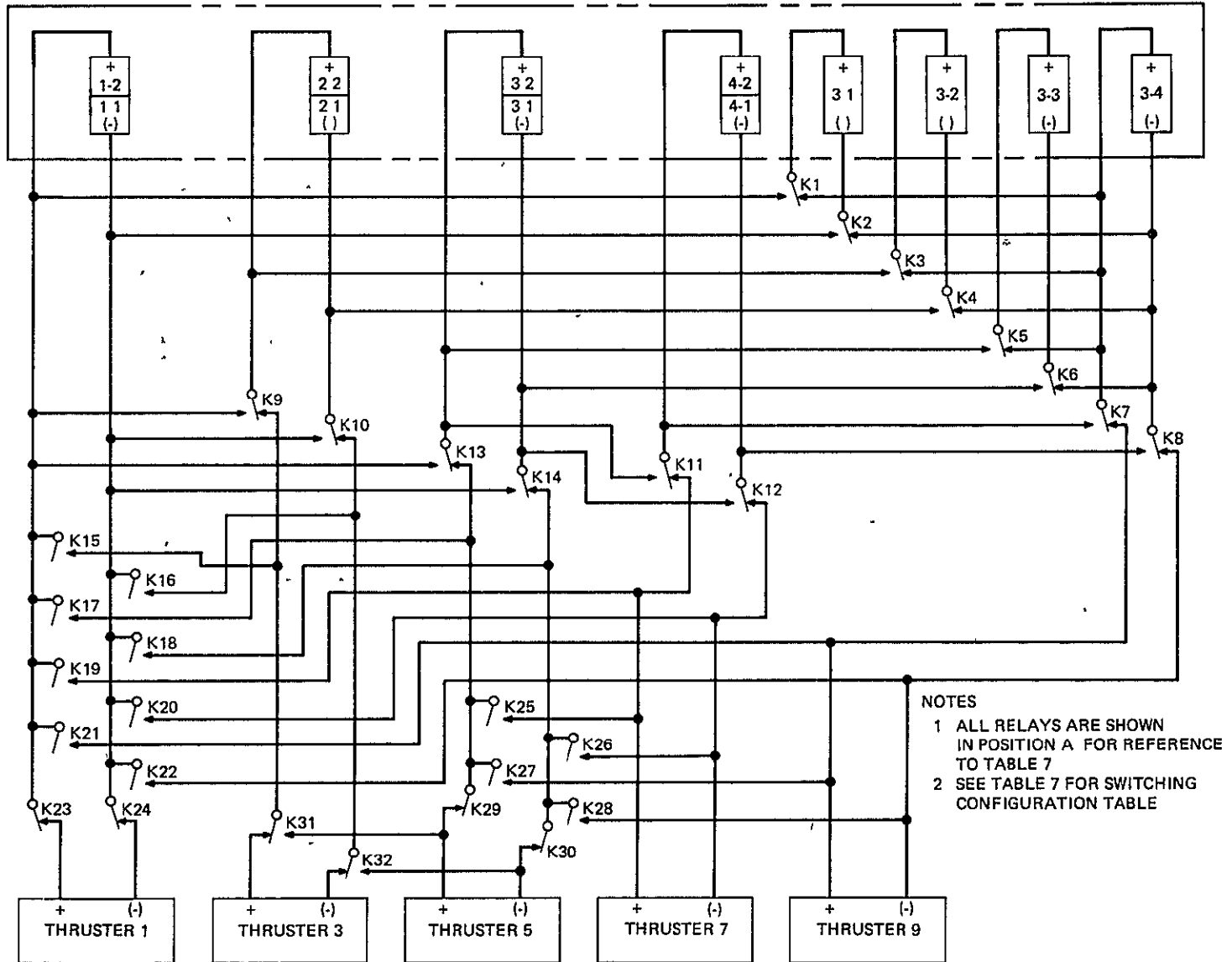
Figure 16.   Schematic of CDVM reconfiguration unit.

6936-5
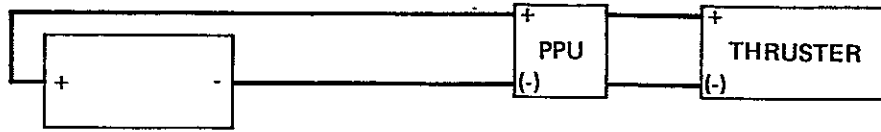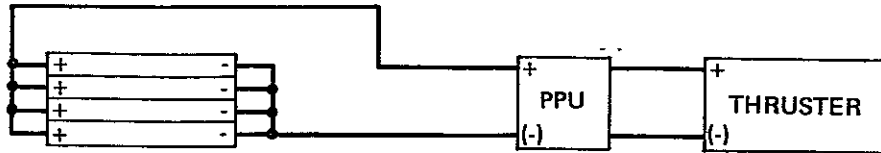
CONFIGURATION A1

CONFIGURATION A2

(a) CONFIGURATION A. (8 CONFIGURATIONS A1 AND 2 CONFIGURATIONS
A2 COMPRISE THE FULL SYSTEM)

6936-6
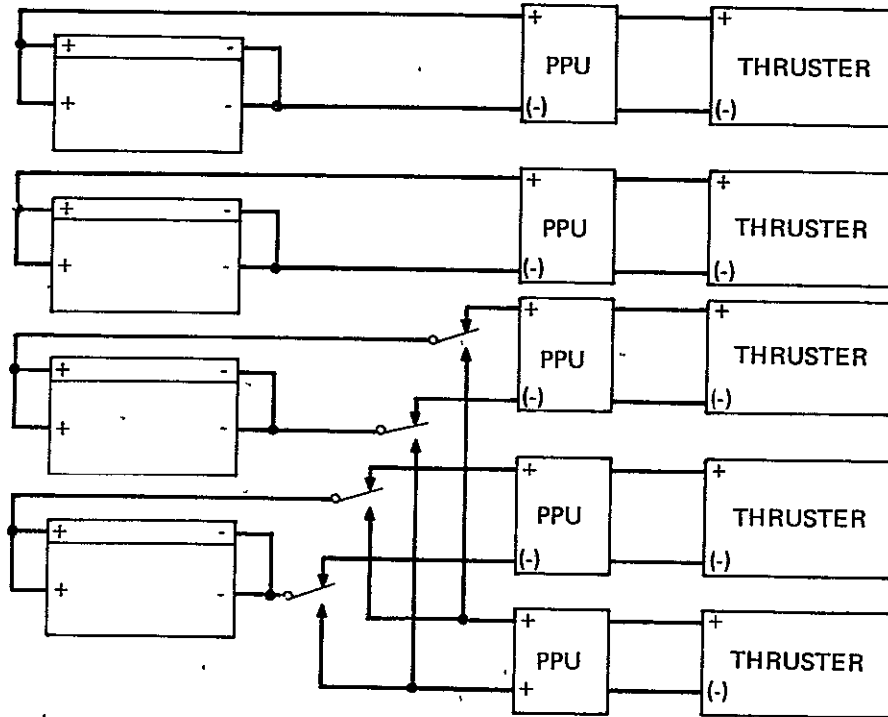
(b) CONFIGURATION B (PER WING, 2 SUCH CONFIGURATIONS
COMPRISE THE FULL SYSTEM)

Figure 17. Switching configurations for CDVM
reconfiguration unit.
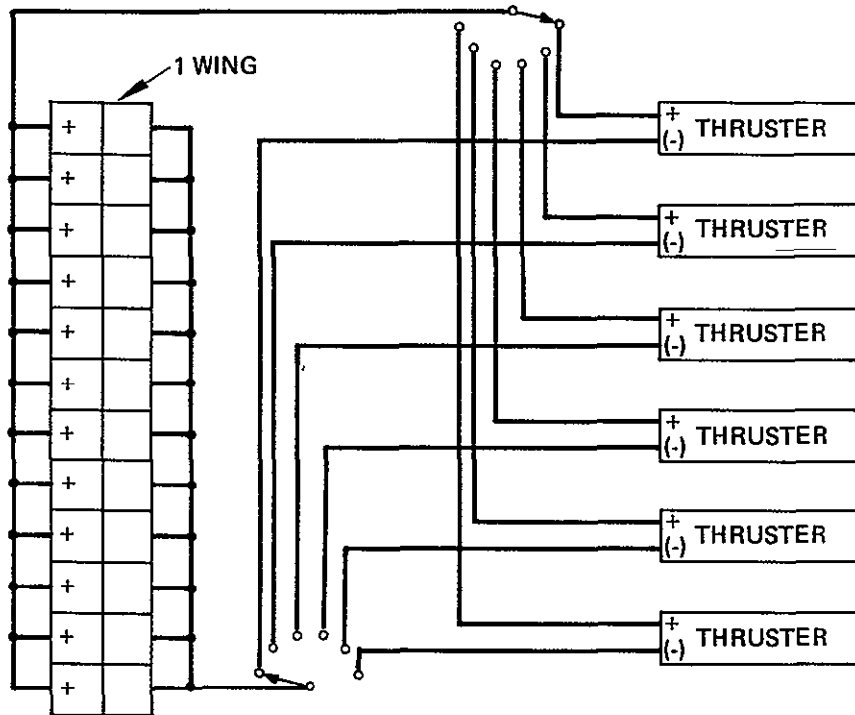
6936-3
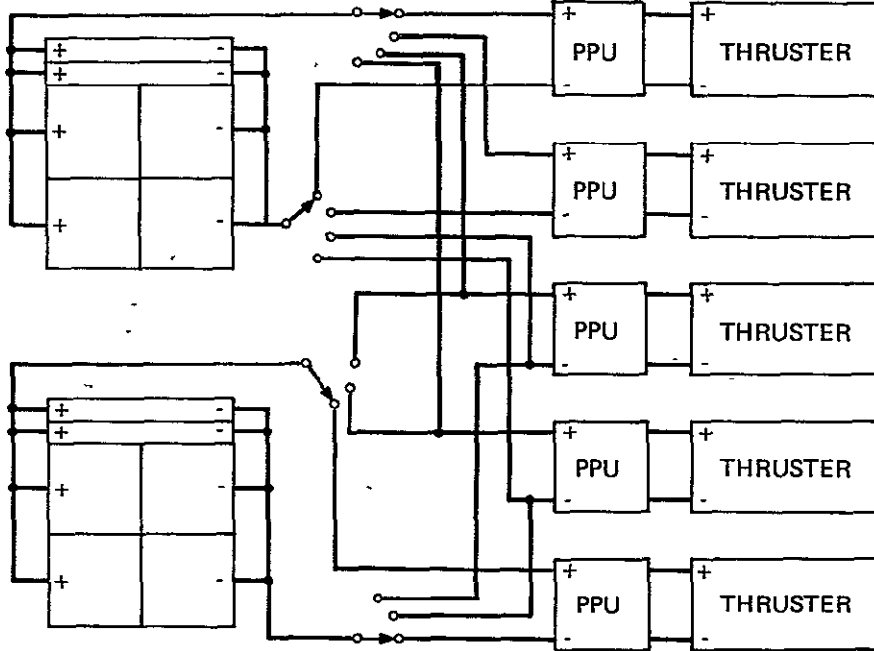
(c) CONFIGURATION C (PER WING; 2 SUCH CONFIGURATIONS
COMPRISE THE FULL SYSTEM)

6936-4
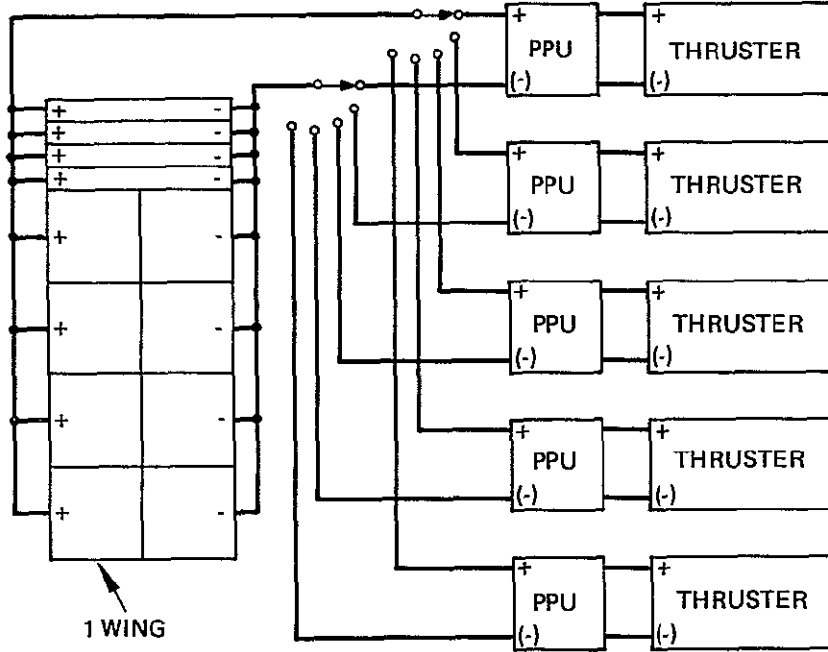
(d) CONFIGURATION D (PER WING, 2 SUCH CONFIGURATIONS
COMPRISE THE FULL SYSTEM)

Figure 17. Continued.

49

Table 8. Switching Diagram of. CDVM Reconfiguration Unit

SHADED AREA INDICATES THRUSTER ON

	1.36 AU		2.52 AU		3.7 AU			WING CONFIGURATION			3.7 AU		3.0 AU			1.2 AU	
Thruster No	A	B1	B2	C1	C2	D1	D2	D3	D4	D5	C3	C1	B2	B1	B3	A

Thruster rows 1–10 (shaded cells indicate thruster ON — see image).

RELAY POSITION

Relay No	A	B	A	B	A	B	A	B	A	B	A	B	A	B	A	B	A	B	A	B	A	B	A	B	A	B	A	B	A	B	A	B
1	X			X		X		X		X		X		X		X		X		X		X		X		X		X		X	X	X
2	X			X	X			X		X		X		X		X		X		X		X		X		X		X		X	X	X
3	X			X		X	X			X		X		X		X		X		X		X		X		X		X		X	X	X
4	X			X		X		X		X		X		X		X		X		X		X		X		X		X		X	X	X
5	X			X		X		X		X		X		X		X		X		X	X			X		X		X		X	X	X
6	X			X		X		X		X		X		X		X		X		X		X		X		X		X		X	X	X
7	X			X		X		X		X		X		X		X		X		X		X		X		X		X		X	X	X
8	X			X		X		X		X		X		X		X		X		X		X		X		X		X		X	X	X
9	X		X		X			X	X			X	X			X		X	X	X			X	X			X		X			X
10	X		X		X			X	X			X	X			X		X	X	X			X	X			X		X			X
11	X		X		X			X		X		X		X		X	X	X		X			X	X			X		X			X
12	X		X		X			X	X	X	X			X		X	X	X		X			X	X			X		X			X
13	X		X		X		X		X			X		X	X	X		X		X		X		X		X		X		X		X
14	X		X		X		X		X			X		X	X	X		X		X		X		X		X		X		X		X
15	X		X		X		X			X	X			X	X			X		X		X		X		X		X		X		X
16	X		X		X		X		X		X	X		X		X		X		X		X		X		X		X		X		X
17	X		X		X		X			X	X			X		X		X		X		X		X		X		X		X		X
18	X		X		X		X		X	X	X			X		X		X		X	X			X		X		X		X		X
19	X		X		X		X		X		X			X		X		X	X	X		X		X		X		X		X		X
20	X		X		X		X		X		X		X	X	X			X		X	X			X		X		X		X		X
21	X		X		X	X		X		X	X		X			X	X			X		X		X		X		X		X		X
22	X		X		X	X		X			X		X		X	X		X		X		X		X	X	X		X		X		X
23	X		X		X	X		X		X		X		X		X	X	X		X		X		X	X	X		X		X		X
24	X		X			X	X		X	X	X		X		X		X		X		X	X			X	X	X		X			X
25	X		X		X		X		X		X		X		X			X		X	X	X		X		X		X		X		X
26	X		X		X		X		X		X		X		X		X		X	X		X		X		X		X		X		X
27	X		X		X			X	X		X		X		X	X		X			X	X		X		X			X	X		X
28	X		X		X		X	X		X		X		X		X	X		X				X	X		X			X	X		X
29	X		X		X		X	X		X		X		X		X	X	X		X			X	X		X			X	X		X
30	X		X		X		X	X		X		X		X		X		X	X	X			X	X		X			X	X		X
31	X		X		X		X		X		X		X		X		X		X	X		X		X		X		X		X		X
32		X		X		X		X		X		X		X		X		X		X	X	X		X		X		X		X		X

WING NO 1

Thrusters: 1 5 9 8 4 / 3 7 10 6 2 — THRUSTERS

WING NO 2

ALUMINUM HONEYCOMB

HIGH-VOLTAGE CONNECTOR
TO WING
12 REQUIRED

45.7

10 2

LOW-VOLTAGE
SIDE OF RELAYS

RELAY DRIVER LOGIC

HIGH-VOLTAGE
SIDE OF RELAYS

63.5

MOUNTING SURFACE

LOW-VOLTAGE
CONNECTOR

GRID CLEARING FILTERS

HIGH-VOLTAGE
CONNECTOR
TO THRUSTER
6 REQUIRED

DIMENSIONS IN CM
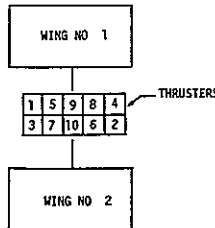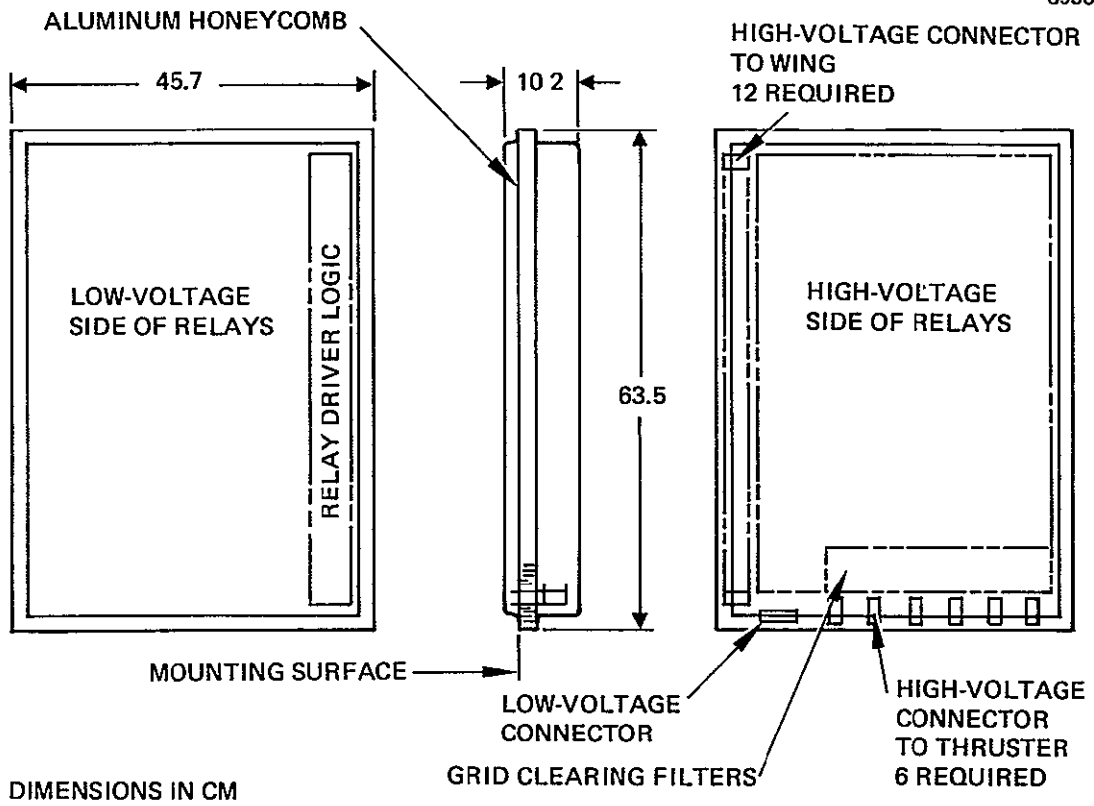
Figure 18.   Physical configuration of a typical reconfiguration
unit.

Table 9. Parts Count and Mass Breakdown of
Reconfiguration Units

Component	Direct Drive Concept 1		Direct Drive Concept 1X		Concept 3	
	Quantity	Mass, g	Quantity	Mass, g	Quantity	Mass, g
High voltage relays	126	7,150	126	7,150	96	5,448
Hybrid circuits	9	360	9	360	7	274
High voltage connectors	18	756	18	756	15	630
Low voltage connectors	1	25	1	25	1	25
Wire	--	500	--	500	--	380
Honeycomb, cm^2	3,064	1,294	3,064	1,294	2,451	1,035
Covers, cm^2	7,418	2,088	7,418	2,088	5,483	1,550
Hardware and miscellaneous	--	1,500	--	1,500	--	1,000
Grid-clearing circuits	6	6,000	0	0	0	0
Inductors	0	0	6	2,700	0	0
Filters	6	2,700	0	0	0	0
Total (single unit)		22,373		16,373		10,342

T5916

Table 10. Summary of Design Parameters of the
Reconfiguration Units
(two units per interface module)

	Direct Drive	Direct Drive Discharge	CDVM
Size, cm^3	29,500	29,500	24,700
Mass, kg	22 4	16.4	10.3
Pd, W	17	17	8.5
Reliability	0 999	0 999	0.999

T5916

52

principal design parameters of the three reconfiguration units (size, mass, power dissipation, and reliability).

D. CDVM PMaC DESIGN CONCEPT

The CDVM PMaC concept 3 design differs from the conventional PMaC design only with respect to the reconfiguration unit and the CDVM beam supply itself. This section summarizes the design features and performance parameters associated with the conceptual design developed during this study.

The output voltage from the CDVM, which is an unregulated supply, varies from 2000 to 4000 V as the input voltage supplied from the reconfiguration units varies from 200 to 400 V. There are 10 CDVM supplies in the five thrust modules (two per module).

Figure 19 is a block diagram of the CDVM. A 2.2-mHz astable multivibrator provides the fundamental timing signal to the 11-phase command generator. The generator outputs two signals to one drive stage for each phase. The power stage switches solar panel power to the capacitor-diode matrix through small aircore inductors. The peak capacitor-charging currents in the transistors and rectifiers are limited to obtain efficient capacitor charging and low component stresses. The primary function of the output filter (a π design) is to inductively limit peak currents in the capacitor-diode matrix during thruster arcing. Since each CDVM beam supply is driven by a dedicated solar array, screen current can be sensed by a resistor between neutralizer return and solar panel return. When an overcurrent is sensed, the protection circuit turns off all transistors in the power stage, thereby protecting the capacitor-diode matrix. Included in each CDVM supply is a grid-clearing circuit that is used in the same way as in the conventional beam supply system.

The principal design tradeoffs pertain to the choice between SCRs and transistors for the power stage and among various alternative circuit configurations (single versus multiple parallel, number of phases) for the driver and capacitor-diode matrix. SCRs and transistors are compared in Table 11. The four most attractive configurations — two using SCRs and two using transistors — are listed in Table 12. The preferred
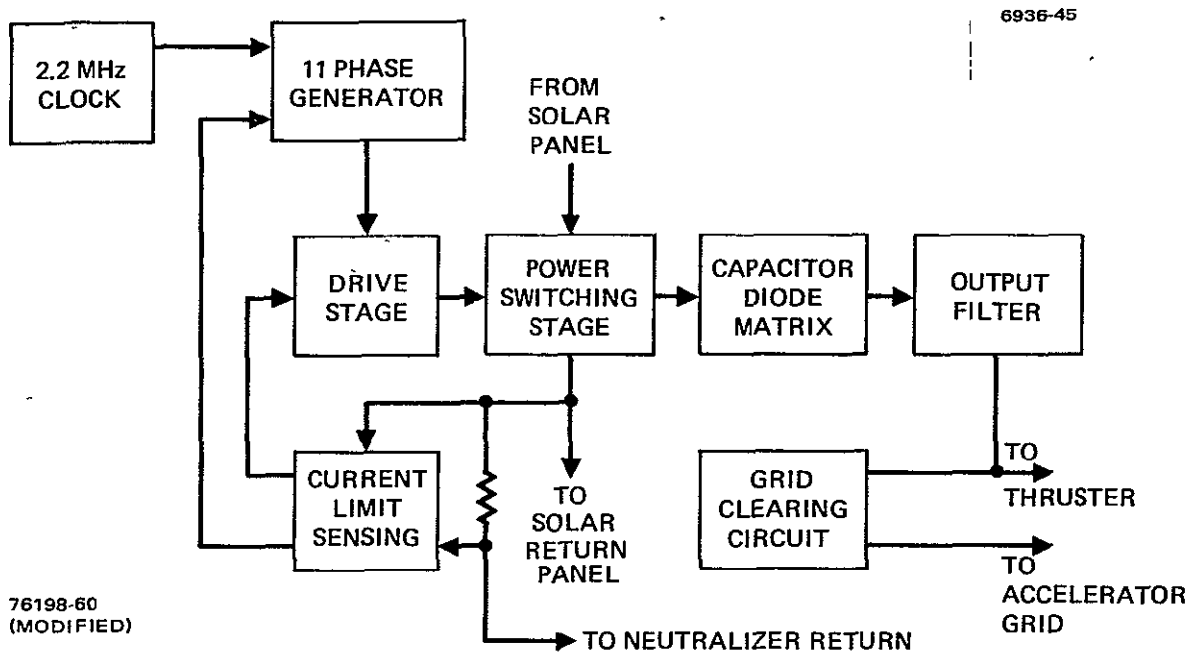
Figure 19. CDVM block diagram.

Table 11 Comparison of SCRs and Transistors
in CDVM Applications

SCR	Transistor
Advantages	
Higher voltage and current, therefore fewer phases required	Higher frequency capability (~100 kHz) Easy to turn off during fault. Low "ON" losses Low switching losses
Disadvantages	
Slow turn-off, therefore lower frequency operation (20 kHz) Require additional components in the CDVM to ensure safe operation during fault Additional components required to commutate SCRs off	More phases required to handle current. Higher drive losses
Apparent Methods to Best Utilize the Devices	
Operate three 2-phase multipliers from a single driver Three 2-phase systems run out of phase.	Multiphase driver and multiplier (eleven phases) Six 2-phase system run out of phase.

T5916

Table 12. Viable CDVM Configurations
(from tradeoff studies)

Concept	Driver Configuration	Capacitor-diode Matrix Configuration
SCR driven	Single -- 2 phase	Three parallel — 2 phase
SCR driven	Three parallel — 2 phase	Three parallel — 2 phase
Transistor driven	Single - 11 phases	Single — 11 phases

T5916

55

design (the third entry in Table 12) was selected on the basis of mass, efficiency, and component stress levels. It utilizes transistors rather than SCRs in the driver, and both the driver and the capacitor-diode matrix are in the single, 11-phase configuration. The rationale for this selection is briefly summarized below.

The fewest phases considered practical were two. Peak currents in the power stage of any single-phase CDVM are twice those in a two-phase CDVM. High peak currents cause severe penalties in the mass of the input filters and capacitor-diode matrices required. At least three parallel, two-phase capacitor-diode matrices are required to maintain average rectifier currents within the ratings of available components. Furthermore, capacitor rms current ratings limit the amount of power that can be handled by a two-phase capacitor-diode matrix. A transistor-driven system requires eleven phases to maintain peak currents within the transistor ratings. The four configurations listed in Table 12 were selected primarily in compliance with component ratings.

The masses of the four configurations in Table 12 are compared in Tables 13 through 16. The comparison, which was based on theoretical capacitor design curves, does not include packaging or input/output connectors. All of these are the major contributors to the total mass of the units, they are not expected to differ significantly from configuration to configuration. Although the mass differences between the four configurations is not very great, this comparison supports the selection of the configuration in Table 15. The two configurations that use transistors are lighter than the SCR configurations primarily because the mass of the capacitor-diode matrix and input filters is lower. This mass is lower mainly because of the higher operating frequency allowed by the transistors and the low ripple content of the input current. The mass penalty from using SCRs is particularly evident with the additional phases in the second configuration in Table 14: although the mass of the input filter would be significantly lower, the higher mass of the power stage would more than offset this. The configuration in Table 15 was also selected because its efficiency is higher because short-circuit protection can be provided relatively easily.

Table 13. Relative Mass of Candidate CDVM Driver-Matrix
Designs (Not Including Packaging): Single 2-phase
SCR Driver; Three Parallel 2-phase Matrices

Circuit	Mass, kg
Capacitor-diode matrix	
Capacitors	0.62
Rectifiers	0.03
Inductors	0.36
Power stage	
Main SCRs	0.12
Auxiliary SCRs	0.08
Commutating rectifiers	0.08
Commutating inductors	0.08
Commutating capacitors	0.01
Input filter	
Inductor	0.27
Capacitors	0.66
Logic/drive circuitry	
ICs	0.02
Drive transformer (0.02 each)	0.16
Miscellaneous resistors and capacitors	0.05
Miscellaneous transistors	0.02
Total	2.56

T5916

Table 14. Relative Mass of Candidate CDVM Driver-Matrix
Designs (Not Including Packaging): Three Parallel
2-phase SCR Drivers; Three Parallel 2-phase
Matrices

Circuit	Mass, kg
Capacitor-diode matrix	
Capacitors	0.62
Rectifiers	0.02
Inductors	0.36
Power stage	
Main SCRs	0.36
Auxiliary SCRs	0.24
Commutating rectifiers	0.24
Commutating inductors	0.24
Commutating capacitors	0.03
Input filter capacitors	0.03
Logic/drive circuitry	
ICs	0.06
Drive transformers	0.32
Miscellaneous transistors	0.06
Miscellaneous resistors/ capacitors	0.15
Total	2.73

T5916

58

Table 15. Relative Mass of Candidate CDVM Driver-Matrix
Designs (Not Including Packaging): Single 11-phase
Transistor Driver; Single 11-phase Matrix

Circuit	Mass, kg
Capacitor-diode matrix	
Capacitors	0.37
Rectifiers	0.05
Inductors	0.40
Power stage	0.77
Input filter capacitors	0.03
Logic/discrete components	
ICs	0.04
Miscellaneous transistors	0.08
Miscellaneous resistors/ capacitors	0.04
Total	1.78

Table 16. Relative Mass of Candidate CDVM Driver-Matrix
Designs (Not Including Packaging): Six Parallel
2-phase Transistor Drivers; Six Parallel
2-phase Matrices

Circuit	Mass, kg
Capacitor-diode matrix	
Capacitors	0.38
Rectifiers	0.05
Inductors	0.44
Power stage	0.84
Input filter capacitors	0.03
Logic/discrete components	
ICs	0.05
Miscellaneous transistors	0.09
Miscellaneous resistors/ capacitors	0.05
Total	1.93

Based on the configuration selected, a preliminary design of the CDVM beam supply was developed. The packaging concept is presented in Figure 20. Because a significant amount of power is dissipated (326 W maximum), components are spread over the largest available area to evenly distribute the approximately 0.156 W/cm^2 (1.0 W/in.^{2}) thermal loading to the heat sink. The height of the CDVM package is low enough (5.1 cm or 2 in.) to closely couple the thermal loads to the heat sink at a minimum mass penalty.

A mass summary estimate for the entire CDVM package, including the grid clearing circuit, is presented in Table 17. Comparison with Table 15 shows the significance of the contribution of packaging to total mass.* Table 18 summarizes CDVM losses and estimated efficiency.

E. SUMMARY COMPARISON OF DESIGN CHARACTERISTICS

The four PMaC design concepts defined above completes the data base required for the design definition of the seven configurations and for their comparative assessment. This section summarizes the key parameters (mass, size, power dissipation, and reliability). Mass, size, and power dissipation are used directly in Section 4 for developing the structural and thermal designs. The structural design data (including total configuration mass), PMaC power dissipation and reliability, and the design information in the preceding sections are used in Section 5 for the overall assessment of the relative masses, efficiencies, reliabilities, and technical risks of the seven configurations.

Mass and power dissipation for the various PMaC units are listed in Table 19. Table 20 summarizes, for each PMaC concept, mass and power dissipation per module for all the thrust modules, for the interface module, and for the entire PMaC subsystem. For the integrated configurations, only the last entry — the overall summary — is significant.

---

*Aside from packaging contributions, the major difference between these tables is that the chassis and cover, output conductor, connectors, circuit board, and wire were not included in the comparative tabulation in Tables 13 through 16.
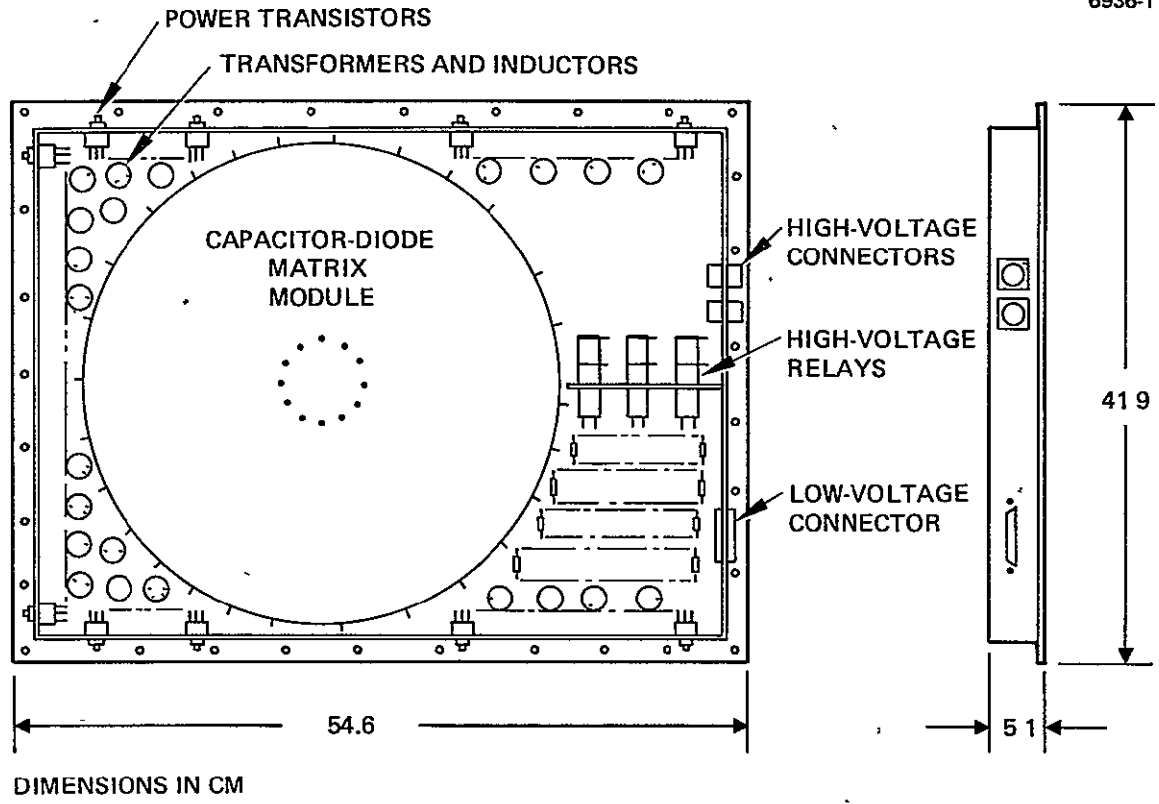
Figure 20. CDVM packaging configuration.

Table 17.   Summary of Estimated CDVM Mass

CDVM Component Subassembly	Quantity	Mass, g
Chassis and cover	1	2,315
Multiplier module	1	6,000
Ceramic capacitors	14	8
Tantalum capacitors	2	2
Zener diodes	1	1
Power transistor	22	561
TO-5 transistor	34	4
Digital ICs	14	7
Drive transformers	11	165
Air core inductors	11	88
Output inductor	1	136
Resistors	56	33
Connectors (high voltage)	2	84
Connectors (low voltage)	1	22
Circuit board	1	49
Wire	–	75
Subtotal		9,550
Grid clearing circuit		1,000
CDVM Total		10,550

T5916

62

Table 18. Summary of Estimated CDVM Losses
and Efficiency

CDVM Subassembly	Losses, W[a]
Capacitor diode matrix	
Rectifiers	78
Capacitors	55
Power Stage	
Transistor drive	63
Transistor forward drop	90
Miscellaneous losses	40
Total	326
CDVM efficiency	95.3%

[a]CDVM operating conditions

Input voltage   225 V
Output voltage   2666 V
Output current   2.5 A
Output power   6.664 kW
Multiplication ratio 12:1

T5916

63

Table 19. Mass and Maximum Power Dissipation of PMaC Units

Unit	Mass, kg				Maximum Power Dissipation, W			
	PMaC Concept				PMaC Concept			
	1	1X	2	3	1	1X	2	3
Each thrust module[a]								
Beam supplies (2)	--	--	28.5	21.0	--	--	950	652
Discharge supplies (2)	10.0	--	10.0	10.0	160	--	160	160
Low voltage supplies (2 sets)	12.5	12.5	12.5	12.5	52	52	52	52
Harness for above	1.0	1.0	5.0	7.0	0	0	0	0
Total per module	23.5	13.5	56.0	50.5	212	52	1.162	864
Interface module								
Reconfiguration units for beam power	45	45	--	21	34	34	--	17
Discharge power	--	33	--	--	--	34	--	--
Power distribution filters	--	--	88	b	--	--	531	b
Distribution inverters (2)	3	3	3	3	60	60	60	60
DC/DC converter	3	3	3	3	65	65	65	65
Controller	8	8	8	8	15	15	15	15
Harness	16	13	28	30	0	0	0	0
Total	75	105	130	65	174	208	671	157

[a]Per two thrusters for integrated configurations
[b]Incorporated in CDVM beam supply.

T5916

64

Table 20. Summary Comparison of Mass and Power Dissipation
for the Four PMaC Concepts

Mass or Power Dissipation of Unit or Module	PMaC Concept			
	1	1X	2	3
Mass summary, kg				
Mass of PMaC units on each thrust module	23.5	13.5	56	50.5
Mass of all thrust module PMaC units	141[a]	81[a]	280[b]	252.5[b]
Mass of interface module PMaC units	75	105	130	65
Total PMaC system mass	216	186	410	317.5
Maximum power dissipation summary, W				
Dissipation in PMaC units on each thrust module	212	52	1162	864
Dissipation in PMaC units in all thrust modules	1272[a]	312[a]	5810[b]	4320[b]
Dissipation in PMaC units on interface module	174	208	671	157
Total maximum PMaC system power dissipation	1446	520	6481	4477

[a]Six modules per PMaC unit.

[b]Five modules per PMaC unit.

T5916

65

Comparing the masses of the various PMaC systems highlights the impact of the absence of beam supplies on the mass of the systems using the direct drive concepts: mass per module for the direct drive is reduced by 50% relative to concepts 2 and 3. Another 50% reduction is achieved by deleting the discharge supplies. The mass of the interface module units depends strongly on the requirement for reconfiguration units and associated filters. The conventional PMaC interface module (concept 2) is heaviest because of the requirement for power distribution filters. The variation in the mass of the interface modules from 65 to 130 kg, however, plays a secondary part in the overall mass comparison.

Power dissipation per module also varies widely among the four PMaC concepts. The low dissipation for concept 1 reflects the absence of beam supplies; for concept 1X it reflects the absence of both beam and discharge supplies. Power dissipation for the conventional system is significantly greater than for the CDVM system because the conventional beam supply dissipates 50% more power than the CDVM. The conventional system also shows a much higher power dissipation on the interface module because of the dissipation in the power distribution filters. But, interface module dissipation has a secondary effect on the overall comparison of the four concepts because thrust module dissipation dominates. The 65 W dissipation* for the dc/dc converter corresponds to the dissipation during the thrust phase, which is the appropriate quantity for determining the thermal control system requirement. Dissipation increases to about 75 W after the thrust phase is completed because the power requirements of the mission module are higher during science payload operations.

For Table 20, it is assumed that all thrusters are operating, as required for the sizing of the thermal control subsystem. The major differences between the four concepts are particularly evident in this

---

*Subsequent design improvements reduce this to 55 W for the selected baseline.

summary. The short radiators required for the direct-drive configurations simplify the design of the thrust system structure. The lower power dissipation of the direct-drive PMaC system also significantly affects the thermal design of the PMaC units. Thermal control of PMaC units is based on a maximum allowable mounting surface temperature* consistent with using proven, high-reliability electrical components. Where units dissipate small amounts of power, as in concepts 1 and 1X, the maximum mounting temperature can be handled relatively easily with small radiators. Electronic packaging is not critical because there are few high-dissipation components. However, in concepts 2 and 3, large amounts of power dissipated in localized high-dissipation components makes it more difficult not to exceed the mounting temperature limits. Electronic packaging becomes critical, which dictates the use of a low-profile chassis and close thermal coupling to the mounting surface.

The approximate sizes of the individual PMaC units used in preparing configuration layouts in Section 4 are presented in Table 21. The length and width of the conventional beam and discharge supplies were later changed for the selected baseline to comply with the ground rules subsequently furnished by NASA LeRC to utilize the 38.1 cm x 101.6 cm (15 in. x 40 in.) area of the Z-frame modular packaging technique. Total volume, however, was not changed. The 25.4 cm (10 in.) length of the low voltage supplies package was subsequently increased to a nominal value of 38.1 cm (15 in.) for the baseline because of the space available within the modular Z frame. The total space required for each PMaC concept depends on the number of units required (as listed in Table 5).

PMaC reliability estimates are presented in Table 22, which shows the calculated reliability of each individual unit and of the entire system for each of the four PMaC concepts. The number of units and the redundancy provided are taken into account in the calculation. Unit

---

*Taken as 60°C during the initial study phase, it was later reduced to 50°C for the selected baseline design.

Table 21. PMaC Unit Size Summary

Unit	Approximate Dimensions, in.			Approximate Volume, cm³ (in.³)
	Length, cm (in.)	Width, cm (in.)	Height cm (in.)	
Thrust module				
Conventional beam supply	45.7 (18)	40.6 (16)	15.2 (6)	28,349 (1730)
CDVM beam supply	54.6 (21.5)	41.9 (16.5)	5.1 (2)	11,634 (710)
Discharge supply	45.7 (18)	22.9 (9)	15.2 (6)	15,895 (970)
Low voltage power supplies	25.4 (10)	15.2 (6)	15.2 (6)	5,899 (360)
Interface module				
Controller	30.5 (12)	20.3 (8)	10.2 (4)	6,309 (385)
DC/DC converter	20.3 (8)	20.3 (8)	5.1 (2)	2,130 (130)
Distribution inverter	15.2 (6)	7.6 (3)	7.6 (3)	901 (55)
Power distribution/ reconfiguration				
Conventional system	30.5 (12)	12.7 (5)	10.2 (4)	3,932 (240)
Direct drive	63.5 (25)	45.7 (18)	10.2 (4)	29,496 (1800)
Direct drive discharge	63.5 (25)	45.7 (18)	10.2 (4)	29,496 (1800)
CDVM	53.3 (21)	45.7 (18)	10.2 (4)	24,744 (1510)

T5916

Table 22. PMaC Reliability Estimates

Unit	Single Unit Reliability	Effective (Functional) Unit Reliability			PMaC Subsystem Reliability			
		Number of Operating Units	Number of Redundant Units	Functional Reliability	Design Concept 1	Design Concept 1X	Design Concept 2	Design Concept 3
Thrust module								
Conventional discharge supply	0.977	2	0	0.955	na	na	0.955	na
CDVM beam supply	0.987	2	0	0.974	na	na	na	0 974
Conventional discharge supply	0.983	2	0	0.966	0.966	na	0.966	0.966
Low-voltage power supplies	0.967	2	0	0.935	0.935	0.935	0.935	0.935
Reliability of PMaC subsystem on each thrust module	--	--	--	--	0.903	0.935	0.863	0.880
Interface module								
Controller	0.797	1	1	0.970	0.970	0.970	0.970	0 970
DC/DC converter	0.979	1	1	0.999	0.999	0.999	0.999	0.999
Distribution inverter	0.984	2	1	0.999	0.999	0.999	0.999	0.999
Power distribution/ reconfiguration								
Conventional system	0.997	5	0	0.985	na	na	0.985	na
Direct drive	0.999	2	0	0.998	0.998	0.998	na	na
Direct-drive discharge	0.999	2	0	0.998	na	0.998	na	na
CDVM	0.999	2	0	0.999	na	na	na	0.999
Reliability of PMaC subsystem on interface module	--	--	--	--	0.967	0.964	0.954	0.967

T5916

reliability estimates were obtained from component parts counts for each unit, using best available component reliability data and accounting for component redundancy provided in unit designs. The reliability of the PMaC subsystem for each thrust module (two sets of power supplies) and for the interface module are tabulated separately (they are used in Section 5 for estimating total thrust system reliability).

Table 22 reflects the rationale for incorporating unit redundancy. Redundancy was considered more critical for the interface module. Accordingly, one spare is provided for the controller, one for the dc/dc converter, and one for the two distribution inverters. The effective functional reliability, taking into account the number of operating units and spares, exceeds 0.97 for all the functional units. The overall reliability of the interface module PMaC units exceeds 0.95 for all four concepts. No redundancy is incorporated in the thrust modules because an excessive mass penalty would be incurred and because the total number of thrust modules permits using one-half module as a spare. Were one set of thrust module PMaC supplies (or one thruster) to fail, it would not be catastrophic to the mission. This is discussed in more detail in Section 5. Furthermore, the lowest single-unit reliability value (0.97 for the low-voltage power supplies) is still reasonably satisfactory without redundancy, and is comparable with the reliability of the controller with redundancy. In any event, the primary objective of these PMaC system reliability estimates (to provide a basis for comparing the alternate concepts) is fulfilled by using the same redundancy ground rules for all four concepts.

SECTION 4

ALTERNATE STRUCTURAL DESIGNS

The preceding sections have described the options available for
specifying the choice of subsystems in designing the seven thrust system
configurations (defined in Table 2). This section discusses the design
of the structure and the thermal control subsystem for these seven
thrust system configurations. The work described produced layouts for
each configuration, defined the structural materials, and consequently
enabled estimation of the total spacecraft mass for comparison of the
seven thrust system design concepts. Analyses were performed to deter-
mine the structural loads and thermal transport processes to support the
minimum mass design goals that guided the design effort for both the
comparison of thrust system configurations and the selected baseline
thrust system.

A. DESIGN APPROACH

Designs were developed for the thrust system structure and thermal
control system (using the data base and the ground rules described in
Section 2) with the overall objective of minimizing mass. The dis-
cussion below explains how ground rules were interpreted and applied; it
also serves to define the approach adopted in establishing the key fea-
tures of the designs.

The thermal design uses cold plates for mounting electronic equip-
ment, radiators, and coplanar Communications Technology Satellite (CTS)-
type heat pipes. The radiators and heat pipes were sized to assure that
the thermal design would comply with component ratings, and that the
interface requirements with the mission module and with the solar array
would also be satisfied. Design parameters were selected on the basis
of tradeoff studies to minimize mass and impact on configuration length.
The seven configurations were compared by postulating a maximum tempera-
ture limit of 60°C (later reduced to 50°C) for the mounting surface of
the PMaC units. The results were validated by computer analysis of a

71

thermal model of thrust system configuration, using thermal-interface
and power-dissipation data available from thruster data and from the
PMaC subsystem design. The distribution of dissipated power in the cold
plates was assumed to be uniform.

The load paths and the sizing of structural members (for the thrust
system structure and for the adapter) were determined by IUS requirements
(see Volume II); a forward cradle supporting the thrust system directly
from the shuttle was assumed. The adapter, thrust system-IUS separation
subsystem, and solar array deployment mechanisms* were sized in compiling
total mass estimates.

The lateral dimensions of the thrust system (perpendicular to the
longitudinal axis of the shuttle) were determined primarily by the
dimensions specified in Section 2 for the PMaC beam and discharge sup-
plies for the modular configurations and by the number of thrusters.
Integrated configurations permitted an additional degree of freedom in
the packaging arrangement. The overall cross-sectional dimensions,
including the stowed array (and the adapter beams), were constrained by
the 4.6-m (15-ft)-diameter shuttle envelope. For some configurations,
this constraint resulted in a tight fit and required design ingenuity
because of the large size of the stowed array, particularly with the
concentrator array concept. For example, the limited space available
with concentrator configuration 2B for the location of adapter tripod
support beams was one of the principal factors that determined the
structural design and mass for this configuration.

Thrust system length was determined by the length of the stowed
array and/or by the required length of the thermal radiators. For all
configurations, length per se was not a critical factor, since ample
space was available in the shuttle. Accordingly, design selection was
based on minimizing the resultant mass. For flat arrays, two alternate
stowed array configurations were considered for modular configurations;

---

*The mass of the solar array deployment mechanisms was not charged
to the thrust system, but was assumed to be a part of the mass
allocation to the solar array in compiling the final mass tabula-
tions for the selected baseline in Volume II.

the one shown in Figure 3(b) was selected because its net mass is lower even though its length is greater.

The requirement for modular construction was interpreted to mean that (1) the thrust modules are identical and have independent structures and thermal control systems, and (2) that the interface module is a separate structure although it does use space on the thrust module cold plates for mounting the interface module power electronics (thermal control). Thus, the additional mass of a separate cold plate and radiator assembly for the interface module is eliminated without loss of the ability to have interchangeable modules and to test and evaluate individual modules. Special test apparatus will be required to provide the appropriate electrical and thermal interfaces for module testing, but this would be the case in any modular design. Each module had an individual cold plate for mounting identical thrust module components on the module side and for mounting interface module components on the interface module side. Interface module components, however, were not identical; they were distributed to obtain near-uniform mass and power dissipation distribution among the modules. This is illustrated in Figure 21. In all other respects, the modules were identical. Additional mounting holes were provided on the cold plates allowed to facilitate module interchangeability. As compared to the alternative of a separate interface module configuration for mounting electronic units with a separate thermal control, this approach significantly reduced mass without violating any of the key provisions of the modular design ground rules discussed in Section 2. In particular, the modularity concept for other mission applications was still essentially preserved, since only a minor design change would be required if, for example, the number of modules were reduced to two or three: appropriately modified interface module units would simply be redistributed on top of the cold plates.

The same criteria were used for all configurations in selecting structural materials. Aluminum was selected for the interface truss, cold plates, and radiators; titanium for the thrust module structure; and beryllium for the adapter tubes, the IUS interface beams, and the

73

6936-43

POWER DISTRIBUTION
21.6 KG, 53.1W

THRUSTER SYSTEM CONTROLLER
7.0 KG, 40W

DISTRIBUTION
INVERTER
3.5 KG, 90W

INV

PD

INV

PD

INV

DC

PD

PD

DC

DC-DC CONVERTER
3.9 KG, 20W

POWER DISTRIBUTION UNIT
1.1 KG, 2.5W

STRUCTURAL
FRAME

COLD PLATE

A   A

BEAM SUPPLY (2)
13 3 KG, 475W

LOW POWER SUPPLY (2)
5.8 KG, 30W

DISCHARGE SUPPLY (2)
5 0 KG, 80W
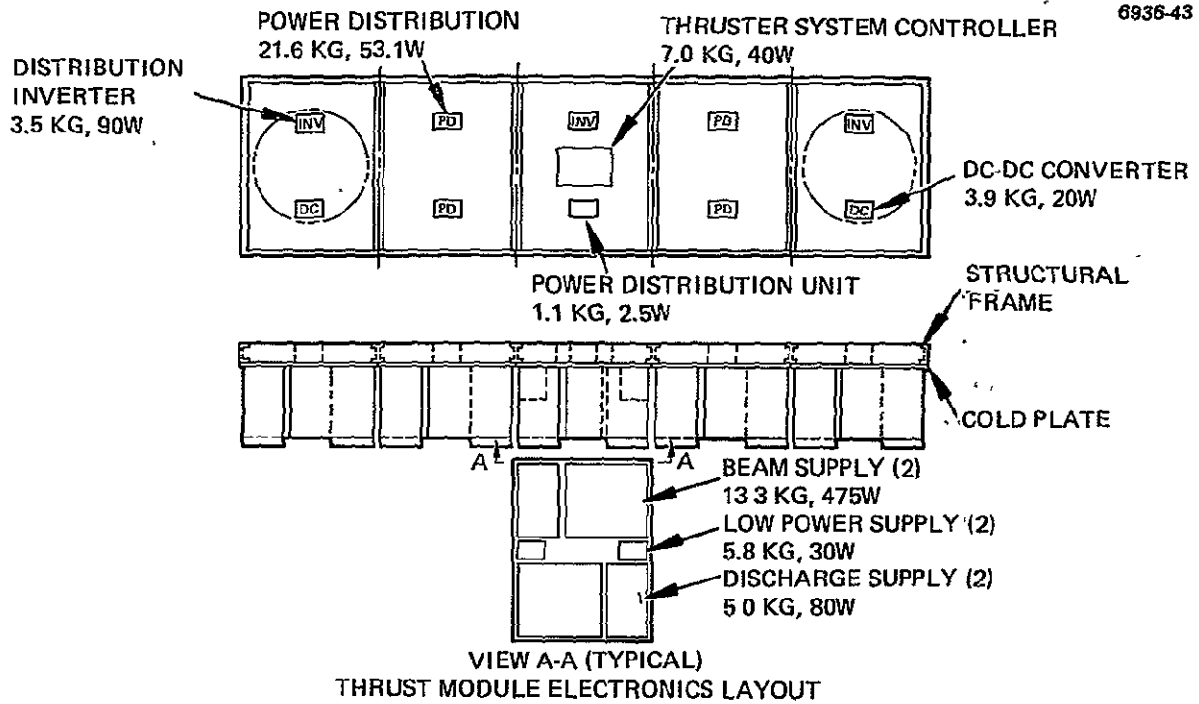
VIEW A-A (TYPICAL)
THRUST MODULE ELECTRONICS LAYOUT

Figure 21. Typical electronics layout.

74

solar panel deployment booms, where stiffness requirements dominate. The design of the selected baseline was later modified somewhat.

A reasonably simple mission module structural interface was sought for all configurations by providing the largest footprint consistent with structural efficiency. In particular, the goal was to maximize the ratio of the circumference to the area of the rectangle formed by the four points of attachment.

The adapter/IUS separation system was designed to minimize mass and to simplify the interface with the IUS. Every attempt was made to utilize the standard interface bolt circle, to minimize requirements for additional IUS interface beams, to provide the simplest separation system consistent with the structural design requirements, and to efficiently use the space available in the shuttle bay outside of the envelope required for the stowed solar arrays. The permissible stowed array locations were rearranged (with NASA LeRC assistance) to help accomplish this. To the extent possible, the accessibility for assembly and test was also considered. Both modular and integrated configuration designs reflect these goals. The designs were carried out in sufficient depth to confirm their feasibility, to identify critical interfaces, and to assess their performance in terms of size, mass, and technical risk.

B.   THERMAL CONTROL

Thermal and structural designs of each configuration evolved from iterative analysis and design tradeoffs. The thermal design for all seven configurations is presented first.

Initial design work and tradeoff analyses related to the thermal control system were performed. The results led to definition of the thermal control subsystem for each configuration and for the selected baseline. The results and a description of the baseline design are presented in Volume II. The basic design is generally applicable to all seven configurations, and will not be repeated here, except for the following differences:

●   The specific design parameters for radiators/heat pipes
     (number and size of radiators and number of heat pipes

75

per radiator) vary, depending on configuration parameters (power dissipations, thermal radiation geometry). These are presented in this subsection.

- Modular thermal design concepts are modified when applied to the 2A/I and 2B/I configurations to accommodate their integrated design features: common cold plate versus individual cold plates for each module, one set of two radiators and a single thermal blanket versus individual sets for each module.

The summary of the radiator/heat pipe design parameters is presented in Table 23. These parameters are derived from the calculations of the maximum (worst case) heat rejection, Q_R, per radiator. This is determined by assuming the worst-case power dissipation in the PMaC units and thrusters, taking into account radiation losses (which, depending on geometry, differ among the various configurations) and solar array view factors and on structural design.

The values in Table 23, which were determined from the analysis* of heat rejection requirements, can be generally explained by correlating them to power dissipation data for the PMaC units and to the other factors considered in the analysis, with the following relationship:

$$Q_R = Q_P + Q_S + Q_T - Q_0 \quad ,$$

where

Q_R ≡ total heat rejected by all radiators under worst-case conditions, which defines radiator size and number of heat pipes (optimized by tradeoff analysis).

Q_R is obtained from Table 23 by multiplying heat rejection per radiator by the number of radiators.

Q_P ≡ total heat dissipation by all PMaC units under steady-state conditions with all thrusters operating at maximum power.

Q_P is directly calculated from Table 20 in Section 3 by adding power dissipation in the interface module to the sum of power dissipations in all the thrust modules.

---

*The analysis was somewhat simplified assuming uniform power dissipation over the cold plates, but is considered adequate for this comparison.

76

Table 23. Thermal Control Subsystem: Key Design Parameters

Thermal Control Factors	Configuration						
	1A	1AX	2A	2A/I	2B	2B/I	3A
View factors							
Radiator — solar array	0.05	0.05	0.04	0-04	0.04	0.04	0.04
Radiator — container	0.05	0.05	0.05	0.03	0.04	0.04	0.03
Radiator — canister	0.05	0.05	0.02	0.02	0.03	0.03	0.02
Radiator — reflector	--	--	--	--	0.11	0.11	--
Heat rejection, W/radiator	140	64	674	3130	659	3169	458
Radiator dimensions, length/width, meters	0.53/0.64	0.25/0.64	2.01/0.76	2.87/2.34	2.08/0.76	1.91/4.06	1.60/0.76
Area per radiator, m^2	0.33	0.16	1.53	6.71	1.59	7.74	1.22
Number of heat pipes per radiator	2	2	5	23	4	22	3
Heat pipe weight per radiator, kg	2.1	1.78	5.3	27.8	3.4	21.1	2.8
Radiator weight per radiator, kg	1.02	0.49	2.1	9.2	2.2	10.6	1.7
Number of radiators	12	12	10	2	10	2	10
Total weight of heat pipes and radiators, kg	37.5	27.3	74.0	74.0	56	63.4	45.0

77

$Q_S \equiv$ incremental power dissipation during thruster start up.

For modular designs, the radiators must be sized to account for Q_S for one of the two thrusters per module.

For integrated designs, radiators must be sized to account for Q_S for one of the ten thrusters.

$Q_T \equiv$ thruster power dissipation (excluding radiation and conduction losses not directly coupled to the radiators).

$Q_0 \equiv$ portion of PMaC power dissipation not coupled to radiators via cold plates/heat pipes (e.g., losses through insulation blankets).

Q_R and Q_P are given in Table 24. Direct correlation between them is not easily evident because Q_S, Q_T, and Q_0 vary from configuration to configuration. Q_S is a much larger worst case relative "surcharge" for modular configurations. Q_0 is greater for the "open" configurations 1A, 1AX, 2B and 2B/I than for configurations 2A, 3A, and 2A/I (for which the radiators extend over the interface module, thereby shielding it). For example:

Configuration 2A versus 2B

- $Q_R > Q_P$ for both because of the contributions of Q_S and Q_T,

  but Q_R is greater for 2A because Q_0 is smaller for 2B than for 2A

Table 24. Comparison of PMaC Power Dissipation with Heat Rejection Requirements of Thermal Radiators

Type of Power Dissipation	Configuration						
	1A	1AX	2A	2A/I	2B	2B/I	3A
$Q_R \equiv$ Total heat rejected by all radiators, in W	1680	768	6740	6260	6590	6338	4580
$Q_P \equiv$ Maximum steady-state power dissipation by all PMaC units, in W	1446	520	6481	6481	6481	6481	4477

T5918

78

Configuration 2A versus 3A

- $Q_R > Q_P$ for both because of the contributions of Q_S and Q_T, but Q_P is greater for 2A than for 3A

- Q_0 is a larger fraction of Q_P for 2A

- $(Q_R - Q_P)$ difference is greater for 2A

Configuration 2A versus 2A/I

- $Q_R > Q_P$ for 2A because of the contributions of Q_S and Q_T, but Q_R is less than Q_P for 2A/I because Q_S is smaller and $Q_0 > (Q_S + Q_T)$

The important design parameters in Table 23 that affect overall configurations are radiator length and total mass. Only one component of total thermal control system mass, the mass of radiators and heat pipes, is included in Table 23. The other components (cold plates, thermal blankets, etc.) are included in the final tabulations in Section 4.

Radiator length impacts the total structural length and, more importantly, the resulting structural mass. In the attempt to minimize this impact, some of the configurations (2A, 3A, 2A/I, and 2B/I) have radiators which extend beyond the cold plates (i.e., over the sides of the interface module). The resulting reduction in the length/mass ratio is added complexity of heat pipe design and individual module testing, because of the additional bend required. This disadvantage is not considered sufficiently important to warrant abandoning the mass advantage.

The thermal design was subjected to a simplified computer model analysis to validate design integrity. The computer model used is shown in Figure 22, and the results are summarized in Table 25. The postulated design limits are not exceeded.
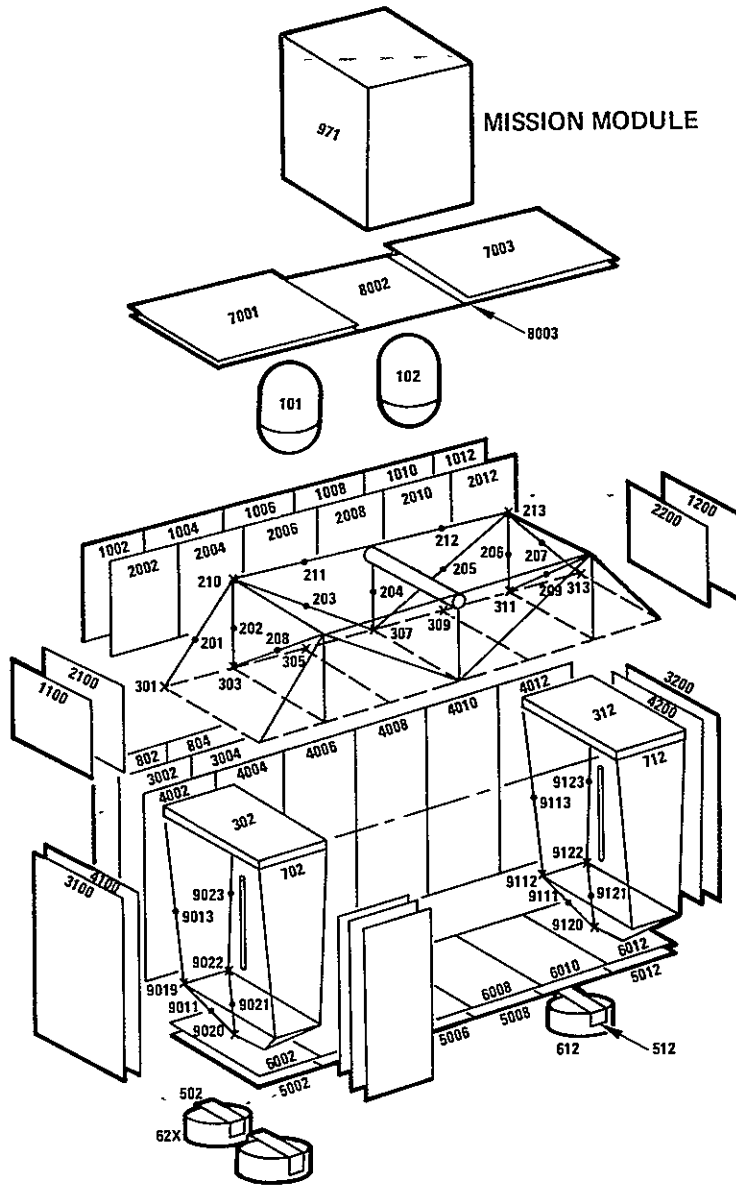
Figure 22.   Computer model for thermal analysis,
             showing Nodal breakdown.

Table 25. Results of Thermal Computer Model Analysis; Comparison with Allowable Limits.

Thrust System Configuration			Subsystem Temperatures, °C[a]						
Solar Array	PMaC System	Designation	PMaC Mounting Surface	Propellant Tanks	Propellant Lines	Solar Array Drive	Thruster	Gimbal	Structure
Flat	Direct drive	1A	59/-20	39/-35	54/-31	55/-25	254/-68	112/-57	63/-43
Flat	Direct drive discharge	1AX	59/-20	39/-35	56/-31	47/-25	254/-68	112/57	63/-43
Flat	Conventional	2A	59/-18	57/-27	58/-8	59/-30	254/-57	112/-57	65/-48
Flat	Conventional	2A/I	58/-3	54/-19	54/4	53/-21	254/-68	112/-57	58/-19
Concentrator	Conventional	2B	59/-21	46/-31	55/-15	57/-30	254/-68	112/-57	65/-43
Concentrator	Conventional	2B/I	50/-8	45/-27	45/-3	43/6	254/-68	112/-57	44/-15
Flat	CDVM	3A	60/-23	57/-32	59/-33	52/-30	254/-68	112/-57	66/-45
Allowable limits			60/-30	150/-40	150/-40	60/-30	300/-100	125/-65	200/-185

[a]Hot/cold conditions.

81

A comparison of the thermal control system design values for configuration 2B with the design values for the selected baseline (Volume II) derived from this configuration shows the principal difference between these to be in power dissipation: 659 W per radiator in 2B compared with 500 W in the baseline. This affords a somewhat shorter radiator for the baseline, and shortens the overall thrust system length (by about 0.2 m). The reasons for the lower power dissipation are: lower maximum thruster power with the revised solar array and thruster profile (7 kW versus 6.4 kW), higher efficiency of beam and discharge supplies (per revised data furnished by NASA LeRC, lower dissipation in the power distribution unit for the revised solar array power profile (530 W versus 326 W).

C. DESCRIPTION OF STRUCTURAL CONFIGURATIONS

The seven structural configurations and one alternate configuration are presented in sequence in Figures 23 through 37. Each configuration is described in terms of a three-view layout, followed by a sketch (except for 1A). Configurations 1A and 1AX are similar, except for mass and thermal control parameters. The three-dimensional sketches for all configurations (except 2B/I) are shown with the solar array stowed; the dimensional envelope specified for the mission module is indicated for reference (it is allowed to extend 2.5 m above the interface module). The sketch of the 2B/I configuration is shown in Figure 35 with the solar array deployed since the large solar array cannisters would hide the key design features in a stowed representation. The sketches for the 2A/I and 2B configurations are shown for both stowed and deployed modes.

Figure 24 shows the layout of an alternate 1A configuration in which the four solar array blanket containment boxes are placed side by side rather than above each other as in the selected 1A design. This is evident in the side views in Figures 23 and 24. Similar alternate layouts, not shown here, were prepared for configurations 2A and 3A. These alternate design approaches were rejected because of a net mass penalty.

2.985m
(117.520 in)
DIA

4.572m
(180.0 in.)
DIA

SHUTTLE BAY
ENVELOPE

4 12m
(162.0 in.)

67.5°
TYP

33 0°

1.054m
(41.5 in.)

1 626m
(64.0 in.)

0 432m
(17.0 in)

2 883m
(113.5 in.)

RADIATOR
0.68m^2
(7.3 ft.^{2})

THRUSTER
& GIMBAL

SOLAR ARRAY
STOWED

1.118m
(44.0 in)

SEPARATION
SPRING

ASTROMAST

IUS LOAD
POINT
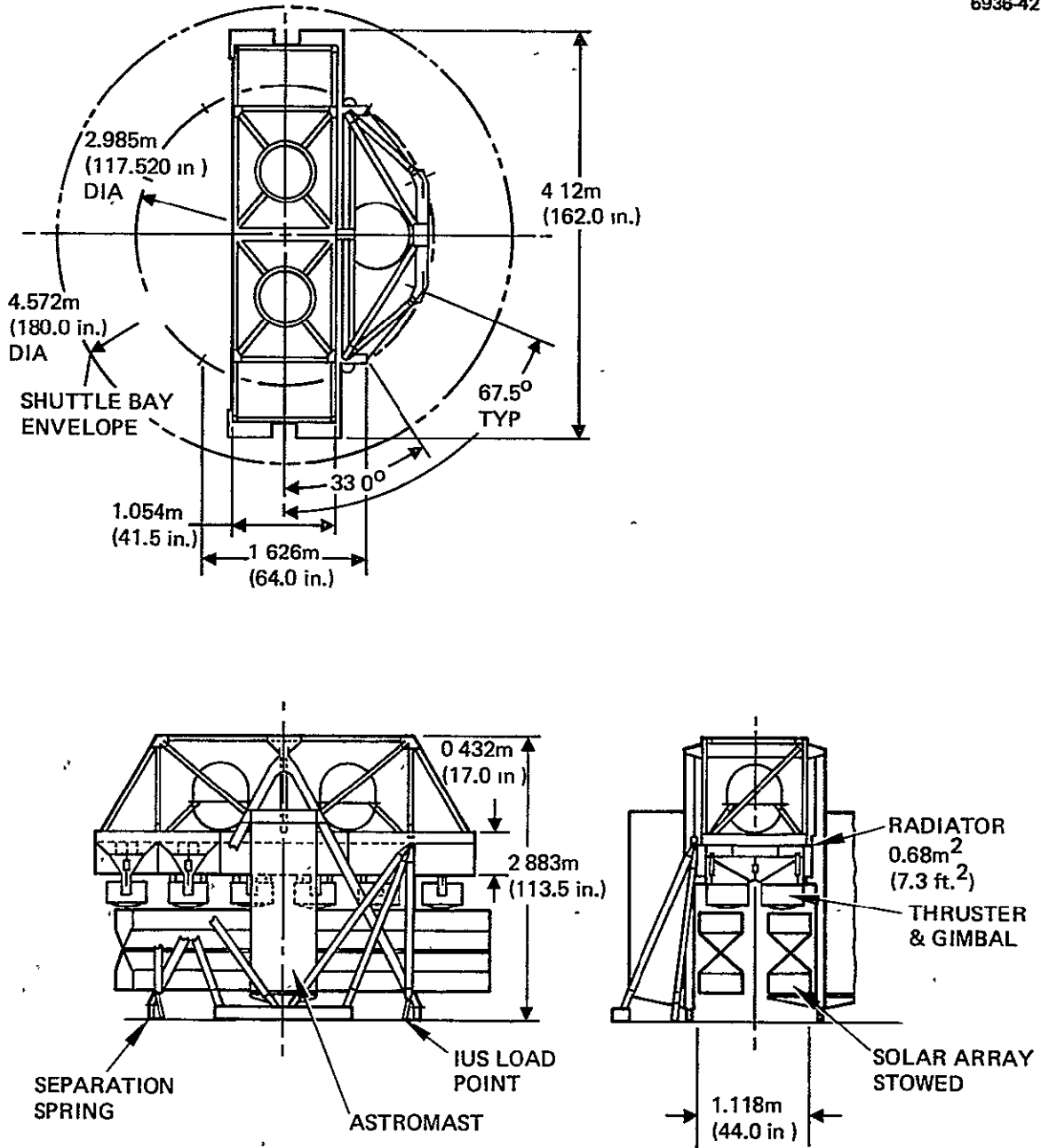
Figure 23.   Configurations 1A and 1AX.

SHUTTLE BAY
ENVELOPE

3 987m
(157.0 in.)

2.985m
(117.520 in.)
DIA

4.572m
(180.0 in)
DIA

1 54m
(41.5 in.)

0.432m
(17 0 in.)

2 44m
(96.0 in)

ASTROMAST

THRUSTER & GIMBAL

RADIATOR
$0.55m^2$
$(5\ 9\ ft.^2)$

SOLAR
ARRAY
STOWED

1 77m
(70 0 in.)

SEPARATION
SPRING
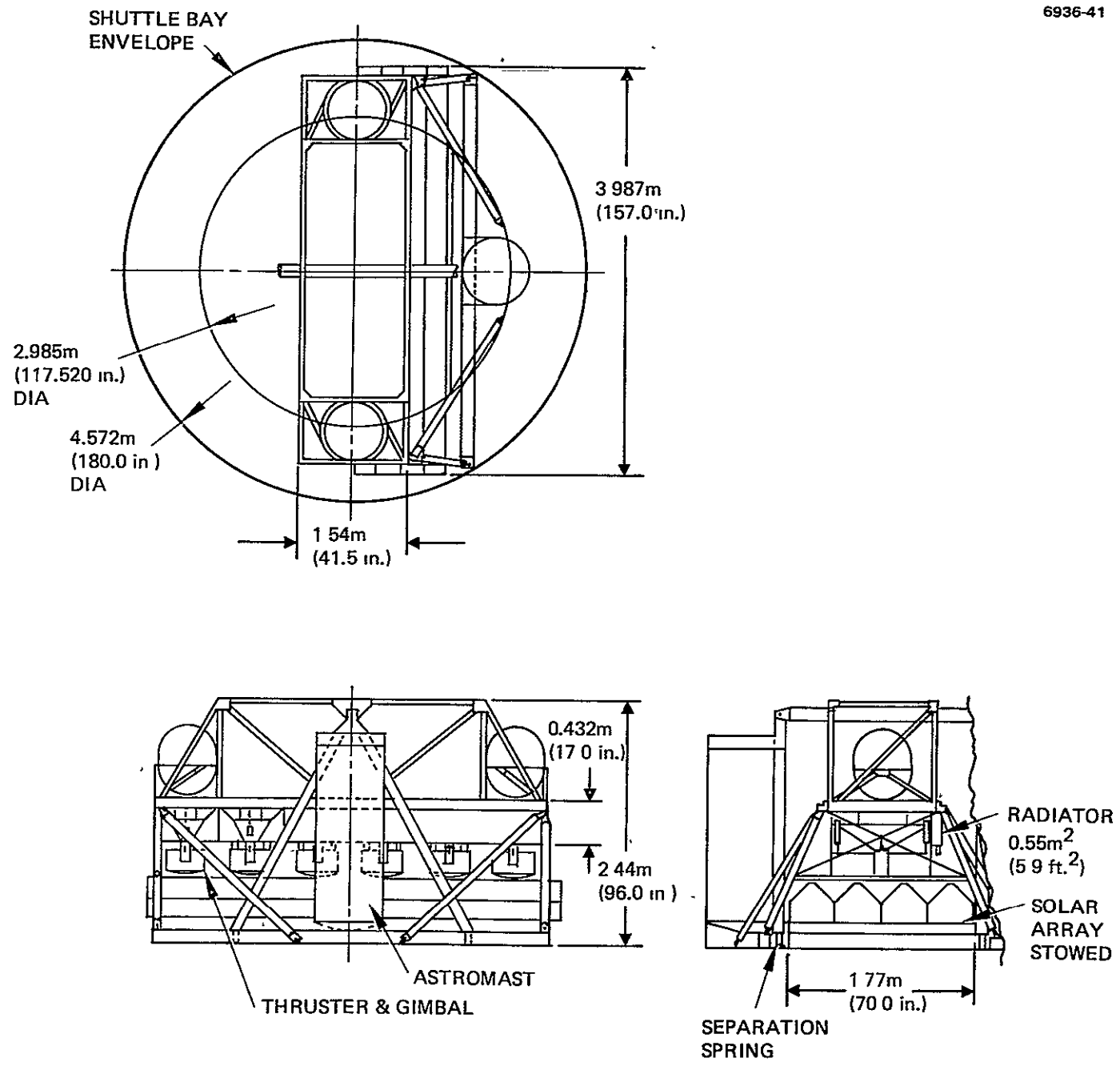
Figure 24.   Configuration 1A alternate.

MAXIMUM ENVELOPE
OF MISSION MODULE
AND SCIENCE PAYLOAD
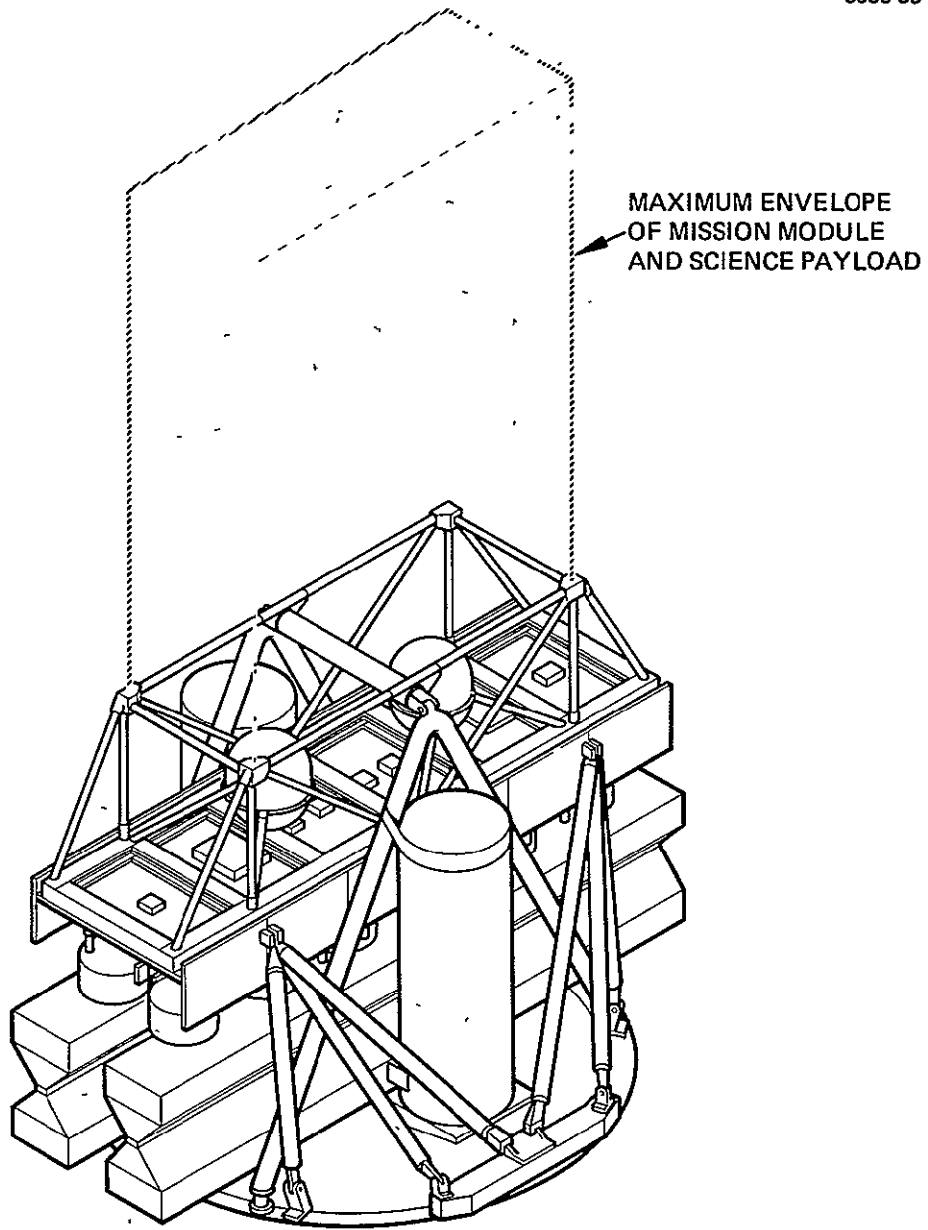
Figure 25.   Configurations 1A and 1AX (stowed array).
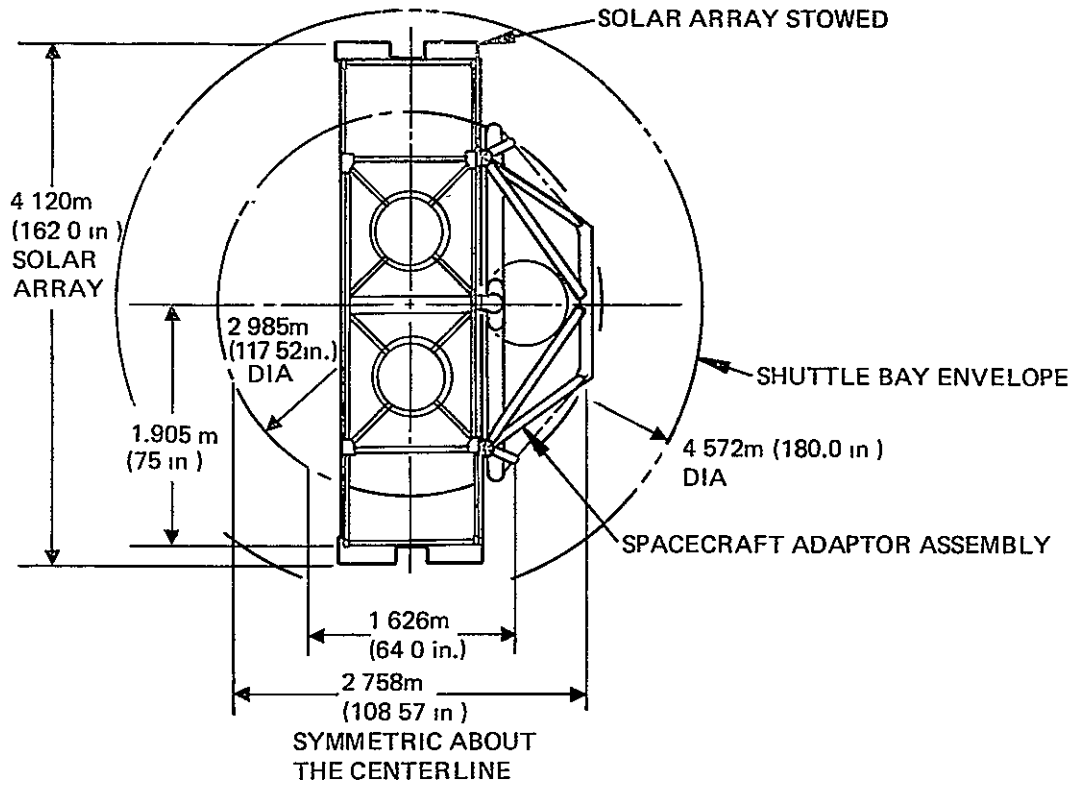
Figure 26.   Configuration 2A.
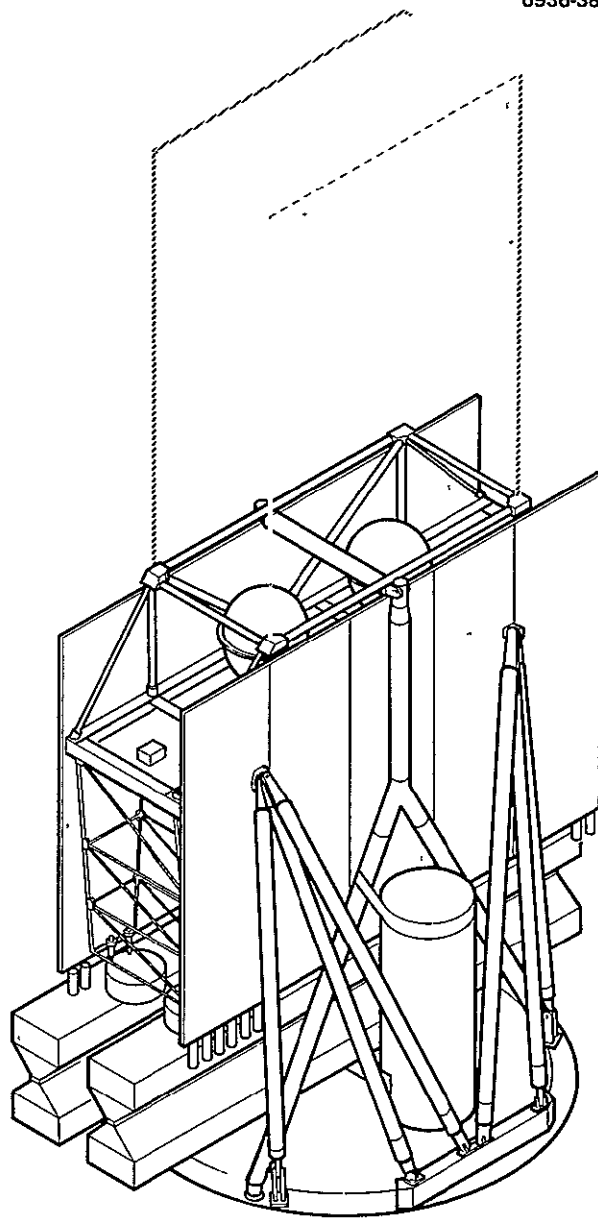
Figure 27. Configuration 2A stowed.

87

Hg TANK

2 34m
(92 0 in)

2 985m DIA
(117.52 in)
IUS BC

ASTROMAST
(STOWED)

½ SOLAR ARRAY
(STOWED)

4 572m DIA
(180.0 in)
SHUTTLE BAY
ENVELOPE

2 11m
(83 0 in)

2 11m
(83 0 in)

RADIATOR
8 9m^2 (96 ft^2) PER SIDE

RADIATOR

HONEYCOMB
PANEL

COLD PLATE
WITH HEAT
PIPES

3 84m
(151 0 in)
RADIATOR

2 67m
(105 0 in)
STRUC-
TURAL
COLD
PLATE

4 72m
(186 0 in)

MAST RETAINER

THRUSTERS

THRUSTER MOUNTING
HONEYCOMB PANEL

IUS INTERFACE
SEPARATION
SPRING

Figure 28.   Configuration 2A/I.

88

6936-36

Figure 29. Configuration 2A/I stowed.
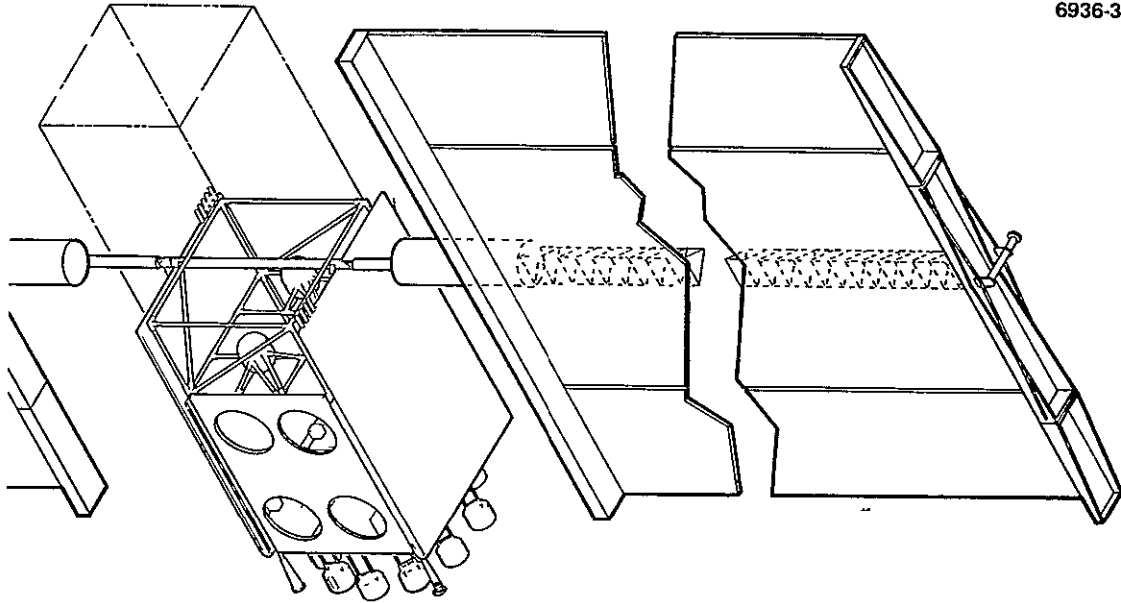
6936-35

Figure 30. Configuration 2A/I deployed.

6934 34

1 00m   0 50m
(39 38 in)   (19 69 in)   SOLAR ARRAY ASSEMBLY

SOLAR ARRAY EXTENSION CONTAINER
SOLAR ARRAY CONTAINER

1.00m
0 50m   (39 98 in)
(19 69 in)

ASTROMAST

REFLECTOR CONTAINER

0 80m DIA
(31 5 in)

2 10m
(82 5 in) TYP

0 75m
(29 5 in)
TYP

2 985m DIA B C
(117 5 in)

0 61m
(24 0 in)   SOLAR ARRAY ASSEMBLY

1 22m   4 57m DIA SHUTTLE ENVELOPE
(48 0 in)   (180 0 in)
SYM
ABOUT ℄

1 02m
(40 0 in)

0 94m
(37 0 in)

SOLAR ARRAY
ASSEMBLY

2 29m
(90 0 in)

MERCURY TANK

SOLAR ARRAY
DEPLOYMENT BOOM

ADAPTER

SEPARATION
DEVICE

ASTROMAST
REF

4 84m
(190 5 in)

ASTROMAST

RADIATOR
4 13m^2
(44 5 ft^2)
PER MODULE

2 72m
(107 0 in)

3 63m
(143 0 in)

ION THRUSTER

Figure 31.   Configuration 2B.

91
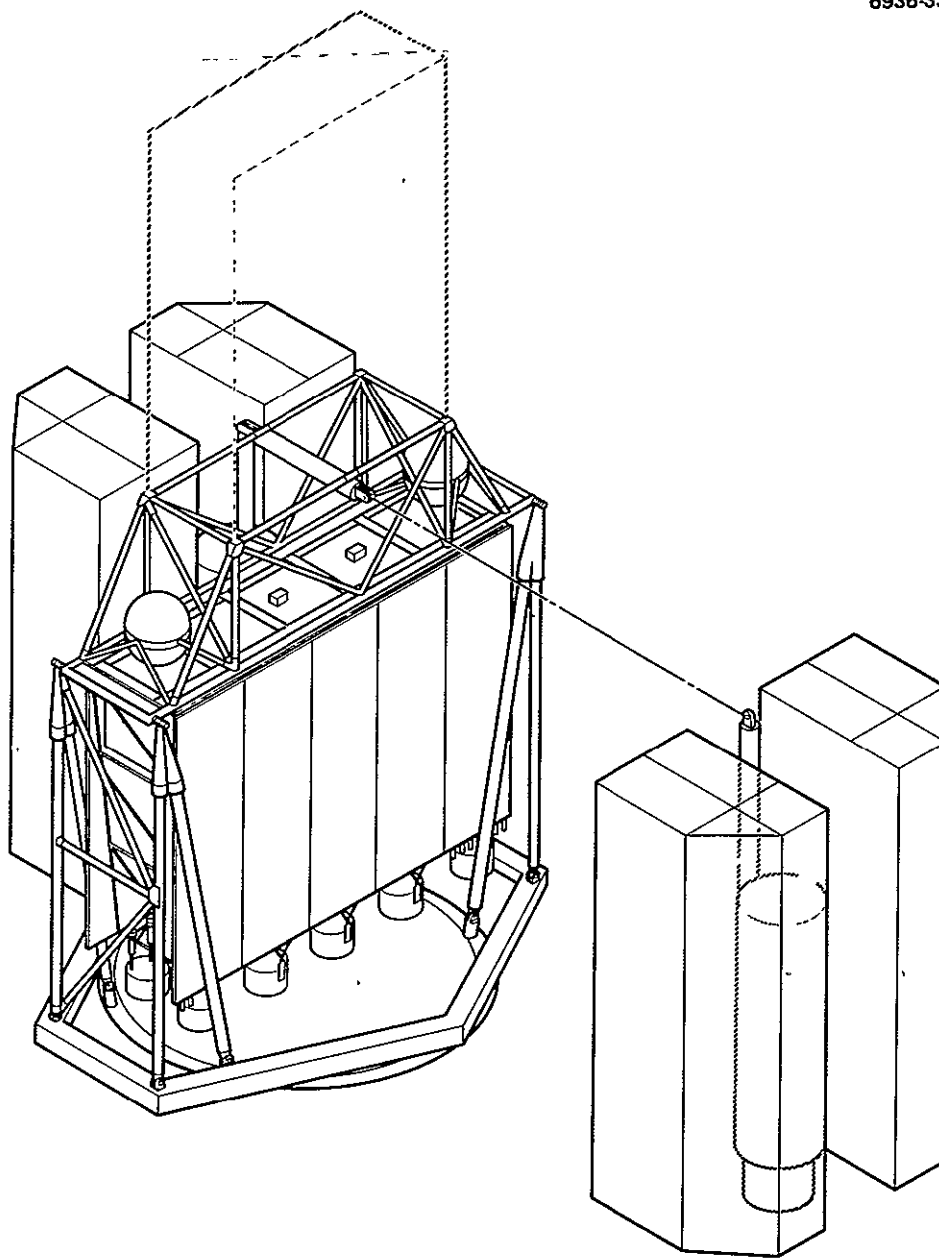
Figure 32.   Configuration 2B stowed.

6936-32

Figure 33.   Configuration 2B deployed.

SOLAR ARRAY AND
EXTENSION MECH

ASTROMAST

2 98m
(117 5 in.) DIA BC
(IUS)

4 57m
(180 in)

SHUTTLE BAY
ENVELOPE

0 93m
(36 5 in)

SYMMETRIC ABOUT
THE CENTERLINE

2 03m
(80 0 in)

MISSION
MODULE
INTERFACE

2 29m
(90 0 in)

SOLAR ARRAY

2 54m
(100 0 in)

4 534m
(178 5in)

RADIATOR
18 2m^2
(196 ft^2)

COLD
PLATE

SEPARATION
SPRING

ION
THRUSTER

ASTROMAST

IUS INTERFACE
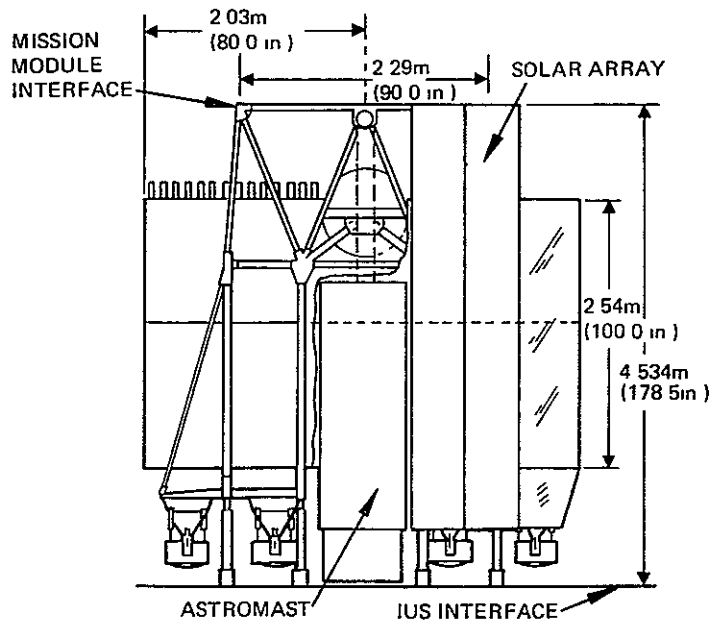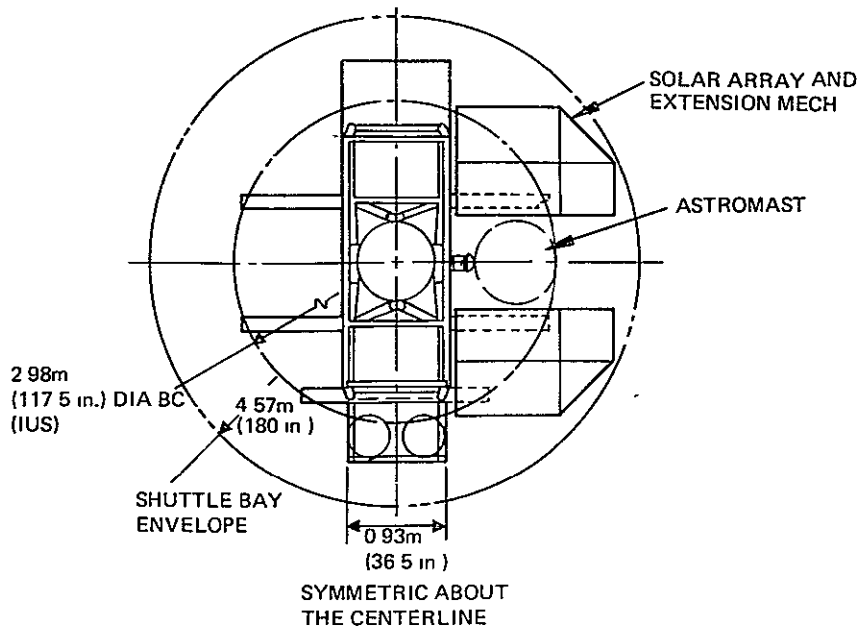
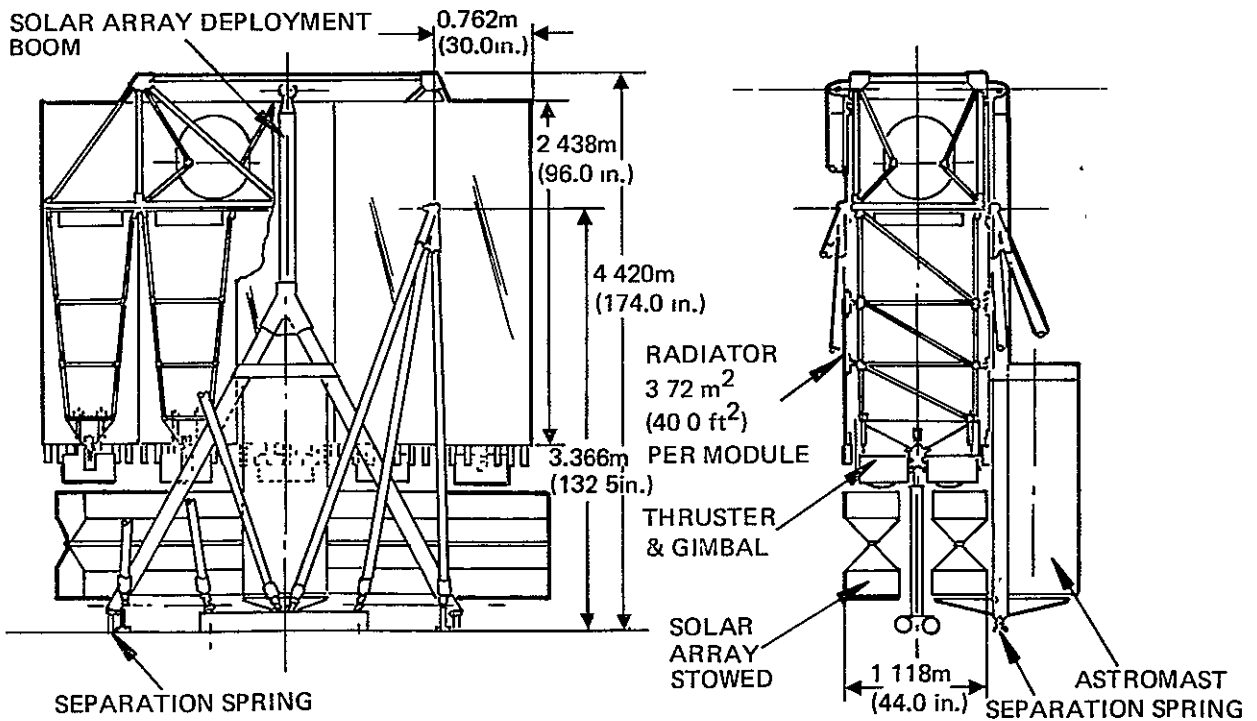Figure 34. Configuration 2B/I.

94
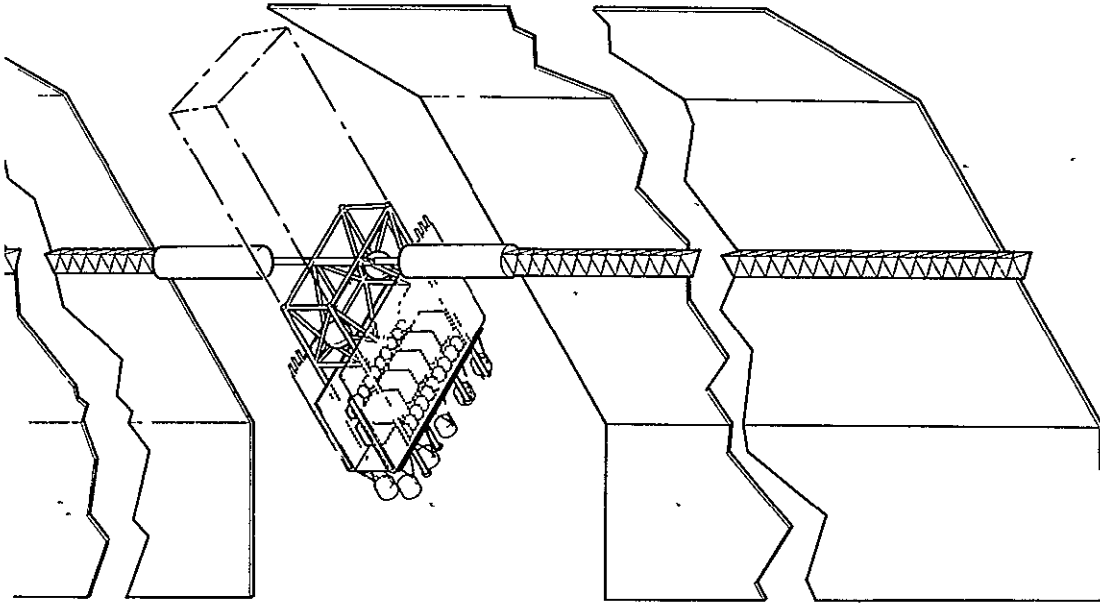
Figure 35. Configuration 2B/I deployed.
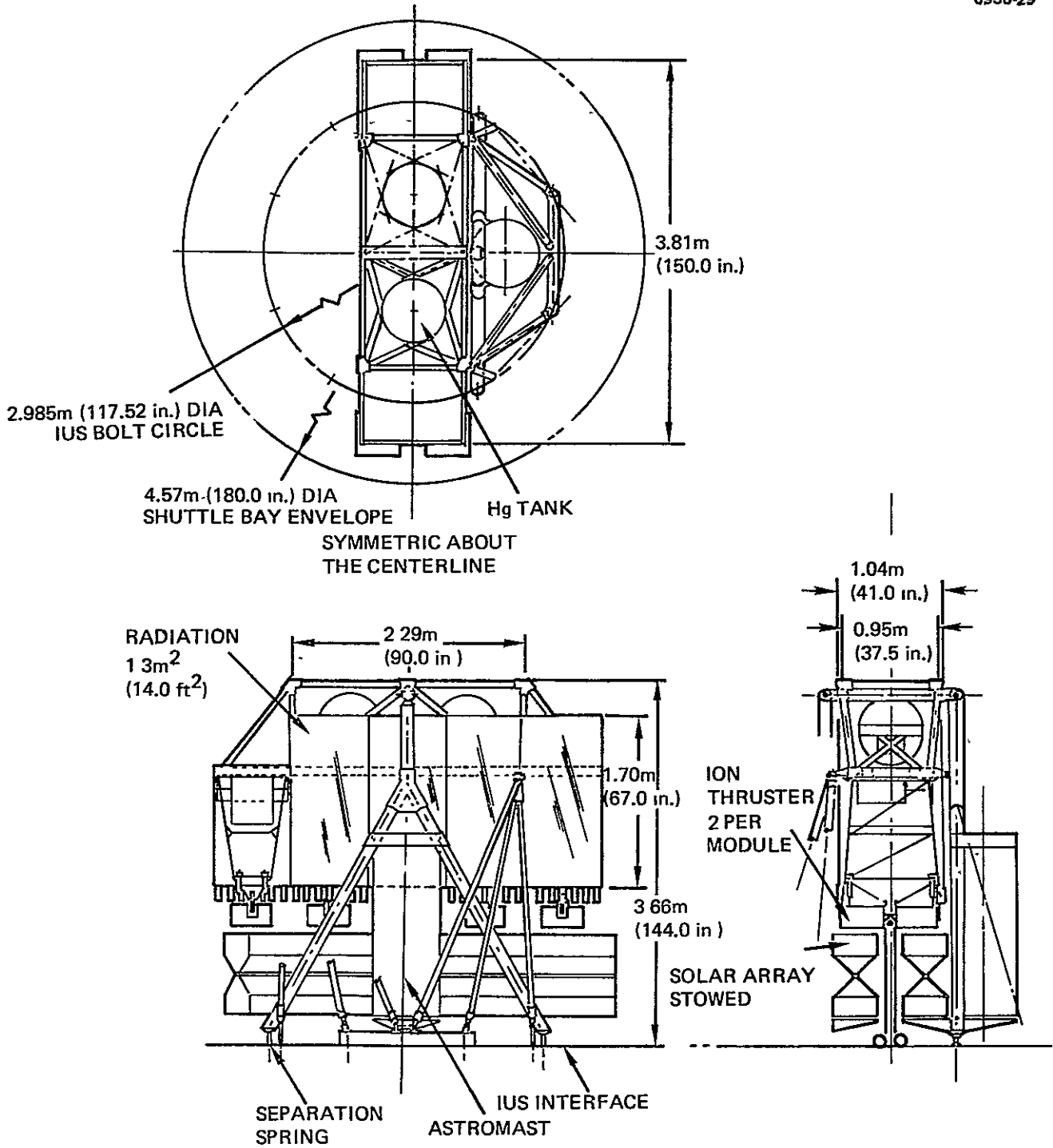
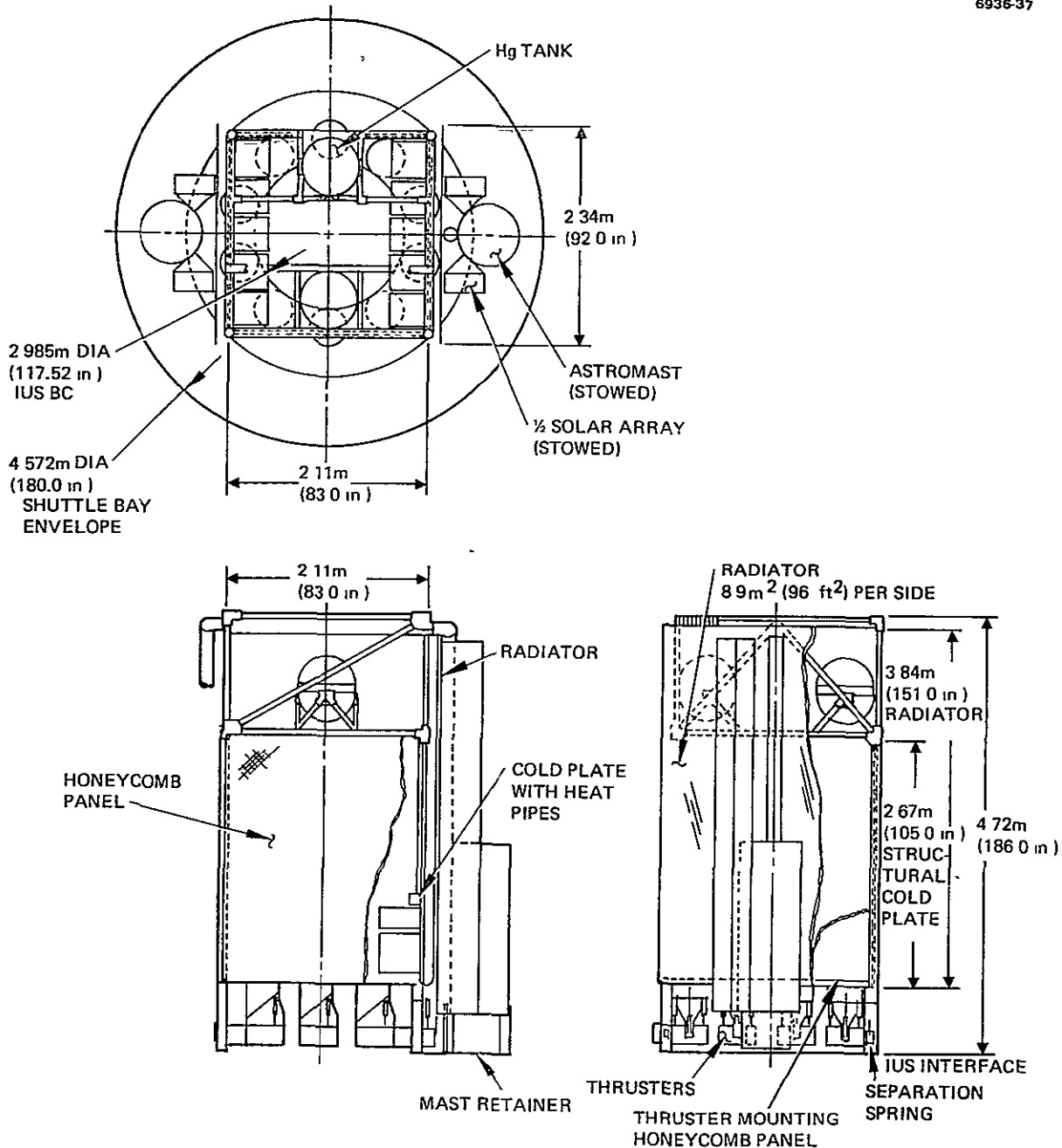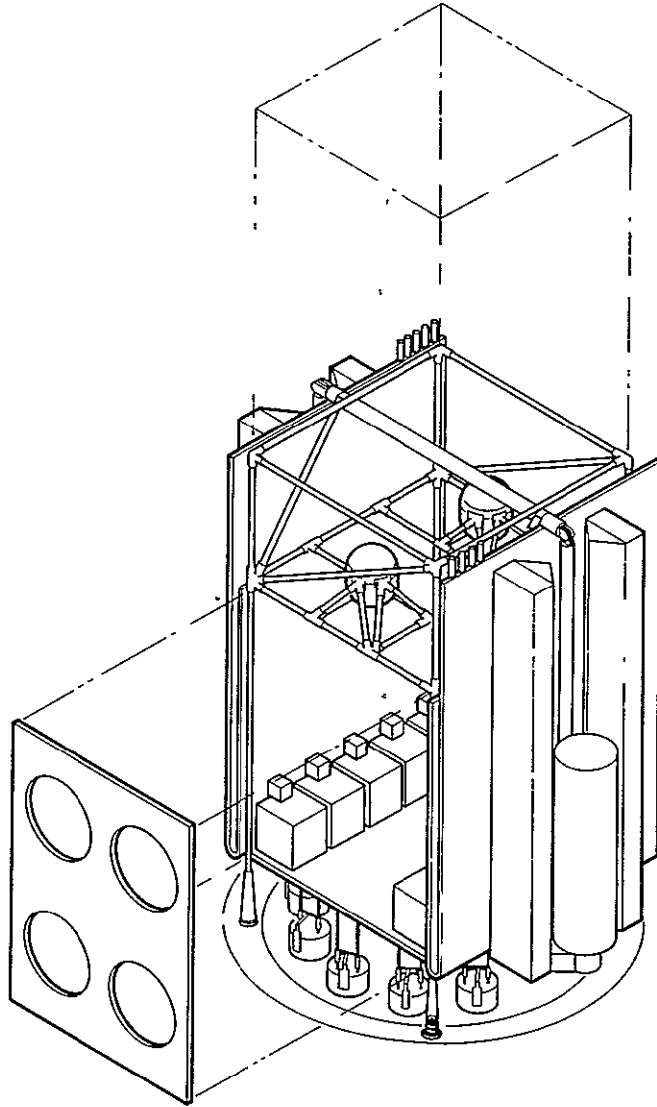Figure 36.   Configuration 3A.

96
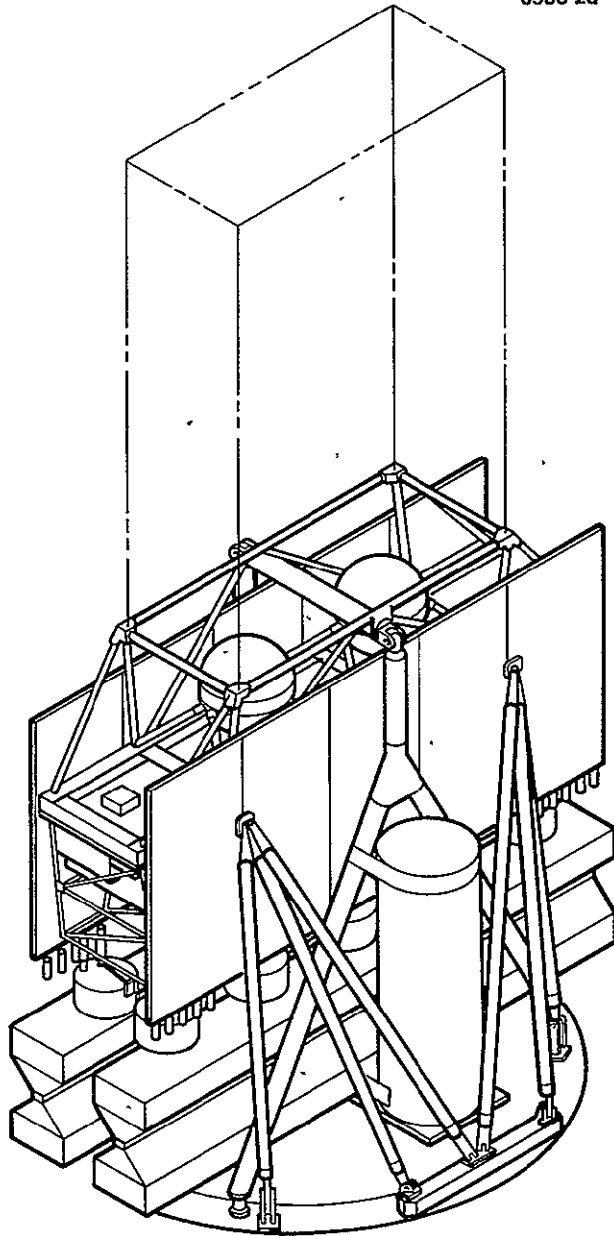
Figure 37.   Configuration 3A stowed.
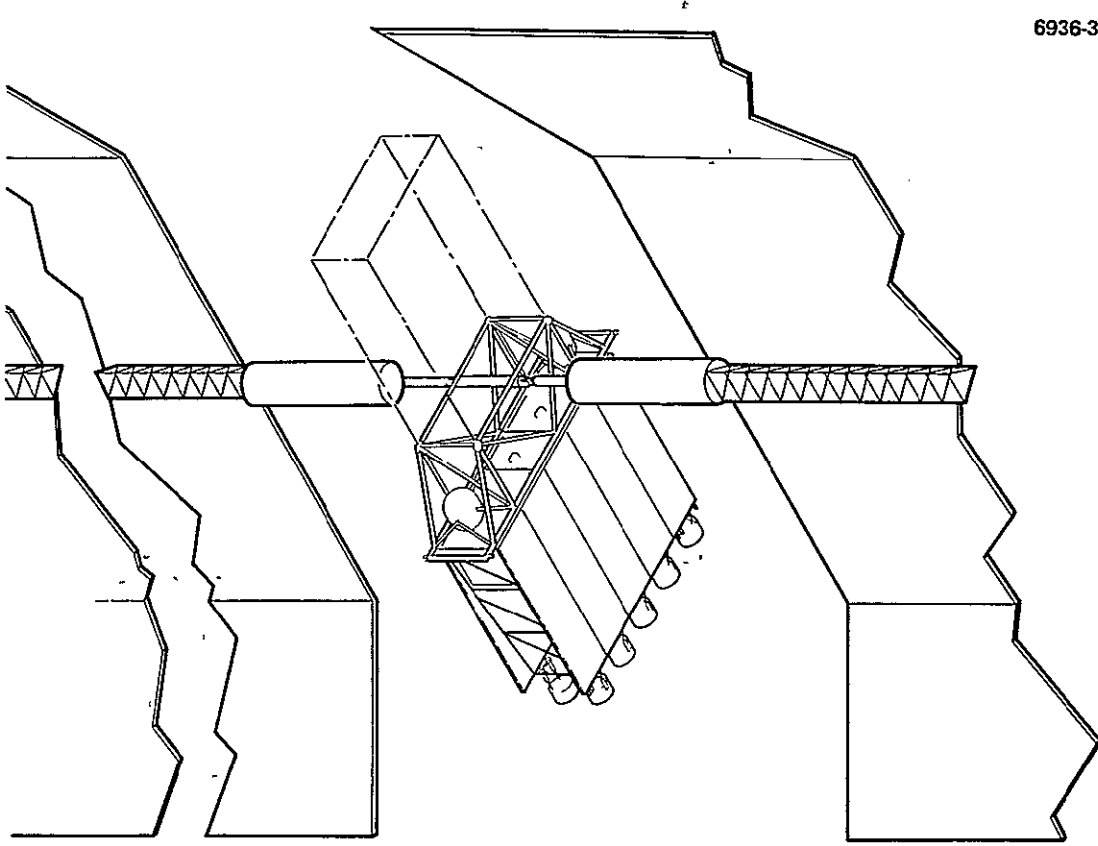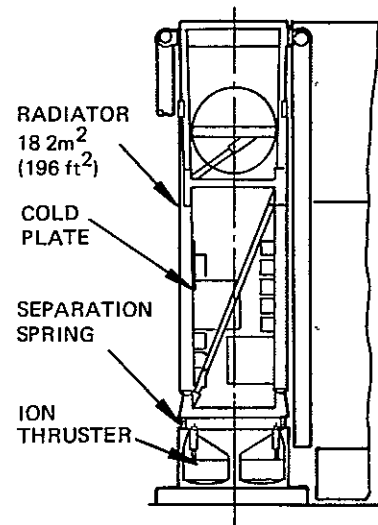
D. COMPARISON OF STRUCTURAL DESIGN CHARACTERISTICS

The seven designs discussed in Section 4 are compared here in terms of their principal design features:

- Design of the support structure to withstand loads

- Adapter design

- IUS separation subsystem design

- Characteristics of structural interface with mission module

- Choice of materials.

In addition, those design features of the integrated configurations that distinguish them from the modular configurations are explained. Several special features of interest for the individual configurations are also discussed: relative complexity of solar array stowage and deployment, assembly/test accessibility, required deployed array-thruster separation distance to prevent mercury ion contamination.

The principal distinguishing features are summarized in Table 26 for the discussion which follows. The materials used are the same for all configurations; they are discussed separately later. Configurations 1A and 1AX are similar and are treated jointly throughout this discussion. The difference in their masses is discussed in Section 4.E.

1. Critical Design Considerations

The principal constraints and requirements that are critical in designing the structure for minimum mass are indicated in Table 26. The reasons for the checked items will become fully evident as design features are explained. The following general observations will be helpful.

The requirements for modular construction constrain all but the 2A/I and the 2B/I configurations. The size of the stowed solar array impacted all configurations; additionally, the length of the 3A and 2A configurations was influenced by the thermal radiator size requirements. The design of configurations 2A, 2B, 2B/I, and 3A was also influenced by the requirement to provide supports for the cantilevered thrusters; the

Table 26. Comparison of Key Structural Design Characteristics

Design Characteristics	Configuration					
	1A and 1AX	2A	2A/I	2B	2B/I	3A
Critical design considerations						
Modularity requirement	Yes	Yes	No	Yes	Yes	Yes
Stowed solar array size	Yes	Yes	Yes	Yes	Yes	Yes
Solar array deployment	No	No	No	Yes	Yes	No
Thermal radiator size	No	Yes	No	No	No	Yes
Cantilevered thrusters	No	Yes	No	Yes	Yes	Yes
IUS adapter mass/loads	No	No	No	Yes	No ˙	No
IUS separation	Yes	Yes	No	Yes	No	Yes
Structural features						
Stowed array orientation relative to thrust axis	Normal	Normal	Parallel	Parallel	Parallel	Normal
Thermal radiator extension over interface module	No	Yes	Yes	No	No	Yes
Flexible, efficient structural arrangement/design	No	No	Yes	No	Yes	No
Supports (snubbers) required for cantilevered thruster storage	No	Yes	No	Yes	No	Yes
IUS extension beams required	No[a]	Yes	No	Yes	Yes	Yes
IUS extension beams protrude beyond bolt circle	No	No	No	Yes	No	No
IUS separation						
Separation plane. at IUS interface or at cold plate (CP)	CP	CP	IUS	CP	IUS	CP
Springs actuate through	Array yoke	Array yoke	Major structure	Astromast canister	Major structure	Array yoke
Adapter leg articulation (rotation) required	Yes	Yes	No	Yes	No	Yes
Mission module interface						
Area of the four-point attachment rectangle, m²	2 6	2 4	4 4	2.2	2.2	2.2
Ratio of rectangle legs	0 42	0 46	0 93	0.44	0.44	0.44
Other						
Accessibility	Fair	Poor	Excellent	Poor	Good	Poor
Minimum Hg impingement angle θ (initial design), deg	45	77	97	26	45	63
Added (deployed) separation of array required[b]	Some	None	None	Significant	Some	None

[a]Not required for structural loads or mass reduction but included for improved IUS separation implementation

[b]Design modification (acceptable to solar array) to attain 50°

T5916

99

short cantilevers in 1A/1AX configurations did not impose this requirement. IUS loads and separation significantly influenced structural and adapter designs for all modular configurations, especially for 2B which required a special design effort to preclude prohibitive mass penalties. Configurations 2B and 2B/I were also influenced by solar array deployment requirements.

2. Structural Features of Configurations 1A (and 1AX), 2A, and 3A

Although thrust system configurations 1A, 2A, and 3A have similar structural designs, they differ significantly in overall length because they require different thermal radiator lengths (in order of length, 1A, 3A, 2A). All three configurations are modular and have the solar array stowed below the thrust modules in the direction normal to the thrust axis. To minimize length (and mass), the thermal radiators for configurations 2A and 3A extend above the separation plane and over the sides of the interface module. This is not required for the lower-dissipation direct-drive thrust system configuration 1A. The design and assembly features of the thrust modules are shown in Figure 38. The four-tripod adapter design is shown in Figure 39 (and fully discussed for the baseline in Volume II); the adapter design is similar for all configurations. The separation plane between the IUS and the thrust system is at the bottom of the interface module (marked CP in Table 26). Two of the adapter tube legs attach to a common fitting at the separation plane; the third leg attaches to a separate adapter end fitting. The legs are hinged at the IUS with a preloaded torsion spring. In all cases, unobstructed egress is provided during separation by spring-actuated articulation (rotation) of the adapter legs and by spring-actuated pushoff through the array yoke.

The difference in the overall length of these three configurations is the main reason for differences in their structural designs (i.e., the length of the cantilevered thruster supports and the inclination of the adapter tripod). Because of the length differences, we had to examine supplementary structures for aft support of the thrusters (snubbers) and extension beams to provide a broader base for the

6936-27
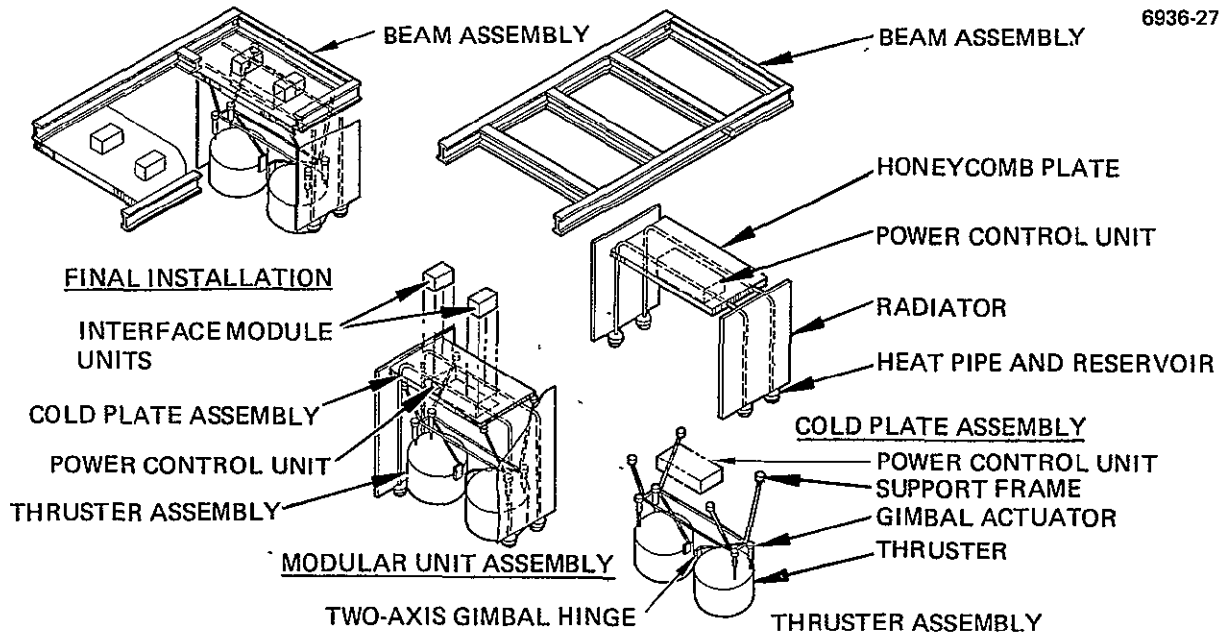
Figure 38. Thrust module design and assembly.

6679-30

INBOARD TUBE

OUTBOARD TUBE

SEPARATION
FITTING

OUTBOARD
TUBE

ADAPTER

ROTATION AXIS

HINGE AND
TORSION SPRINGS

IUS CROSS-BEAM

TO IUS BOLT CIRCLE
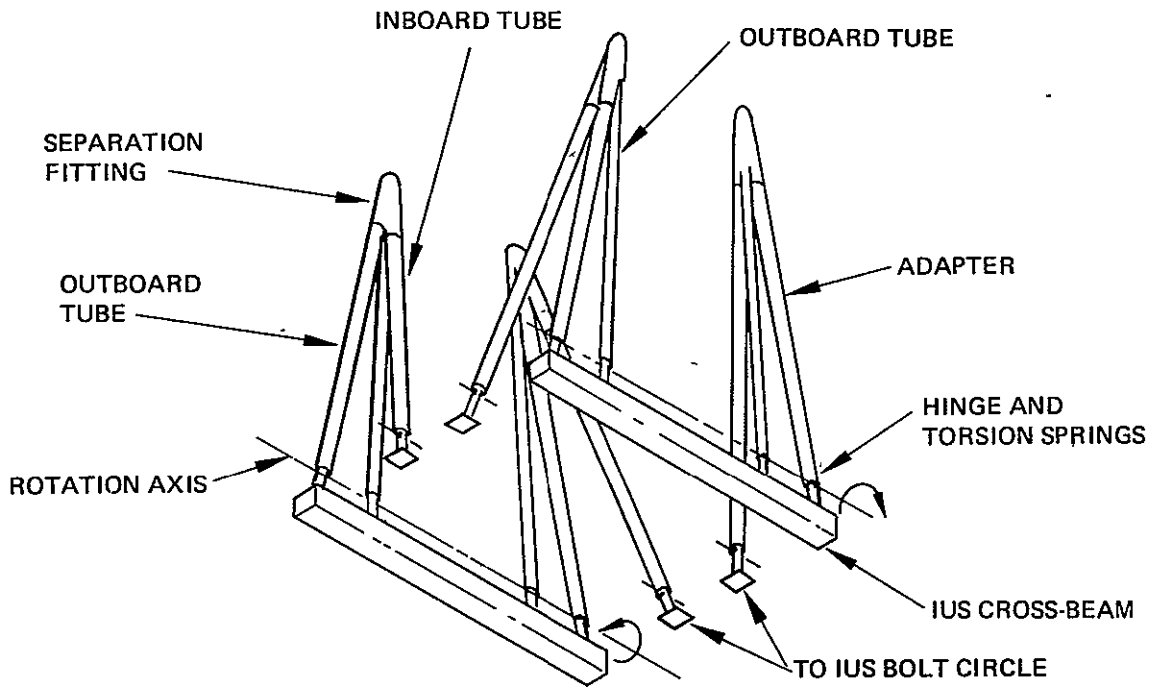
Figure 39.   Adapter design for configurations 1A, 1AX, 2A,
and 3A.

102

adapter tripod than is available on the IUS interface bolt circle. The relatively long cantilever support of the thrusters in configuration 2A implies a highly flexible support structure and a relatively large displacement at the thruster end if the structure is subjected to vibrational loading at low excitation frequencies. This results in a correspondingly high load magnification. Of the two solutions possible — larger support members (increased stiffness) with resulting mass penalty, and lateral restraint of thrusters with additional aft supports (snubbers) — the latter approach was selected (as is evident in the side view in Figure 26). The relatively short cantilever length in configuration 1A does not require such snubbers. Configuration 3A falls somewhat between the cases mentioned above: requirements for snubbers are marginal, and the proposed design incorporates them. Efficient transmission of lateral forces axially through the adapter tripod tubes (i.e., with small magnification) is achieved with a large relative inclination of the tubes. The short length of configuration 1A permits an efficient adapter structure design without using extension beams at the IUS interface. For the longer thrust system, configurations 3A and 2A, such extension beams are required to avoid a significant mass penalty that would be incurred if the same function were performed by increasing the adapter tube diameter. These IUS extension beams are reflected in the entries in Table 26 and in the configuration layouts in the previous subsection.

Increasing the inclination of the adapter tubes would also facilitate deploying the adapter at separation. Therefore, two small IUS beams were also incorporated in the 1A design. For thrust system configurations 1A, 2A, and 3A, however, the IUS extension beams can be confined within the limits of the IUS interface bolt circle.

An alternate to thrust system configuration 1A was considered for the alternate stowed array arrangement shown in Figure 24. The length of the thrust system is shorter in this configuration (by about 0.4 m) and the inclination of the adapter tubes is greater. However, the resultant saving in mass was more than offset by the mass of the relatively long support beams required at the IUS interface. Also, these

103

support beams would extend beyond the IUS bolt circle. The net mass penalty of the alternate to configuration 1A relative to 1A was estimated to be about 10 kg. Similar assessments were made regarding possible alternate designs for configurations 2A and 3A. Accordingly, the alternate solar array stowage concept was abandoned, although this decision perhaps should be reconsidered if later it is desired to minimize post-deployment on-orbit mass at the expense of IUS payload mass and IUS interface complexity.

IUS separation is accomplished using pin pullers and separation springs. Pin pullers rather than concentric bolts were selected for the 2A and 3A configurations because there are several potential interface problems associated with thermal radiators that extend over the separation plane. Concentric bolt with explosive separation nut devices, although more reliable in assuring positive separation, could seriously affect the radiators. Pin pullers were also included in the 1A design, subject to future reassessment. During separation, axial forces are transmitted in double shear through the pin to the adapter fittings, and lateral forces are transmitted by bearing against adjustable stops. Separation springs are located at the base of the solar array boom support. When the pin is withdrawn, the legs of each tripod fall away: two legs as a unit, and the third leg independently. The pushoff springs provide the desired separation velocity.

3. Structural Features of Thrust System Configuration 2B

Thrust system configuration 2B required special design measures because of the constraints imposed by the stowed solar array. The dimensions of the array's stowage cannister are so large that it would have barely fit within the space allowed. These constraints were significantly reduced for the selected baseline derived from this configuration by a smaller solar array envelope that was subsequently specified by NASA LeRC.

Since the large array cannisters could not be oriented horizontally within the shuttle envelope, they were stowed parallel to the thrust axis, overhanging the IUS interface ring. This required a heavy adapter

104

structure, as shown in Figures 31 and 32. The modular structure comprising the interface module and the thrust modules, similar to that for configurations 1A, 2A, and 3A, is supported by the two cradle-type structures attached to the ring of large beams at the IUS interface. The adapter tripods embrace the extreme ends of the thrust system — two on each side. Four end posts are laced with diagonal members to transmit the lateral forces and to reduce the effective column length. The large IUS beams, which necessarily extend beyond the IUS bolt circle to prevent a large mass penalty, carry the loads to the IUS. The solar array is supported by the astromast canister and snubbers. As shown in Figure 31 and noted in Table 26, support snubbers are also required here to support the cantilevered thrusters. Among the seven configurations, this is the only instance where it is necessary to have the IUS beams extend beyond the circumference of the bolt circle.

The height of the stowed array influenced the length of configuration 2B since the mission module space above the interface plane must not be encroached upon. The thrust modules, and the overall 2B configuration, are longer than for 2A, and the thermal radiators do not extend over the interface module.*

The thrust system-adapter separation plane at the bottom of the interface module, and the method of IUS separation by articulation of adapter legs, are similar to those discussed previously, but the load paths and mechanization are necessarily different. The solar array loads are carried through the astromast canister. Because thermal radiators do not extend beyond the thrust system-adapter separation plane, concentric bolts and shear cones, and push-off springs, are used for separation. A high-strength bolt inserted into an oversize hole and isolated from bending forces is threaded into an electro-explosive separation nut. The shear cones align the adapter with the thrust system and transmit the lateral forces across the separation plane. The push-off springs are compressed when the adapter and spacecraft are mated. Because their location is optimal, the springs provide a

---

*Volume II, Section 9.B.

positive, accurate separation force. A cursory separation analysis indicated that a separation force of approximately 17,800 N (4000 pounds) would be required. This could be produced with four springs with a spring rate of 1400 N per cm (800 pounds per inch) and a deflection of 3.2 cm (1.25 in.).

The design approach is also dominated partially by the deployment of the large volume array. To assure design integrity, a preliminary conceptual deployment sequence was analyzed, (one not furnished as part of the data base) and is illustrated in Figure 40. Many more articulation steps than those required for the flat array are evident, but the compatibility of solar array deployment with structural configuration design was shown conceptually.

4. Structural Features of Integrated Thrust System Configurations 2A/I and 2B/I

Thrust system configurations 2A/I and 2B/I were structured and sized to determine the possible advantages of abandoning modular construction and allowing greater flexibility in efficiently arranging the thrust system components on an integral structure. The principal aim was to determine the degree to which mass could be reduced. Thrust system configurations 2A and 2B were selected for this study (as directed by NASA LeRC) because the mass savings were expected to be larger for these configurations because they are heavier than are configurations 1A and 3A.

Since the mass of the adapter was relatively large for the 2A and 2B configurations (compared to 1A and 3A), and we were concerned that the total mass might exceed IUS payload capabilities, the effort was directed towards minimizing the total mass on the IUS rather than mass of the injected spacecraft. In retrospect,* mass minimization of the injected spacecraft is a more desirable objective. Nevertheless,

---

*Subsequent inputs from NASA LeRC indicated that IUS payload capability could be assumed to be significantly greater than originally stipulated, pending mission trajectory tradeoffs. This was used in baseline design, described in Volume II, to minimize the mass of the injected spacecraft.

6936-28
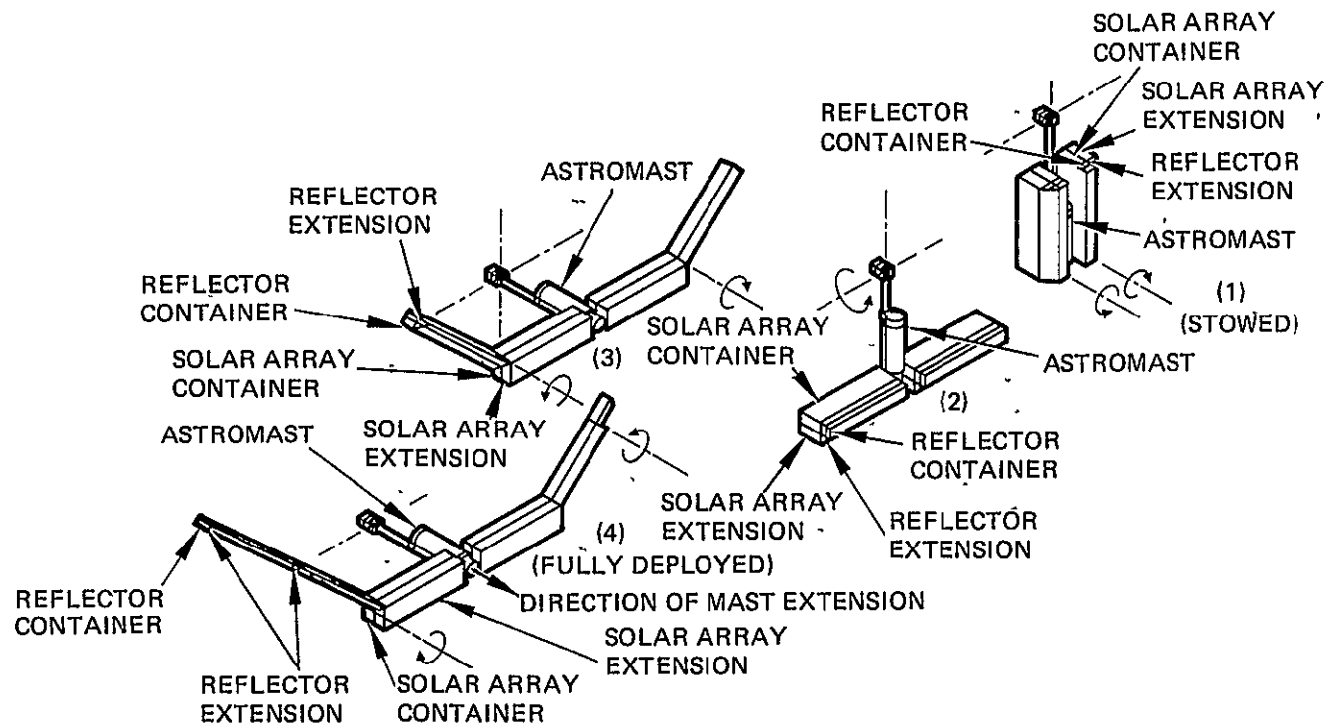
Figure 40. Conceptual deployment sequence of concentrator solar array.

107

the conclusions of the study are basically valid with respect to assessing the relative benefits of integrated versus modular designs.

Several different integrated structural arrangements were explored. Although the design development for these configurations was not as extensive as for the modular configurations, the analysis did identify the major benefits and disadvantages of integration and estimate potential mass savings. Because the volume occupied by the stowed concentrator array is larger in thrust system configuration 2B/I, design of configurations 2A/I and 2B/I was approached somewhat differently. The difference between modular and integrated configurations is reflected in the features common to both integrated designs 2A/I and 2B/I. Both integrated configurations have a common cold plate and only two radiators, one on each side of the integrated thrust system structure. Shear web panels are used on the two opposite sides. Loads are partially carried by these panels and partially by the radiator/cold plate assemblies. The solar arrays are stowed alongside the radiators, in the direction parallel to the thrust axis. They are coupled to the IUS with a simple adapter at the bottom of the thrust structure. The separation plane is at the IUS interface. Neither the tripods nor the associated articulation (rotation) of support arms that are required for the modular configurations are necessary. Separation is accomplished using concentric bolts with springs actuating against the major structure.

The differences between configurations 2A/I and 2B/I relate to the size of the stowed concentrator array. These differences are in the arrangement and support of the thrusters and in the design details of the adapter (including the requirement for IUS support beams). An integrated design for the smaller stowed array of the baseline configuration would have led to a configuration closer to 2A/I.

Configuration 2A/I has the ten thrusters arranged in a circle and supported by a common shelf. As in configuration 2A, the thermal radiators extend over the mercury tanks above the cold plate to minimize thrust system length. The holes shown in the side panels in Figures 29 and 30 reduce structural mass and provide access to the assembled configuration. The outside dimensions of the square structure

(2.1 m x 2.1 m) place it within the IUS bolt circle. The simple adapter is comprised of four columns which attach the bottom of the thrust system directly to the bolt circle.

Configuration 2B/I, which is constrained by the space available, features a rectangular integrated truss structure with the thrusters in line, five on each side. The main truss supports six thrusters, and two overhanging extension shelves support the remaining four thrusters, two on each side. Because the length of the configuration is determined by the length of the solar array (as for configuration 2B), there is no requirement for the thermal radiators to extend above the common cold plate. The structure is also supported on the bottom with a simple four-column adapter. The structural geometry, however, requires that IUS extension beams be added to carry the loads; these extension beams, as indicated in the top view in Figure 34, need not extend beyond the circumference of the IUS interface bolt circle.

Configuration 2B/I differs somewhat from the other configurations in that it utilizes only one mercury tank. A two-tank system was selected for the other configurations, which were designed earlier than 2B/I, for reasons discussed in Volume II. The reasons for this choice are not very compelling, and a single-tank system could be easily adapted to each configuration with only minor penalties and a negligible mass difference. In the two-tank systems, the tanks are located close to the adapter supports to minimize bending stresses and to raise the structural frequencies. In configuration 2B/I, it would have been awkward to place the two tanks in the three bays, and a single-tank design was chosen (with the tank located in the center bay along the thrust system axis). The tank diameter was increased from 0.6 m for the two-tank system to 1.0 m. The impact of this design difference on the overall comparison of the seven configurations is negligible.

Although the integrated configurations were not optimized, significant conclusions can be drawn relative to the mass difference between modular and integrated designs. The discussion below is based on the mass breakdown analysis (summarized in Section 4.E).

Comparing configurations 2A/I and 2A indicate that there is likely to be no significant difference in mass for any subsystems other than the structure and the adapter. Different integrated design approaches merely reflect tradeoffs between the masses of these two subsystems. Configuration 2A, the design selected, was intended to minimize IUS payload. In that design, the adapter mass has been drastically reduced — from 110 kg to 20 kg. This 90 kg saving was, however, partly negated by the heavier (by about 60 kg) on-orbit mass, which was largely due to the increase in the mass of the structure by about 55 kg. That increase is largely attributable to the side panels and to the bottom shelf of configuration 2A/I. Alternate integrated design approaches that minimize on-orbit mass might reduce structural mass relative to 2A, at the expense of adapter mass, but the design analysis conducted during this study indicates that a significant reduction in on-orbit mass would be very unlikely.

Comparing configurations 2B/I and 2B indicates that adapter mass was significantly reduced (150 kg versus 220 kg for 2B) and that total injected spacecraft mass was reduced somewhat (1020 kg versus 1050 kg for 2B). A net reduction in IUS payload mass of about 100 kg (70 kg for the adapter and 30 kg for the thrust system) was thereby achieved. Here the basic similarities between thrust system structures for configurations 2B/I and 2B, which were necessitated by stowed array volume constraints, precluded a significant change in thrust system structural mass: again, some increase was necessary ($\sim$5 kg), primarily because of the mass of the extension shelf for the outside thrusters. The principal reduction (about 35 kg) stemmed from the more compact (single blanket) design of the thermal control subsystem.* In any event, the same

---

*This conclusion may not be entirely valid. The mass of the thermal control system for 2B is somewhat suspect, since subsequent, more detailed analysis for the baseline in Volume II led to lower mass estimates. Time did not permit a full reassessment of the mass of the thermal control subsystem for configuration 2B.

general conclusions reached for the comparison between 2A/I and 2A
-above apply here: no significant-reduction in on-orbit mass is expected
with an integrated design; a significant saving in IUS payload mass
might be obtained by simplifying the adapter structure; and tradeoffs
are available between adapter and structural designs that reflect on
potential IUS payload mass reduction versus the extent of reduction (or
increase) in injected spacecraft mass.

5. Materials

The criteria used in selecting structural materials were (1) to
satisfy structural requirements, (2) to minimize mass (without an exces-
sive cost penalty), (3) to facilitate manufacture, and (4) to be obtain-
able on a procurement cycle that is compatible with the required schedule.
As a further ground rule, the same materials basically were selected for
all the configurations because this eliminated materials as a variable
without compromising design optimization. The selection was governed
by the availability of state-of-the-art materials. High-modulus fiber
composites (such as graphite/epoxy, boron epoxy, and fiber reinforced
materials) should be considered in the final design of the selected
baseline.

Table 27 summarizes the materials used for structural members.
Aluminum and beryllium were used as principal structural materials.
Aluminum was used for components that do not greatly influence overall
spacecraft rigidity and for parts that require a significant amount of
machining. Beryllium was only used in elements for which stiffness
requirements were critical. In particular, beryllium was selected for
the long adapter columns (because a prohibitively large tube diameter
would be required with aluminum) and for the IUS beams (because this
provides a rigid support with less mass). Aluminum was selected for
interface truss tubes and corner fittings. In the subsequent design
definition of the baseline configuration (Volume II), aluminum was
replaced with beryllium for the interface module truss. Aluminum sheet
(alloy 6061-T6) was chosen for fabricating the radiator and cold plate
face sheets because of its strength, stiffness, and high thermal

Table 27. Materials

Component	Material
Heat pipes	Stainless steel
Interface truss[a]	Aluminum
Cold plate	Honeycomb — aluminum face sheet
Radiators	Aluminum
Solar panel deployment booms	Beryllium
Thruster support beams	Titanium
Thrust module structure	Titanium
Adapter	Beryllium
IUS interface beams	Beryllium

T5816

conductivity. Titanium was selected for the small-diameter thruster truss structures to isolate the high-temperature thruster environment from the electronics. Materials selected for the elements of the various subsystems not shown in Table 27 were described in Volume II.

6. Mission Module Structural Interface

One design objective was to achieve favorable structural interface with the mission module. All seven designs provided a four-point attachment to the mission module, but differed somewhat in the location of these attach points. The relative "figure of merit" is determined by the geometric properties of the rectangle formed by the four points of attachment. The structural interface is improved as the rectangle approaches a square and as its area increases.

These two parameters — rectangle area and length-to-width ratio of the rectangle — are shown in Table 28 for the seven configurations. Configurations 2B, 2B/I, and 3A have identical mission module interfaces.

Table 28. Summary of the Mass and Length of the Seven Structural Configurations

Design Characteristic	Structural Configuration						
	1A	1AX	2A	2A/I	2B[a]	2B/I	3A
Number of thrusters/modules	12/6	12/6	10/5	10/NA	10/5	10/NA	10/5
Mass, kg							
Thrust modules (sum)	355	290	600	NA	650	NA	525
Interface module (including Hg residuals, solar array drive and booms, and solar array deployment mechanisms)[a]	235	265	310	NA	305	NA	240
Subtotal	590	555	910	965	955	930	765
Contingency[b]	60	55	90	95	95	90	75
Thrust system on orbit, dry	650	610	1000	1060	1050	1020	840
Adapter (including contingency, supports, and separation subsystem)	50	50	110	20	220	150	110
Length, m							
Thrust system, overall	2.9	2.9	4.4	4.6	4.9	4.6	3.7
Solar array height (dimension X in Figure 3)	2.7	2.7	4.2	NA	NA	NA	3.5

[a]Mass budget for selected thrust system baseline did not include solar array deployment mechanisms, considered part of solar array mass budget.

[b]10% assumed in this task, versus 15% in sizing selected baseline.

113

T5916

Although all configurations provide an acceptable mission module structural interface, the one provided by configuration 2A/I is by far the best . The differences among the other six configurations are not sufficient to substantially influence selection, although configuration 2A is somewhat better than the remaining five (highest length-to-width ratio, second in area).

7. Accessibility

Accessibility during assembly and testing was also considered in developing the seven designs. Different constraints arose in each case. Table 26 gives relative accessibility ratings, which strongly favor the integrated design approach.

8. Mercury Ion Impingement

The potential for contamination of the solar array by the mercury ions in the thruster plume was a concern, as discussed in Section 2.A, and illustrated in Figure 9. This concern would be eliminated if the angle between the thrust axis and the line to the corner of the deployed array could be kept above 50° throughout the mission. The worst impingement condition would occur when the solar array is fully opened and co-planar with the thrust system. The corresponding "worst case" (minimum) angle will be called θ in this discussion.

That θ will be more than 50° is assured for all designs with a sufficiently large separation distance between the deployed array and the thrust system. In accordance with ground rules in Section 2, assurance of $\theta > 50°$ was not the determining factor in the design of the thrust system (i.e., its length) and the location of the thrusters. The rationale was that the length of the solar array deployment arm could later be increased, if necessary, to meet this requirement.

Table 23 contains the calculated θ's for each configuration. This permitted rating the configurations in terms of the extent of design modification that would be required (i.e., the additional separation distance required to achieve $\theta > 50°$). This is also indicated qualitatively in Table 23. Concentrator arrays are particularly susceptible

114

to Hg impingement, and added separation distance is especially needed for configuration 2B. The short length of configuration 1A also calls for some additional separation. The potential impingement problem with configuration 2B from which the selected baseline was derived did not prove formidable when the modified solar array configuration was defined and a modest increase in solar array separation essentially eliminated it.

E. MASS SUMMARY OF THE ALTERNATIVE THRUST SYSTEM CONFIGURATIONS

Table 28 summarizes the masses of the seven configurations. Table 29 gives a mass breakdown by major subsystem, excluding contingencies. The mass tabulations included the estimated mass of the solar array deployment mechanism to highlight the potential mass penalties of the concentrator array configurations. The final tabulation for the selected baseline in Volume II allocates this mass component to the solar array mass budget. As noted in Table 28, the 10% contingency used initially was later changed to 15% for the selected baseline.

Table 28 also shows the lengths of the seven configurations and, for reference, dimension X (from Figure 3). Dimension X is the required overall height of the flat solar array in the stowed configuration for the four modular designs employing this array. The mass and length of the selected baseline differ slightly from those of configuration 2B. The selected baseline is 0.2 m shorter (4.7 versus 4.9 m, primarily as a result of reduced power dissipation and radiator length) and 130 kg lighter (notwithstanding the 40 kg penalty of using a higher contingency of 15%). The mass comparison is shown in Table 30. A large contributor to the lower mass is that the adapter is 90 kg lighter. The total net reduction in total injected spacecraft mass is therefore only 40 kg.

Table 29. Thrust System Mass Breakdown

Subsystem	Mass of Modular Configurations, kg[a]					Subsystem	Mass of Integrated Configurations, kg[a]	
	1A	1AX	2A	2B	3A		2A/I	2B/I
Thrust module						Thrusters	90	90
Thrusters	17.5	17.5	17.5	17.5	17.5	Gimbals	30	30
Gimbals	6.0	6.0	6.0	6.0	6.0			
PMaC	23.5	13.5	56.0	56.0	50.5	PMaC	410	410
Structure	3.0	3.0	6.0	11.5	5.0	Structure	125.	115
Thermal control	8.0	7.0	32.5	37.0	24.0	Thermal control	170	155
Hg distribution	1.0	1.0	2.0	2.0	2.0			
Total	59.0	48.0	120.0	130.0	105.0	Hg storage and distribution	80	80
Number of modules	6	6	5	5	5	Solar array drive	10	10
Total, all thrust modules	355	290	600	650	525	Array booms and deployment	50	40
Interface module								
PMaC	75	105	130	130	65			
Structure	45	45	45	50	45			
Thermal control	5	5	5	5	5			
Hg storage and distribution	70	70	70	70	70			
Solar array drive	10	10	10	10	10			
Array booms and deployment	30	30	50	40	45			
Total	235	265	310	305	240			
Thrust system total	590	555	910	955	765	Thrust system total	965	930

Table 30. Mass Comparison: Selected Baseline Versus Configuration 2B

Comparison Element	Mass of Baseline Minus Mass of Configuration 2B, kg	Comments
Thrust modules (five)		
PMaC units	+ 55	Increase from 14 5 to 20 kg per unit (as specified by NASA LeRC)
Structure	- 20	New solar array; redesign
Thermal control	- 70	Update Previous estimate found too high, plus redesign 615 for baseline versus 650 for 2B
Net, thrust modules	- 35	
Interface module		
Electronics	+ 10	Addition of solar array control unit
Mercury storage and distribution	- 10	Design update
Structure	- 5	Design update (new array)
Solar array deployment mechanism	- 40	Deleted from thrust system budget (included in solar array budget)
Net, interface module	- 45	260 for baseline versus 305 for 2B
Subtotal	- 80	875 for baseline versus 955 for 2B
Contingency	+ 40	135 (15%) for baseline versus 95 (10%) for 2B
Thrust system on orbit, dry	- 40	1010 for baseline versus 1050 for 2B
Adapter (including contingency)	- 90	130 for baseline versus 220 for 2B (simpler, new solar array)
Total	-130	Main truss -50 -50 IUS support beam -25 -25 Aft support snubbers deleted -15

T5916

117

SECTION 5

COMPARISON OF ALTERNATE THRUST SYSTEM CONFIGURATIONS

The seven thrust-system configurations are compared in this section in terms of their principal design parameters (mass, length, efficiency, reliability) and in terms of the key criteria of technical risks and system interfaces. The other elements of the spacecraft (the solar array and the mission module), although not part of this study, are considered to the extent to which their characteristics affect this comparison. A baseline thrust system configuration was selected on the basis of this comparison. The analysis does not consider cost or schedule (program) impact. The program plan and cost estimates were subsequently prepared for the selected baseline, and are presented in Volume II.

A. THRUST SYSTEM PERFORMANCE PARAMETERS

The two principal performance parameters required for a comparative assessment of the alternative thrust system configurations are efficiency and reliability. To compute thrust-system efficiency requires defining the total power input and mass flow rate for operating the thrust system at a given thrust value. To estimate reliability requires defining all the PMaC and structural elements and their failure modes. A simplified preliminary analysis of these requirements made during the design phase of the study is sufficient for comparing alternative configurations.

Thrust system efficiency and reliability are both influenced by the plan for determining the number of thrusters to be operated and for specifying the beam voltage and current to utilize the available power. Ideally, one would use a logic chart like the one shown in Figure 41 to optimize the thruster operating plan for any given mission. For this study, we were constrained to use the data for a single trajectory for each configuration with both the available power and thrust requirements specified at each point on the trajectory. Consequently, the only loops shown on the logic chart that could be closed were those to

119

```
                    ┌─────────────────────────────────────┐
                    │       TRAJECTORY SPECIFICATION       │
                    ├─────────────────────────────────────┤
                    │        ⊚ POWER AVAILABLE             │
                    │        ⊚ THRUST REQUIRED             │
                    │        ● TOTAL PROPELLANT            │
                    │        ● SUBSYSTEM WEIGHT            │
                    └─────────────────────────────────────┘
```

```
            ┌──────────────────────────────────────────────┐
            │      THRUST SUBSYSTEM REQUIREMENTS            │
            ├──────────────────────────────────────────────┤
            │   ● NUMBER OF THRUSTERS OPERATING            │
            │   ● BEAM CURRENT PER THRUSTER               │
            │   ● BEAM VOLTAGE                             │
            └──────────────────────────────────────────────┘
```

```
 ┌─────────────────────────────────────┐   ┌─────────────────────────────┐
 │      THRUSTER REQUIREMENTS           │   │     PMaC REQUIREMENTS        │
 ├─────────────────────────────────────┤   ├─────────────────────────────┤
 │ ● AMPERE—HOURS PER THRUSTER         │   │      ● REGULATION            │
 │ ● VOLTAGE/CURRENT (PERVEANCE)       │   │      ● CONTROL               │
 │ ● EFFICIENCY                         │   │      ● WEIGHT                │
 └─────────────────────────────────────┘   └─────────────────────────────┘
```

```
            ┌──────────────────────────────────────────────┐
            │      COMPARISON OF CAPABILITIES              │
            │           WITH SPECIFICATIONS                │
            ├──────────────────────────────────────────────┤
            │        ● POWER REQUIRED                      │
            │        ● THRUST PRODUCED                     │
            │        ● PROPELLANT REQUIRED                 │
            │        ● SUBSYSTEM WEIGHT                    │
            │        ⊚ EFFECT OF DIFFERENCES              │
            │             ON TRAJECTORY                    │
            └──────────────────────────────────────────────┘
```

```
 ┌─────────────────────────────────────┐   ┌─────────────────────────────┐
 │      RECOMPUTE TRAJECTORY            │   │    THRUST SUBSYSTEM          │
 │   USING NEW POWER/THRUST            │   │       DEFINED                │
 │      PROPELLANT, ETC                │   │                              │
 └─────────────────────────────────────┘   └─────────────────────────────┘
```
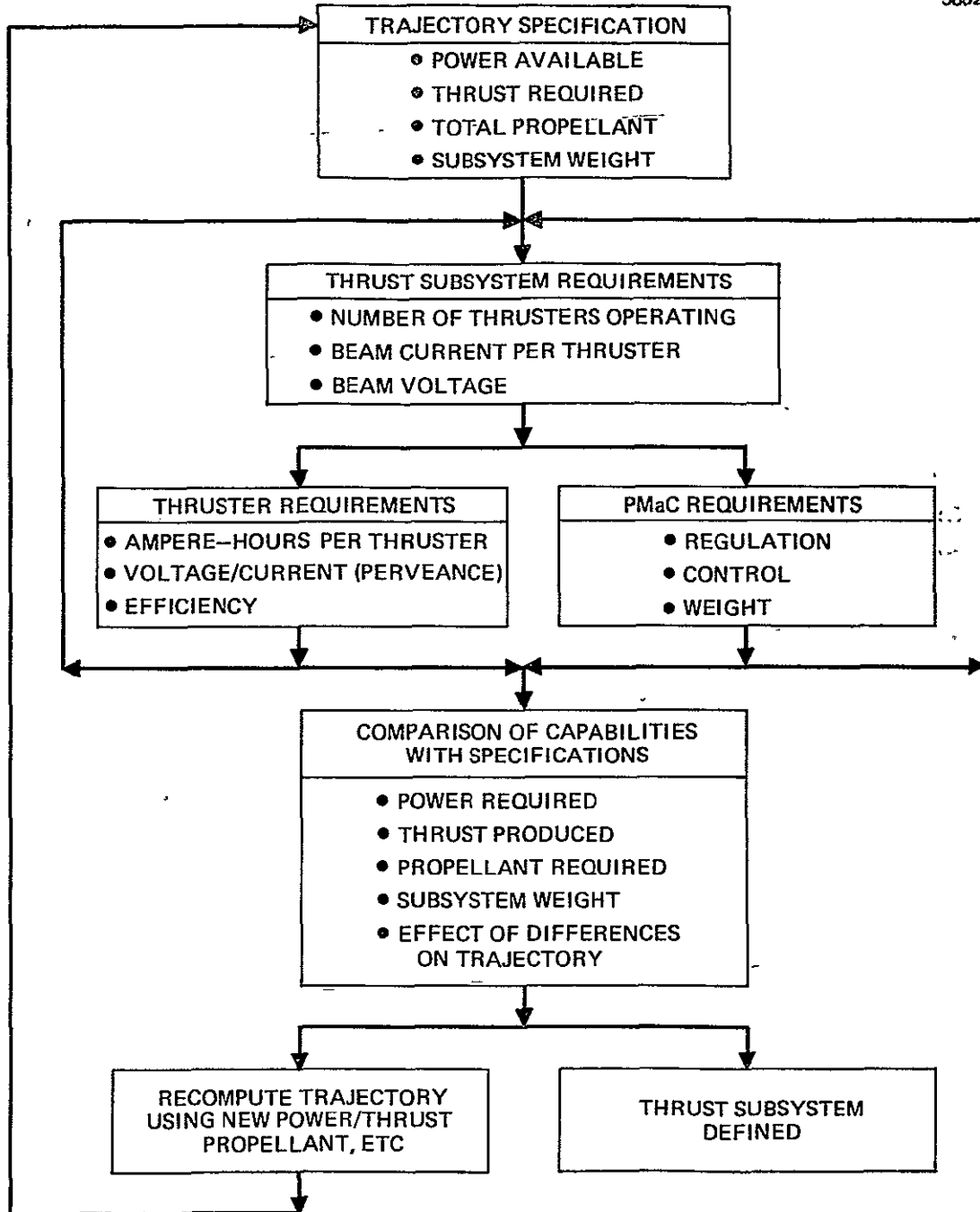
Figure 41. Logic chart for determining logistics and specification
for operating thrusters to achieve the mission
objectives.

meet the constraints on thruster technology or PMaC approaches. During this phase of the study, the thruster technology limits were set as follows:

- A maximum beam current of 2.5 A per thruster

- A maximum beam voltage of 4000 V

- A maximum operating time of 15,000 hr per thruster.

The power available per thruster and the beam voltage depend on the PMaC approach followed and type of solar array used. For a conventional ion-beam power supply, the beam voltage can be specified arbitrarily. For CDVM power supplies, the beam voltage varies with heliocentric distance and can be controlled or specified only by the solar array. Specifying solar array reconfiguration was outside the scope of the study. Therefore, we took as given NASA LeRC's thruster operation plan for both the direct-drive and CDVM PMaC approaches. Figure 42 compares thruster sequencing for a thrust system using a CDVM beam supply and a flat solar array with one using a conventional beam supply and a concentrator solar array. To be consistent, we followed the pattern set by NASA LeRC in that thrusters were turned on and off in pairs to match the solar array power output (as contrasted with one thruster at a time). The operating thrusters were operated at the highest beam current possible (limited by the power available) to maximize propellant efficiency.

Having established a plan for thruster sequencing (shown in Figure 42), it is a straightforward process to add up the total thruster operating hours and obtain the average operating time per thruster. Similarly, the total ion beam ampere-hours can be obtained by using the thruster operation plan for varying ion beam current as a weighting factor to provide an average value for ion beam current. The performance model described in Volume II was used to determine the average propellant efficiency (by using the propellant utilization corresponding to the average ion beam current). This allows converting the total ion beam ampere-hours (for all the thrusters) to total mercury propellant requirement. When the beam voltage remains constant (Figure 42(b)), the average current can be used with the analytic performance model to obtain

THRUSTER SEQUENCING
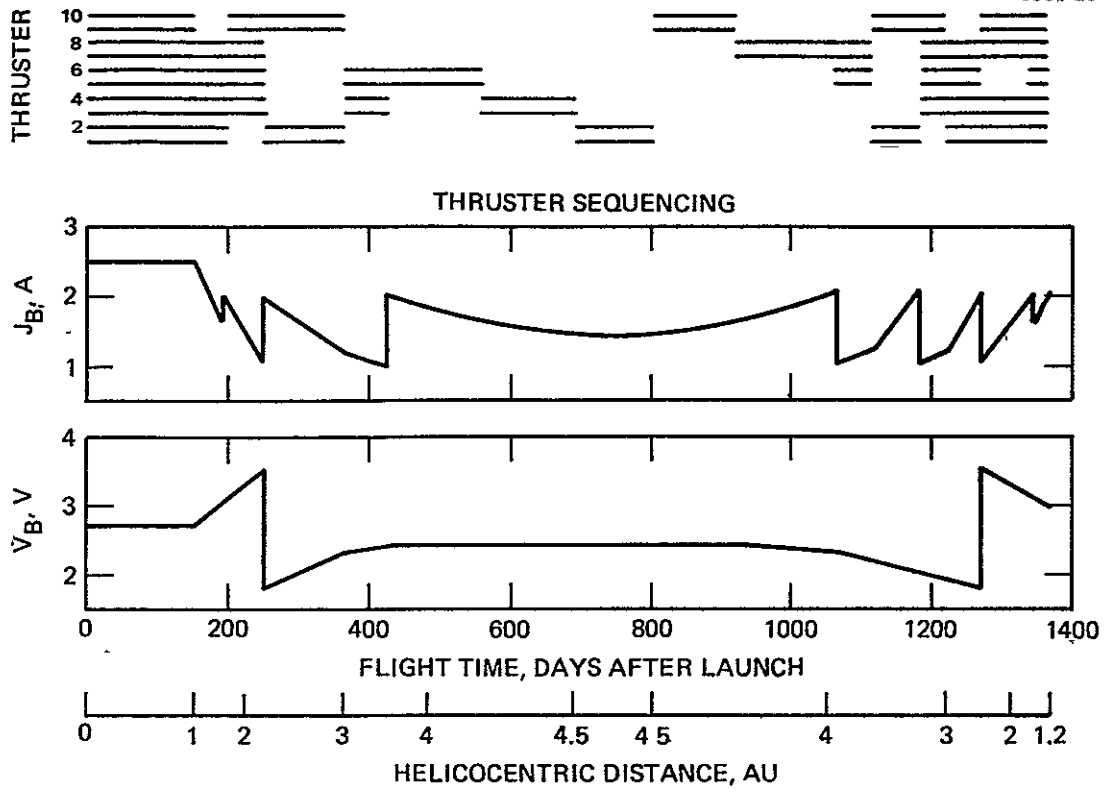
a) VOLTAGE MULTIPLIER PMaC APPROACH, FLAT SOLAR ARRAY

THRUSTER SEQUENCING
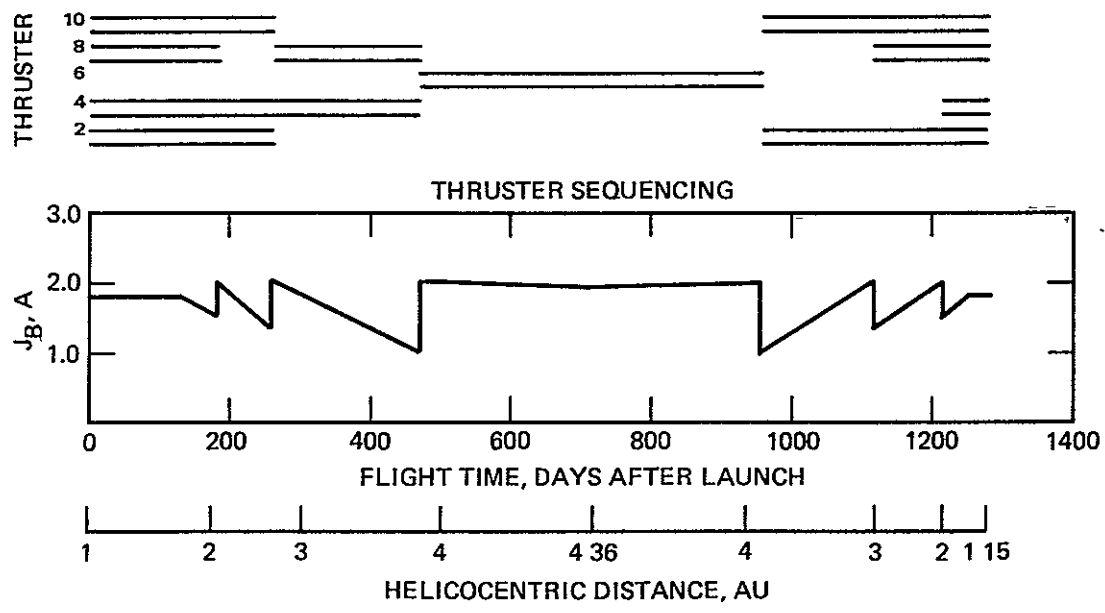
b.) CONVENTIONAL PMaC APPROACH, CONCENTRATOR SOLAR ARRAY

Figure 42. Plan for thruster sequencing and beam parameter control
to match trajectory thrust requirements.

122

the average power input required by the thruster. Thus, all the elements required to compute thruster efficiency can be obtained by specifying a plan for thruster sequencing (as shown in Figure 42). When beam voltage varies (Figure 42(a)), both the average beam power and the average current must be determined for performance characteristics to be evaluated using the analytic model. This requires only performing another summation and then weighting the thruster operating time by beam power to obtain a value for total watt-hours. Thruster efficiency determined in this manner was then used with the appropriate PMaC unit efficiency factors to compute thrust system efficiency.

Analysis of the alternative configurations in the manner described above produced the parameters shown in Table 28. Since, as the only parameters that can be varied in selecting a thruster sequence plan are the beam voltage and current, the direct-drive and voltage-multiplier PMaC approaches offer no appreciable flexibility. Some latitute in beam voltage and current is available for the configurations using a conventional PMaC approach. Consequently, the seven alternatives considered can be reduced to the four cases shown in Table 31. Comparing the conventional PMaC approach configurations that use a flat array (2A, 2A/I) with those that use a concentrator array (2B, 2B/I) shows the effect of changing beam voltage. The power available from the flat array declines so severely at large heliocentric distances that beam voltage must be lowered to avoid operating at very low beam currents and to reduce the power-to-thrust ratio so that the thrust required by the trajectory can be matched. The consequences are an increase in the operating time per thruster and in the total propellant requirement. These consequences are to be expected from reducing specific impulse (beam voltage). Using a concentrator array (and a different trajectory) permits operating at a constant beam voltage over the entire mission without deep throttling (low beam current) and without increased operating time and propellant requirements. Variations in propellant mass of several hundred kilograms can be found by varying the beam voltage over a 200 V range, but it would be necessary to recompute the trajectory before any significance could be attached to the variation.

Table 31. Comparison of Thruster Parameters for the
Design Concepts Considered

Thruster Parameter	Configuration			
	1A, 1AX	2A, 2A/I	2B, 2B/I	3A
Beam current (max), A	2.5	2.5	2.0	2.5
Beam current (min), A	1.0	1.0	1.0	1.0
Beam current (avg), A	1.76	1.76	1.7	1.72
Beam voltage (max), kV	3.9	3.2	2.9	3.5
Beam voltage (min), kV	2.0	1.6	2.9	1.8
Beam voltage (avg), kV	2.7	2.8	2.9	2.5
Maximum thruster power, kW	7.4	8.6	6.3	7.3
Thruster efficiency (avg), %	75.1	75.3	75.2	74.4
Operating time, hr	11,521	14,520	13,056	14,952
Operating time, A-hr	20,326	25,582	22,237	25,653
Number of thrusters	12	10	10	10
Total operating time, hr	138,256	145,200	130,560	149,520
Total operating time, A-hr	243,912	255,816	222,368	256,536
Total propellant, kg	2,130	2,240	1,950	2,250
Average specific impulse, sec	4,500	4,580	4,640	4,340

T5916

124

The parameters in Table 31 can also be analyzed in terms of reliability. We have assumed that thruster reliability can be described by a constant failure rate over the operating period and that wearout lifetime is greater than 15,000 hr. Consequently, the configuration that requires the least number of operating hours should have the best reliability. Since actual failure rate data is not available for ion thruster hardware, it is necessary to examine operating conditions that might affect failure rates adversely. Since the beam parameters are the most important, a perveance relationship (Figure 43) between voltage and current was selected as the best method of comparing operating conditions. Thruster design criteria are best satisfied when thruster parameters are adjusted to produce beam voltage and current values that follow a perveance line such as given in Figure 43 (actually, the voltage should be slightly larger than the value determined from the perveance line for any given current). The operating ranges required for the alternative PMaC approaches are shown in the figure. Since the CDVM and direct-drive PMaC approaches require the largest parameter variation, thruster operation in these approaches must deviate the most from the optimal conditions. This could reasonably be expected to increase the failure rate. The configuration with a conventional PMaC approach and a flat solar array also has two operating voltage regimes and thereby is, to some extent, in the same category. Ideally, the operating region would be parallel to a required perveance line that is drawn through a point representing the maximum beam current and a beam voltage slightly less (200 to 500 V) than the beam voltage specified at that point. The configuration having a conventional PMaC approach and a concentrator solar array is the most amenable to this sort of operation.

B. THRUST SYSTEM EFFICIENCY

Thrust system efficiency is defined as the ratio of the thruster power output to the total power furnished to the thrust system. It is a significant performance parameter because it is one of the key quantities used for evaluating the total performance of the Halley's comet spacecraft system. For this comparison, the average thrust system efficiency
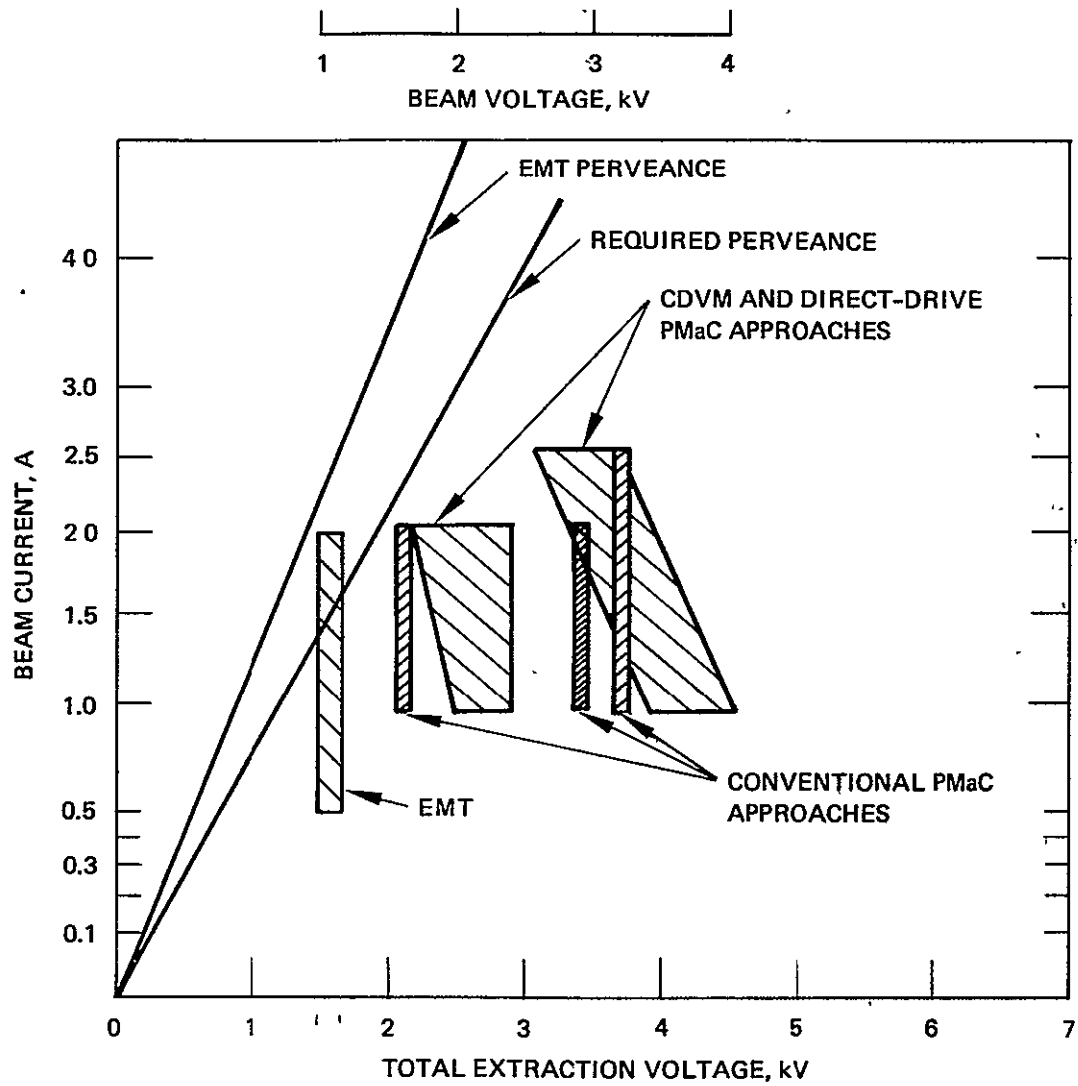
Figure 43. Thruster perveance requirements for different PMaC
approaches.

(time-weighted over the mission) was calculated for each of the seven thrust system configurations. After these calculations were made, NASA LeRC directed that such calculations should exclude the power furnished to the mission module for housekeeping purposes. Since we had included this power, the average efficiencies presented below are somewhat lower than they otherwise would have been. But the difference is so small as to have no effect on the comparative evaluation.

The quantities required to calculate thrust system efficiencies are power profile, thruster efficiencies, and PMaC unit power dissipations. The calculated thrust system efficiencies are listed in Table 32.

Table 32. Thrust System Efficiency
(Time-weighted average over the mission)

Configurations	1A	1AX	2A and 2A/I	2B and 2B/I	3A
Efficiency, %	73.0	73.7	67.5	68.1	68.5
Note: Calculations include housekeeping power furnished to mission module.					

T5816

C. THRUST SYSTEM RELIABILITY

Thrust system reliability calculations are based on the reliability model used for the selected baseline (Volume II). The notation used is given below:

- $r_p \equiv$ reliability of one set of PMaC thrust module units (i.e., per thruster)

  $r_T \equiv$ reliability of one thruster/gimbal $= \exp(-\lambda T)$

where

  T = average hours per thruster (from Table 28)

  λ = failure rate, in failures per hour

  $10^{-6} \leq \lambda \leq 10^{-5}$

$r_M \equiv$ reliability of each thruster/gimbal/PMaC supplies string (half-module) = $r_p \cdot r_T$

$R_M \equiv$ reliability of all thrust modules = $F(\lambda, T, r_p, N)$

where

$N \equiv$ number of thrusters

$R_p \equiv$ reliability of the PMaC units on the interface module

$R \equiv$ reliability of the thrust system = $R_M \cdot R_p \cdot R'$

where

$R' \equiv$ reliability of other subsystems (principally mercury storage and distribution).

Note that $R' = 0.95$ will be assumed for all configurations.

Reliability strongly depends on λ, T, N, and thruster utilization (i.e., the number of spares, number required to be operational at the end of the mission, etc.). T also depends on N, the thruster utilization plan, the solar array power profile, and the assumed values for thruster parameters (maximum voltages and currents, etc.). Initial calculations assumed specific (nonoptimized) thruster profiles and led to the values of T listed in Table 32. With N and T specified for each configuration, calculations of reliability thus depend on the value assumed for λ and on the formula for R_M (which depends on whether spare thruster/PMaC units are retained).

Reliability calculations summarized below were performed for the two estimated extreme limits of λ, and for the following three cases considered for thruster utilization:

- Case 1: All N thrusters considered operational when calculating T (i.e., no spares), and all N operational at the end of the mission.

- Case 2: N-1 thrusters considered operational (i.e., one spare), and N-1 operational at the end of the mission.

128

●   Case 3:   Same as Case 2, except that N-2 thrusters
               are operational at the end of the mission
               (i.e., mission performance degraded but not
               catastrophically).

The corresponding equations for R_M corresponding to these cases (derived in Volume II), reveal a strong dependence on λ and also that Case 2 is significantly better than Case 1 (especially for low values of λ) and Case 3 is somewhat better than Case 2 with respect to reliability.

Results of an analysis of Case 1 for $\lambda = .10^{-6}$ (considered to be a representative value) are presented in Table 30. The formula for R_M is $R_M = r_M^N$. All entries are identical for the corresponding integrated and modular configurations, reflecting the earlier assumption that structural reliability would have a negligible effect. Accordingly, the columns for configurations 2A and 2A/I and for 2B and 2B/I will be combined in subsequent tables.

Table 33 indicates that R ranges from 38% for 2A to 53.4% for 1AX. R depends on T, N, and r_p. Configuration 1AX is best because it has the highest value for r_p and the lowest value for T. Both direct-drive configurations are better than any of the other configurations because the higher r_p and the lower T contributions overshadow the effect of larger N. Configuration 2A is the worst one because of its low r_p. For this case ($\lambda = 10^{-6}$) the effect of T is not nearly as pronounced in the expression $\exp(-\lambda T)$ as it is for the upper limit of λ ($\lambda = 10^{-5}$) discussed below. Therefore, the reliability of 3A is greater than that of 2A or 2B, notwithstanding its larger T.

Relative reliability, ρ, is the most useful measure for comparisons for two reasons. First, it shows the relationships between the estimated system reliabilities explicitly. Second, it at least partially is isolated from the effect of assumptions made in estimating the absolute reliability magnitudes. Variations from assumed values that affect all configurations proportionally will be reflected in R but not in ρ. But those variations that affect some configurations more than others will affect both R and ρ. A sensitivity analysis on the effects on R and on ρ of varying the assumptions in Table 30 was performed, and the results

Table 33. Thrust System Reliability Estimates[a]

Reliability Factor[b]	Configuration						
	1A	1AX	2A	2A/I	2B	2B/I	3A
r_P	0.950	0.967	0.930	0.930	0.930	0.930	0.940
T, (10^3 hr)	11.5	11.5	14.5	14.5	13.0	13.0	15.0
r_T	0.9885	0.9885	0.9855	0.9855	0.987	0.987	0.985
r_M	0.939	0.956	0.9165	0.9165	0.918	0.918	0.926
N	12	12	10	10	10	10	10
$r_M = r_M^N$	0 470	0.583	0.418	0.418	0.425	0.425	0.464
R_P	0 967	0.964	0.954	0.954	0.954	0.954	0.967
R	0 432	0.534	0.379	0.379	0,385	0.385	0.426
Relative[a] Reliability, ρ	0.81	1.00	0.71	0.71	0.72	0.72	0.80

[a]Assuming $\lambda = 10^{-6}$ failures/hour and all thrusters operational for the full mission with respect to configuration 1AX.
[b]Defined in the text.

for several cases are given in Table 34. The first case, $\lambda = 10^{-6}$, is taken for reference from Table 33. The three other cases shown are

● $\lambda = 10^{-5}$; Case 1 of thruster utilization

● $\lambda = 10^{-6}$; Case 2 of thruster utilization

● $\lambda = 10^{-6}$; Case 3 of thruster utilization.

Increasing λ to its upper limit drastically reduces R for all configurations. However, ρ is largely unaffected, except that configuration 3A becomes less attractive. This can be traced to the specific (nonoptimized)) thruster profile selected for this particular configuration, and basically stems from the fact that the CDVM beam supply is unregulated. The correspondingly larger thruster power swings (from minimum to maximum) which would require using more thrusters during the mission in the selected thrust profile. This is reflected in a larger T (see Table 31). Because the increase in T is pronounced for larger value of λ, the relative ratings of configurations 2B and 3A appear to reverse for the particular set of thrust profiles selected.

In Case 2 above (one thruster as a spare), all values of R are significantly improved. This case was selected for the baseline (see Volume II). Since the improvement relative to Case 1 is greater for the less reliable configurations, the spread among them is reduced, but the relative ordering remains unchanged: again 1AX is best and 2A is worst.

The last case in Table 31 indicates the improvement expected over the previous case by allowing one less thruster to be operational at the end of the mission (with some potential mission degradation). The value of $\lambda = 10^{-6}$ was maintained for direct comparison. Reliability would be further improved and the values of ρ bunched still closer, and the relative ratings left unchanged.

The most significant result from the above analysis is the identification of the relative reliability ratings of the seven configurations, which can be used in the subsequent overall comparative assessment. The absolute magnitudes of estimated reliability vary rather widely in response to changes in λ, in thruster profiles, and in the manner of their utilization. Relative reliability ratings, however, remain — at least in the examples given — unchanged.

Table 34. Estimated and Relative Reliability of Alternate Thrust Systems

Thruster Failure Rate (λ), Failures/hr	Number of Thrusters			Reliability	Configurations				
	Considered Operational	Considered as Spares	Operational at End of Mission		1A	1AX[a]	2A and 2A/I[b]	2B and 2B/I[b]	3A[b]
10^{-6}	N	0	N	R	0.432	0.534	0.379	0.385	0.426
				ρ[c]	0.81	1.00	0.71	0.72	0.80
10^{-5}	N	0	N	R	0.125	0.154	0.103	0.119	0.110
				ρ	0.81	1.00	0.67	0.77	0.71
10^{-6}	N-1	1	N-1	R	0.768	0.828	0.724	0.730	0.766
				ρ	0.93	1.00	0.87	0.88	0.92
10^{-6}	N-1	1	N-2	R	0.788	0.841	0.752	0.757	0.790
				ρ	0.94	1.00	0.89	0.90	0.94

[a]12 thrusters operational.

[b]10 thrusters operational.

[c]ρ is normalized to R_{1AX}.

T5916

D. RISK ASSESSMENT

The relative risk associated with the seven thrust-system configurations is an important consideration in selecting a configuration. The study attempted to develop some measures of overall technical risk for each of the seven designs to furnish an input to NASA LeRC for the overall assessment of risks at the total spacecraft level. Only risks associated with the thrust system and with interfaces with the solar array and with the mission module were considered. The rationale for the final selection made by NASA LeRC is presented in Section 5.D. The risk factors associated with the solar array (and considered by NASA LeRC) are also noted.

The factors considered in assessing thrust system risks included:

● Novel technology requirements

● Engineering design complexity and difficulty

● Test validation requirements and feasibility

● Operational and design flexibility

● Predictability and resolution of interfaces (including environmental susceptibility).

Engineering design risks considered here were those relating to factors other than those pertaining to the nominal reliability estimates. The purpose of risk assessment was not to determine which configurations are feasible and which are not, since it can reasonably be expected that each of the seven designs could be implemented in time for a successful Halley's comet mission. This confidence stems primarily from four factors· (discussed in more detail in Volume II):

● The maturity of electric propulsion technology, which would be the basis for the ion thruster proposed for this application.

● ·Analyses and tests conducted during this study that demonstrated that the extended performance required of the 30-cm thruster can be achieved.

133

o   The extensive background in power processing technology
    that is directly applicable to the conventional beam
    and discharge supplies. Also, the results of breadboard
    tests of the CDVM (performed during this study) were
    promising, thus increasing our confidence in the voltage
    multiplier PMaC concept.

o   Current (1977) technology for electronics and system
    design is adequate, and no new components are required.
    Hence, what was assessed was the degree of risk, not
    overall feasibility.

1.   Technology

Comparing the seven thrust system concepts purely on a technological
basis — basic physics and new technology requirements — indicates that
the only significant difference among them arises from the requirement
for high-voltage switching gear for the direct-drive PMaC concepts.
High-voltage solar array design and panel switching is a relatively new
concept for space application, one not yet tested in a space environ-
ment. The risk it presents is significantly higher than for the other
design concepts. And the direct-drive discharge concept obviously pre-
sents an even greater risk than use of only the direct drive beam supply.
The components of novel technology in high-voltage array design and
switching are also reflected in the associated relative risks in the
areas of design implementation, test validation, interfaces, and
environmental susceptibility (discussed later).

Another area of technology risk is the requirement for a high-
voltage propellant isolator. This risk is included here rather than in
the engineering risk category because the design required is so novel.
Intensive effort during this study (see Volume IV) is believed to have
resulted in an isolator design approach that could be implemented within
the necessary time frame. However, that design must be evaluated further
before its performance can be confined. This risk does not affect the
selection from among the seven candidate thrust system configurations
because all seven require this new component.

No novel technology requirements exist in any other area of thrust
system design. In particular, 1977 technology is deemed adequate for all
electronic designs, and no novel electronic components are necessary.

2. - Engineering and Design

The seven configurations differ significantly with respect to
engineering design of the thrusters and PMaC subsystems. These differ-
ences are reflected in the risks assignable to design implementation.
Structural and thermal design aspects, although differing somewhat among
the seven configurations in terms of relative design complexity, are not
considered to present any significant technical risks. Accordingly,
structural and thermal design differences will not be considered further
in this subsection, but will be accounted for in the overall comparative
assessment in Section 5.4.

The engineering/design areas that present some risk, and for which
a difference arises among the various thrust systems, are:

- Thruster design scalability to required power levels

- PMaC design maturity

- Thruster/PMaC interactions.

The differences in thruster and PMaC design complexity and in thruster
life requirements among the configurations has already been accounted
for in the relative reliability estimates. The above engineering risk
categories address other design factors. Fault protection is not
included in the above listing because it is equally present and equally
resolvable in all four PMaC concepts.

All configurations require extended performance operation from the
thruster. One concern is the risk associated with scaling thruster per-
formance to higher voltage and power operation. Greater energy dumped
into the accelerator grids during arcing and the increased stress placed
on insulators by higher voltage may increase the failure rate. This
concern exists even though the (previously noted) experimental work
conducted has given us confidence that higher power/voltage operation
is feasible. The differences among the various design concepts stem
from the differences in thruster voltage, current, and power level and
operating time (on a performance basis) required over the mission. The
actual differences suggest a significant advantage for the conventional

135

PMaC concentrator array configurations (2B or 2B/I) and a significant disadvantage for the direct drive configurations (1A and 1AX).

Comparing the PMaC electronic designs on the basis of design maturity clearly places the CDVM approach in the highest risk category. The CDVM concept is a novel, unproven design in an initial stage of development, which has yet to be scaled to the required power level or to be tested with thrusters. Furthermore, no life testing of CDVM circuits has been conducted.

Because the CDVM electronics has only begun to be developed, it had to be assessed as a high-risk technology, even though no real problem areas have been identified as yet. On the other hand, there are funda-mental, relatively well-defined, technology risks associated with the high-voltage switchgear of the direct-drive approach and the high parts count (low reliability) of the conventional PMaC electronics.

Thruster-PMaC interactions at high power levels pose additional problems to be solved that differ somewhat for the four PMaC design concepts. These problems fall in three general categories:

- The identification of potential EMI sources and effects, and provision of corrective design measures.

- The definition of and recovery from thruster malfunction.

- The implementation of maximum power tracking for multiple thruster operations.

Potential EMI sources and effects and the measures available for reducing or eliminating these effects are discussed in Volume II for the conventional PMaC design. EMI problems are generally equally applicable to the CDVM design. The basic mechanisms are associated with the high noise currents caused by thruster high-power operation and by thruster arcing. Detrimental effects on sensitive circuits in the thrust system and in the mission module could result from conducted interference and from radiated emissions. The most serious interference mechanism (conducted and radiated) is associated with the PMaC harness. Localized shielding, and filters in the conventional and CDVM power supplies can significantly alleviate the potential problems. The inability to predict

current paths and the nature of detrimental effects on circuit performance must, however, place the technology for solution of this problem in a potentially high-risk category because the questions raised can only be resolved by extensive tests at the subsystem and system levels.

The causes, effects, and remedial measures against EMI are significantly different for the direct-drive concepts. Although the radiated emissions generated by the thrusters are similar for all concepts, the nature of noise current sources and current paths, and the measures for noise suppression and filtering, are inherently different for the direct-drive concepts. Without a beam power supply to act as a buffer, only a limited amount of filtering can be reasonably incorporated between the thrusters and the solar panels. The conducted and radiated current paths and effects are even less predictable than for conventional PMaC electronics. In addition, direct-drive concepts pose potentially an even more serious problem resulting from the presence of higher voltage. High-level transients may occur as a result of thruster arcing. Solar panel voltage potential may change drastically during thruster malfunctions. Unpredictable plasma interactions may occur. But it is not easy to shield, isolate, or reroute (between the thrusters and the solar panel) the high-voltage wiring harness to prevent or reduce EMI effects. Therefore, potential EMI problems appear to be more severe for the direct-drive concepts (especially for concept 1AX). The testing required to resolve them is both more comprehensive and more difficult, and the remedial measures will be less predictable.

All thrust system designs must provide for recovery from thruster malfunctions. Possible malfunction modes and controller design concepts for automatic recovery on board the spacecraft from some of these malfunctions are discussed in Volume II for the conventional PMaC design. Defining the thruster malfunction modes for which automatic recovery provisions can be incorporated and mechanizing these provisions will vary among the different PMaC concepts. This difference stems from the degree to which each design allows for sensing, adjusting, and controlling thruster operational parameters. Conventional and CDVM designs inherently possess this capability because the beam and discharge supplies provide

137

for PMaC-thruster closed loop control: thruster operational parameters can be measured and adjusted by corresponding measurements and adjustments in the beam and discharge supplies.

Providing for identification of and automatic recovery from thruster malfunctions will be less certain and more difficult for the direct drive and for the direct-drive discharge concepts 1A and 1AX. A controllable discharge supply is available for concept 1A, but neither beam nor discharge supplies are available for concept 1AX. The risk of adequately providing for thruster malfunction recovery is therefore greater for concept 1AX.

Each thrust system concept, to operate efficiently, must have automatic maximum power tracking. Implementing this requirement in the controller for multiple thruster operation involves a greater risk for the direct drive concepts than for the conventional and CDVM designs for reasons similar to those given above for thruster malfunction recovery. The risks are especially significant for direct-drive discharge concept 1AX. For this concept, direct coupling to the high-voltage solar panel is required for sensing and adjustment, and the resulting impact on thruster operations is less predictable than it is for the other configurations.

3.   Test Validation

All PMaC concepts require extensive tests at both the subsystem and system levels to validate thruster PMaC interactions and operational performance. It is difficult to assure in advance that all potential problems, especially the EMI effects, can be resolved. The fact that the CDVM design has not been previously tested with an operating thruster is a source of some risk relative to the conventional design. The risk assignable to testing the validity of the direct drive concepts is substantially higher because simulation, identification, and validation of corrective measures for potential EMI effects is extremely difficult, if not impossible, on a full-scale basis.

4. Flexibility

The operational flexibility available is an important measure of the relative performance of the various designs. Flexibility is needed in adjusting the performance parameters of the multiple operational thrusters to ensure the success of the mission. Efficient performance must be maintained as the solar array power level changes, as the number of operating thrusters is altered, as the thruster performance varies (e.g., as a function of wear-out), and during the recovery from malfunctions. This flexibility, although related to provision for malfunction recovery, is a broader design requirement. Real-time closed-loop control is required for adjusting operating parameters, and would be provided by using a discrete set of control algorithms incorporated in the controller design. The problem is compounded by the fact that the flexibility requirements are largely unpredictable until late in the development program or until after the mission begins. The PMaC subsystem design must therefore incorporate flexibility in terms of control loops and operating points, with simple provisions for real-time changes.

The task of providing operational flexibility is not equally tractable for each of the four PMaC concepts. The conventional approach (concept 2) offers the greatest flexibility because of the adjustments available for controlling and modifying the set points in the beam and discharge supplies. The CDVM approach (concept 3) also offers good flexibility, although regulation (not included in the design evaluated under this study) would be required. The CDVM design used for this study could be readily modified (with some performance degradation) to include regulation. The direct drive concept poses a much greater risk with respect to flexibility. The thruster beam supply is directly tied to the solar array via the reconfiguration unit, and a change in operational parameters would require special provisions in the design of the solar array reconfiguration unit. The performance and the associated risks are still greater for the direct-drive discharge concept, since both the beam power and the discharge power depend directly on the characteristics of the solar array design and of the associated reconfiguration units.

5. Interfaces

Defining the interfaces between the thrust system and the other major vehicle components (the mission module, and solar array) and complying with the resulting interface specifications pose a difficult, if not the most difficult, problem in the thrust system design. There are likely to be problems concerning the responsibility for and the ability to predict specifications for certain interfaces. These problems stem from the possibility of interactions caused by the electromagnetic environment; the risk differs among the various thrust system design concepts. These risks involve a broad, system-level class of EMI effects. One potential problem is the impact on mission module communication and computer functions of high-noise thruster operations (especially during malfunction or recovery). As another example, solar array arcing within the direct-drive configurations may significantly affect the mission module and the thrust system. These effects are a concern because many of the potential interactions can only be guessed at, but not definitely pinpointed, a priori. Again, the direct-drive concepts present greater risks.

E. COMPARATIVE EVALUATION

A summary comparison of the seven thrust system configurations is presented in Table 35. The major categories listed are those considered to furnish the principal criteria for the comparative assessment. In each category, the factors that distinguish among the seven configurations are presented. Modularity is included because it is important to the final selection. Thrust system length, although it varies significantly by configuration, is included for reference only since each configuration would fit easily in the shuttle bay (assuming the specified 2.5-m-long envelope for the mission module and a maximum IUS length of 8.4 m).

Mass data is included for the total spacecraft. Mass data is given for the significant trajectory times:

- On orbit at rendezvous (after the expenditure of mercury propellant)

140

Table 35. Summary of Principal Features and Characteristics of the Candidate Thrust System Configurations

Parameters/Characteristics	Configuration						
	1A	1AX	2A	2A/I	2B	2B/I	3A
Modularity	Yes	Yes	Yes	No	Yes	No	Yes
Length, m	.2.9	2.9	4.4	4 6	4 9	4.6	3 7
Spacecraft, kg							
On orbit, at rendezvous	1800	1760	2150	2210	2200	2170	1990
On orbit, at IUS deployment	3930	3890	4390	4450	4150	4120	4240
On IUS, at shuttle deployment	3980	3940	4500	4470	4370	4270	4350
Efficiency, %	73 0	73 7	67.5	67.5	68.1	68.1	68.5
Reliability[a]							
Estimated, %	77	83	72 5	72 5	73	73	76 5
Relative, normalized with respect to 1AX	0 93	1 0	0.87	0 87	0 88	0 88	0 92
Technology risk	High	High	Low	Low	Low	Low	Low
Engineering/design risk							
Thruster operating parameters level (scalability)	High	High	Medium	Medium	Low	Low	Medium
PMaC electronics design maturity	Medium	Medium	Low	Low	Low	Low	High
Thruster-PMaC interactions (E'1I, malfunction recovery, P_{max} tracking)	High	High	Low	Low	Low	Low	Low
Other risk[b]	High	High	Low	Low	Low	Low	Medium
Structural design and interfaces complexity of							
Design complexity	Medium	Medium	High	Low	High	Low	High
Accessibility	Medium	Medium	Poor	Good	Poor	Good	Poor
Solar array interface	Medium	Medium	Good	Good	Poor	Poor	Good
IUS interface	Medium	Medium	Medium	Good	Poor	Good	Medium

[a] Estimated upper limit with no mission degradation

[b] Test, operations, interfaces

141

T5916

● On orbit at the start of thrust phase (after deployment from the IUS)

● On the IUS (after deployment from the shuttle).

This data reflects the relative mass contributions of the various thrust system designs. However, the comparison is somewhat artificial and inconclusive. A true comparative assessment would be based on a full mission trajectory analysis at the spacecraft level, an analysis that considers the relative thrust system masses as inputs and that derives the relative available mission module payload masses using the actual IUS capabilities for each trajectory and the updated mercury propellant requirements resulting from mission profile optimization. Nevertheless, the data in Table 35 is judged to be adequate for a relative assessment of the configurations in terms of their masses.

The comparison of relative thrust system reliabilities takes into account the reliability and wear-out of the thrusters (i.e., in terms of the relative thruster operating time required) for the reliability and complexity of the PMaC electronics, and for redundancy provisions. These relative values therefore also implicitly account for differences in potential single point failures. Structural reliability contributions, which are relatively insignificant and essentially the same for all configurations, are, in effect, also included. The values presented in Table 35 correspond to the third case in Table 34 (i.e., one spare thruster, all other thrusters operational for the full mission duration, and thruster failure rate taken at the lower limit of $\lambda = 10^{-6}$ failures per hour). This yields upper limits for reliability estimates with no mission degradation. This case is considered as the most representative since it corresponds to the case selected (one spare half-module) for the baseline. The rankings of the configurations are not significantly different for the other reliability estimates. Both the estimated reliability values and the relative reliabilities with respect to configuration 1AX are listed.

Results of the risk assessment are summarized in three separate categories; these reflect the relative importance of the factors in the overall assessment. Risks related to high-voltage technology are highlighted for the direct-drive configurations. Engineering and design risks are broken down into the three areas previously considered. The scalability of thruster parameters is of most concern with the direct-drive configurations, since these require the highest variations in the parameters, and of least concern with the configurations using conventional PMaC systems and a solar concentrator array. From a design maturity standpoint, the configuration using the CDVM PMaC subsystem is rated as most risky because the CDVM beam supply has not yet been designed for the required power levels, and has not yet been operated with thrusters. Interactions between the thruster and the PMaC unit are the least understood and their effects are of the greatest potential concern for the direct-drive configurations.

The other potential risks (adequate test validation, provision of required operational flexibility, and interactions between the solar array and the mission module) are grouped together. The highest risk is again assigned to the direct-drive configurations because with them it is the most difficult to incorporate the design measures required for operational flexibility. Because full-scale testing would probably not be possible, a flight test would probably be necessary for validating system integration procedures for a direct-drive spacecraft configuration. Of the other configurations, the CDVM configuration is considered somewhat more risky in this respect because test data is lacking.

The last entry in Table 35 relates to all the other design and interface factors that distinguish among the seven configurations and that are considered of significance. These factors all reflect a relative degree of complexity, although none of them presents any serious concern regarding design implementation.

The integrated configurations are preferred from a structural design complexity standpoint. Of the modular designs, the short direct-drive configurations are structurally the simplest and have the best accessibility for assembly and testing.

Comparing the configurations, with respect to the adequacy and complexity of the interfaces leads to some changes in the above rankings. The superiority of the integrated configurations still emerges essentially unchanged, but the ranking of the concentrator-array configuration (2B) is significantly reduced with respect to all the others. This is because of the potential interface problems with the solar array and with the IUS, caused by the large volume that was specified for the stowed array. Changing the stowed array packaging significantly improved the structure of this configuration and contributed to its selection as the baseline concept.

The interface between the thrust system and the solar array was considered with respect to the difficulty of array stowage and deployment and the requirements for preventing mercury ion contamination (i.e., the length the deployment arm must be to provide adequate separation). The two concentrator array configurations receive the lowest ratings. The rating of a configurations structural interface between the thrust system and the IUS was made with regard to required IUS attachment modifications (e.g., extension beams), the design of the adapter and of the separation system. Again, the integrated configurations are rated highest and the concentrator array configuration of the modular was rated lowest. Rating of a configuration's interface with the missing module was made in terms of structural adequacy; all configurations are basically satisfactory, but the integrated, flat array configuration (2A/I) appears to be distinctly superior.

F. BASELINE SELECTION

The comparative analysis of the seven configurations (summarized in Table 35) was used as the basis for selecting the baseline thrust system. The conventional PHaC approach, and a concentrator solar array configuration (2B) was selected. The selection process consisted of three steps. The first step, carried out as part of this study, was to recommend the thrust system. The second step, which was carried out by NASA LeRC, considered (in addition to the thrust system) the risks associated with the solar array configurations and the net mass available

144

for the science payload (by considering the mission trajectory profile).
The result was a tentative preference for configuration 2B. The third
step was the introduction of a design modification for the concentrator
solar array. The improvement from the modification was significant and
led to the selection of configuration 2B as the baseline.

This section primarily addresses our analysis of the thrust system
(step 1 above). The data in Table 35 was translated into a comparative
assessment matrix, given in Table 36. Disregarding length differences,
rankings were assigned for each of the parameters and characteristics
by assessing the corresponding entries in Table 35, with an A repre-
senting the most desirable configuration, a B representing the next
desirable, and a C representing the least desirable. This was admittedly
a rather arbitrary and subjective method for comparing configurations;
however, it serves to point out the fact that none of the configurations
can be considered an obvious best choice. Our recommendations were
therefore based on the arguments that follow.

Of the assessment criteria shown in Table 36, the risk assessments
are probably the least likely to be influenced by refinements in design
and could be changed only by intensive development. The Halley's comet
rendezvous mission is constrained to an exact time frame and it is
unlikely that sufficient activity could be supported (within a reason-
able budget) to alleviate the risks within the time frame required.
The direct-drive configurations (1A and 1AX) were therefore eliminated
on the basis of risk. Thrust system mass, efficiency, and reliability
were used to differentiate among the remaining configurations. The
configurations employing the flat solar array and a conventional PMaC
subsystem were judged least desirable and were eliminated on that basis.
Ranking the three remaining system configurations is most subjective
and requires further consideration of the weighting of the assessment
criteria.

As in the initial comparison, risk was weighted most heavily with
reliability next in order of importance. This weighting allowed
selecting the conventional-PMaC subsystem configurations (2B and 2B/I)
over the CDVM configuration (3A). This is not a clear-cut choice

Table 36. Assessment of Thrust System Configurations

Assessment Criteria	Configuration						
	1A	1AX	2A	2A/I	2B	2B/I	3A
Technology risk	C[a]	C	A	A	A	A	A
Engineering risk	C	C	A	A	A	A	B
Other risk	C	C	A	A	A	A	B
Reliability	B	A	C	C	C	C	B
Mass	A	A	C	C	B	B	B
Efficiency	A	A	C	C	B	B	B
Structure and interface complexity	B	B	B	A	C	A	B
Modularity	A	A	A	C	A	C	A

[a]A ≡ Best

B ≡ Medium

C ≡ Worst

146

because, by assuming some additional engineering and integration risk, it might be possible to obtain a thrust system with higher reliability (lower parts count and complexity). In comparing the remaining two configurations, 2B and 2B/I, the desirability of modular construction overshadows the interface criteria and resulted in the recommendation of the modular configuration 2B as the baseline concept for further design and evaluation. Our recommendation is made with the reservation that the mass, efficiency, and reliability of configuration 2B might not be adequate to satisfy the mission requirements without significant design modifications (notably to the stowed array). We also observe that a configuration using a concentrator solar array with a CDVM PMaC subsystem would make a good alternate if some additional risk could be tolerated.

Results of steps 2 and 3 (carried out by NASA LeRC) strengthened this selection. During step 2 process, two basic factors were considered: The acceptability of the mass of configuration 2B (with respect to available payload mass) was confirmed by a system-level analysis (which also confirmed the relative mass ratings of the other configurations). Also, the relative risk disadvantages of the other configurations (especially direct drive) were significantly increased by the analysis of the relative risks of the solar arrays. Table 37 summarizes NASA LeRC's ratings of the risk factors for the various solar array configurations. Step 2 further confirmed our selection and pointed out the need to simplify the concentrator solar array design in a way that would improve performance and strengthen the validity of this selection. Subsequent investigation initiated by NASA LeRC did lead to the identification of several alternate concentrator array designs that would meet those goals. As reported, the final recommended concentrator array design exhibited significant performance and structural design improvements for this application relative to the concentrator design considered during this task. This significantly reduced some of the concerns reflected in Table 35. In particular, the mass of the thrust system was reduced and the structure was simplified, thereby effectively removing the C rating in Table 36. As modified, configuration 2B therefore emerged as the clear choice and was used for defining the selected baseline (presented in Volume II).

Table 37. Comparison of Solar Array Configurations
(From a NASA LeRC Initiated Study)

Comparison Category	Parameter or Comment			
Solar array configuration	Flat	Flat	Flat	Concentrator
Thrust system configuration Designation Type of PMaC system	 1A and 1AX Direct drive	 2A Conventional	 3A Voltage multiplier	 2B Conventional
Technology risk(s)	High-voltage effects Thin cells	Thin cells	Thin cells	
Engineering risk(s)	High voltage design Manufacturing and blanket handling	Manufacturing and blanket handling	Manufacturing and blanket handling	Mechanical integrity in space (alignment/ pointing) Deployment
Test validation risk	High voltage			Deployment
Operational flexibility	Low			
Environmental susceptibility	Degradation of the thin cell	Thin cell degradation	Thin cell degradation	

T5916

In summary, the final selection of configuration 2B may be stated evolved from the following sequence:

- Direct-drive configurations were rejected because of high risk.

- Flat solar array configurations were rejected because of their high mass and because of risks associated with the thin cells.

- Integrated configurations were rejected because their relatively small potential mass savings, their efficiency and reliability benefits, and their relative structural and interface simplicity did not warrant abandoning the benefits of modularity. (Modularity is desired because it would permit the thrust system components to be adapted for other missions at a much lower cost than for adapting an integrated configuration.)

- The concentrator array was considered superior, particularly given the modified design that was expected to lower total system mass and to make packaging more manageable.

- The conventional PMaC approach was adopted because of its relatively low risk and acceptable system mass, reliability, and efficiency.

- The concentrator array with the CDVM PMaC subsystem (not explicitly studied) was considered as a potential alternative to the baseline, pending progress in CDVM development.

REFERENCES

1. IUS System/Subsystem Summary, Boeing Aircraft Company, Document
    No. D-290-10051-1, 25 January 1977.

2. System Specification, Performance and Design Requirements for the
    Department of Defense Space Transportation System, Vol. 3, Interim
    Upper Stage System Segment, Basic Requirements for, August 19, 1976.

3. DoD STS Payload Requirements Data Book, Boeing Aircraft Company,
    Document No. D-290-10077-1, 10 June 1977.

4. Level II Program Definition and Requirements, Vol. XIV — Space
    Shuttle System Payload Accommodations, JSC-07700, Change No. 18.

DISTRIBUTION LIST

Recipient		Copies

NASA Lewis Research Center
21000 Brookpark Road
Cleveland, OH 44135

Dr. Bernard Lubarsky	MS 3-3	1
Dr. Seymour C. Himmel	MS 3-7	1
Daniel J. Shramo	MS 303	1
Elmer H. Davison	MS 3-3	1
Howard W. Douglass	MS 501-5	1
H. Warren Plohr	MS 501-5	1
Robert R. Lovell	MS 501-4	1
James F. DePauw	MS 501-4	1
James E. Cake	MS 501-4	24
Allan Jones	MS 500-313	1
Library	MS 60-3	1
Report Control Office	MS 5-5	2
Public Information Office	MS 3-11	1

NASA Scientific and Technical Information Facility   10
P.O. Box 8757
Baltimore Washington International Airport
Baltimore, MD. 21240

NASA Headquarters
Washington, D.C. 20546

James Lazar	Code RP	1
Wayne R. Hudson	Code RPE	1
Jerome P. Mullin	Code RPP	1
Fred J. DeMeritte	Code RC	1
Edward A. Gabris	Code RS	1
Frank T. Rosenburg	Code BR	1
John H. Disher	Code MT	1
Lester K. Fero	Code MTE	1
A. Thomas Young	Code SL	1
Daniel H. Herman	Code SL	1
Paul F. Tarver	Code SL	1

NASA George C. Marshall Space Flight Center
Marshall Space Flight Center, AL. 35812

R.E. Austin	PS04	3
L.E. Young	EC12	1
J.L. Miller	EC12	1

Jet Propulsion Laboratory
4800 Oak Grove Drive
Pasadena, CA   91103

Dr. Bruce C. Marray,	M.C. 180-905	1
J.N. James	M.C. 180-901	1
Norman R. Haynes	M.C. 180-704	1
Dr. K.L. Atkins	M.C. 180-700	3
J.M. Cork	M.C. 233-307	10
J.E. Graf	M.C. 122-123	1

Jet Propulsion Laboratory   1
Attn: E.N. Costogue FH-B201
2500 Foothill Blvd.
Pasadena, CA   91103

TRW Defense and Space Systems Group   1
One Space Park
Redondo Beach, CA   90278,

J.J. Biess	M.C. 82/2367	1
A.D. Schoenfeld	M.C. 82/27200	1

Rockwell International   1
Attn: Dr. James B. Weddell SK71
12214 Lakewood Blvd.
Downey, CA   90241

Boeing Aerospace Co.   3
Attn: Charles Terwilliger   M.C. 84/95
Seattle, Washington

Fairchild Space and Electronics Co.   1
Attn: Steven S. Myers
Germantown, MD   20767

Science Applications, Inc.   1
Attn: John Niehoff
One Woodfield Place Bldg., Suite 109
1701 East Woodfield Road
Schaumburg, IL   60196

Battelle Columbus Laboratories   1
Attn: R.R. Teeter
5058 King Avenue
Columbus, OH   43201

```
General Dynamics                                                    1
Convair Division
Attn:  J.W. Streetman
P.O. Box 80847
San Diego, CA  92138


Wright-Patterson Air Force Base
AFAPL
Wright-Patterson Air Force Base, OH

    Hans VonOhain                                                  1
    J. Reams                                                       1


SAMSO/YAT
P.O. Box 92960
Worldway Postal Center
Los Angeles, CA 90009

    Col. Woods                                                     1
    Capt. Robert Ford                                              1
    Capt. Paul Heartquist                                          3


The Aerospace Corporation
P.O. Box 92957
Los Angeles, CA 90009

    John Mosich                                                    1
    T. Silva                                                       1
```